CHARACTERIZATION OF MEMBRANE PROTEIN PRIMARY STRUCTURE AND PROTEIN COVALENT MODIFICATION BY MALDI-TOF-MS

by

Jian Huang
B.Sc., Sichuan University, 1992

THESIS SUBMITTED IN PARTIAL FULFILLMENT OF
THE REQUIREMENTS FOR THE DEGREE OF

MASTER OF SCIENCE

In the
Department
of
Chemistry

SIMON FRASER UNIVERSITY

Fall 2005

APPROVAL

Name: **Jian Huang**

Degree: **Master of Science**

Title of Thesis: **CHARACTERIZATION OF MEMBRANE PROTEIN PRIMARY STRUCTURE AND PROTEIN COVALENT MODIFICATION BY MALDI-TOF-MS**

Examining Committee:

Chair: **Dr. Michael H. Eikerling**
Assistant Professor of Department of Chemistry

Dr. George R. Agnes

Senior Supervisor
Associate Professor of Department of Chemistry

Dr. Paul C. H. Li

Supervisor
Associate Professor of Department of Chemistry

Dr. Erika Plettner

Supervisor
Assistant Professor of Department of Chemistry

Dr. Byron D. Gates
Internal Examiner
Assistant Professor of Department of Chemistry

Date Defended/Approved: Nov. 28/2005

ABSTRACT

The subjects of this thesis were to illustrate membrane protein primary structure determination, protein covalent modification and protein-protein interaction by using matrix assisted laser desorption/ionization time-of-flight mass spectrometry (MALDI-TOF-MS). First, in one mode of sample preparation referred to as wall-less sample preparation, an increase in sequence coverage of a model membrane protein, bacteriorhodopsin, increased from 81% using traditional sample methodology to 89%. Second, chemical modification sites of proteins, pheromone binding protein 2 (PBP2) and cytochrome $P450_{cam}$ ($P450_{cam}$), were characterized by MALDI-MS. This finding contributed to further studies of protein-ligand interaction of PBP2, and also provided information about native conformation of $P450_{cam}$. Third, co-immunoprecipitation and MALDI-MS was used to identify the interaction of synapse-associated protein (SAP97) with potassium voltage-gated ion channel Kv1.5. This study provided the first direct mass spectral evidence to support their protein-protein interaction. In addition, to better understand one of MALDI ionization pathways, a simple two-plate method was used to examine the MALDI gas-phase cationization.

献给我的父亲黄代国和母亲米建湘

以及我的先生

For my parents, Dai Guo Huang and Jian Xiang Mi,

And my husband, Walter Selent.

ACKNOWLEDGEMENTS

I would like to thank my senior supervisor Dr. George. R. Agnes for the opportunity to study and do research in his group. Characterizing proteins and peptides using MALDI-MS is a very interesting project. During my two-year master program, Dr. Agnes serious academic attitude and creative ideas inspired me. I have greatly benefited from his scientific training.

I must thank my supervisor Dr. Erika Plettner for allowing me to work with her group on identification of protein covalent modification sites. And her suggestions on protein study are appreciated.

I also wish to thank another supervisor, Dr. Paul C. H. Li, for his encouragement and suggestion along my study and research.

Furthermore, I must extend my gratitude to all my co-workers and friends in the Department of Chemistry and the Department of Molecular Biology and Biochemistry at Simon Fraser University. Especially I have to thank Diem Ly Van and Teresita M. Cruz Sanchez for their help on wall-less samples preparation.

Most of all, my appreciation goes to my dear parents, Dai Guo Huang and Jian Xiang Mi, who are my true motivation. Finally I want to thank my husband, Walter Selent, for his incredible patience and understanding.

TABLE OF CONTENTS

LIST OF FIGURES

LIST OF TABLES

LIST OF ABBREVIATIONS AND SYMBOLS

ACN	Acetonitrile
ACTH 18-39	Adrenocorticotropic hormone fragment 18-39
BR	Bacteriorhodopsin
7C-BIPY	5'-(4-Bromo-heptyl)-5-methyl-[2,2']bipyridinyl
CHCA	α-Cyano-4-hydroxycinnamic Acid
CNBr	Cyanogen bromide
DHB	2,5-Dihydroxybenzoic acid
DTT	1,4-Dithiothreitol
EDB	Electrodynamic balance
GRAVY	Grand average of hydropathicity
HPLC	High performance liquid chromatography
IAEDANS	5-((((2-iodoacetyl) ethyl) amino)-naphthalene-1-sulfonic acid
IR	Infrared
Kv1.5	Potassium voltage-gated ion channel subfamily A member 5
MALDI	Matrix assisted laser desorption/ionization
MS	Mass spectrometry
m/z	Mass-to-charge ratio
NCBInr	the National Center for Biotechnology Information database
OG	Octyl-β-D-glucopyranoside
PAGE	Polyacrylamide gel electrophoresis
PBP2	Pheromone binding protein 2
PEG 1000	Polyethylene glycol average molecular weight 1000
PMF	Peptide mass fingerprinting
PDZ	Named after three proteins, Postsynaptic density protein, molecular weight 95 kDa (PSD-95), Discs-large protein (Dlg) and Zonula occludens-1 (ZO-1)

$P450_{cam}$	Cytochrome $P450_{cam}$
SA	Sinapinic acid (3,5-dimethoxy-4-hydroxycinnamic acid)
SAP 97	Synapse associated protein, molecular weight 97 kDa
SDS	Sodium dodecyl sulfate
S/N	Signal-to-noise ratio
TFA	Trifluoroacetic acid
TOF	Time of flight
TM	Transmembrane region
UV	Ultraviolet

CHAPTER 1:
INTRODUCTION: CHARACTERIZATION OF PROTEINS AND PEPTIDES USING MALDI-TOF-MS

1.1 Context

In this thesis, matrix-assisted laser desorption/ionization time of flight mass spectrometry (MALDI-TOF-MS) was used to characterize proteins and peptides. Specifically, this thesis covers development of general methods for improving the sequence coverage of membrane proteins, identification of covalent modification sites on proteins, and characterization of ion channel protein-protein interactions. This chapter describes some applications of MALDI for the study of proteins and peptides.

1.2 Introduction

MALDI and electrospray (ESI) are two soft ionization techniques.[1-3] Both sources ionize the low volatility, high molecular weight compounds, including proteins and peptides, and they offer a detection limit as low as attmomoles.[4,5] Both are widely used in proteomics research. MALDI and ESI are viewed as being complementary techniques.[6] ESI produces multiple charged molecular ions,[5] and has a low tolerance to salts and buffers, but it can be coupled on-line with separation techniques, such as liquid chromatography and capillary electrophoresis.[5-7] In contrast, the predominant production of singly charged molecular ions in MALDI makes the interpretation of mass spectrum straightforward,[8] and MALDI tends to be more tolerant to common contaminants such as salts and buffers which are often present in biopolymer samples.[9] MALDI-MS is often

used for the direct analysis of complex biological samples, such as human blood and serum, due to its relative higher tolerance to contaminants that are often present in sample.[10] MADLI-MS was used to study proteins and peptides in this thesis. More details about MALDI are described in chapter 2.

1.3 MALDI-MS and protein study

To study cellular and gene function at the protein level, many techniques have been used, some of which include cell imaging by light microscopy, or protein-protein interaction analysis by two-hybrid assays.[11] When studying low abundant proteins in highly complex biological samples, more sensitive techniques with a high specificity such as MALDI-MS, are being successfully applied.[11]

1.3.1 Molecular weight determination of proteins and peptides

MALDI-MS can provide information about the molecular mass of proteins or peptides.[12] Every protein has a unique set of peptides digested by an enzyme (e.g. trypsin or chymotrypsin) or a chemical (e.g. cyanogen bromide), leading to unique peptide masses, which together form a "peptide fingerprint" for a protein.[11,13] Figure 1.1 shows the flowchart of the detection of peptide mass fingerprint by using MALDI-MS. The detected peptide mass from a protein digest can be used to map protein sequence and further for protein identification through peptide mass fingerprinting. [11,14]

The theoretical monoisotopic m/z of a peptide or protein was calculated by using a common used web tool, PeptideMass. (http://www.expasy.ch/tools/peptide-mass.html).[15] This program can calculate a peptide or protein theoretical mass for a

submitted the peptide or protein sequence. It was used to calculate the theoretical m/z of peptides in this thesis.

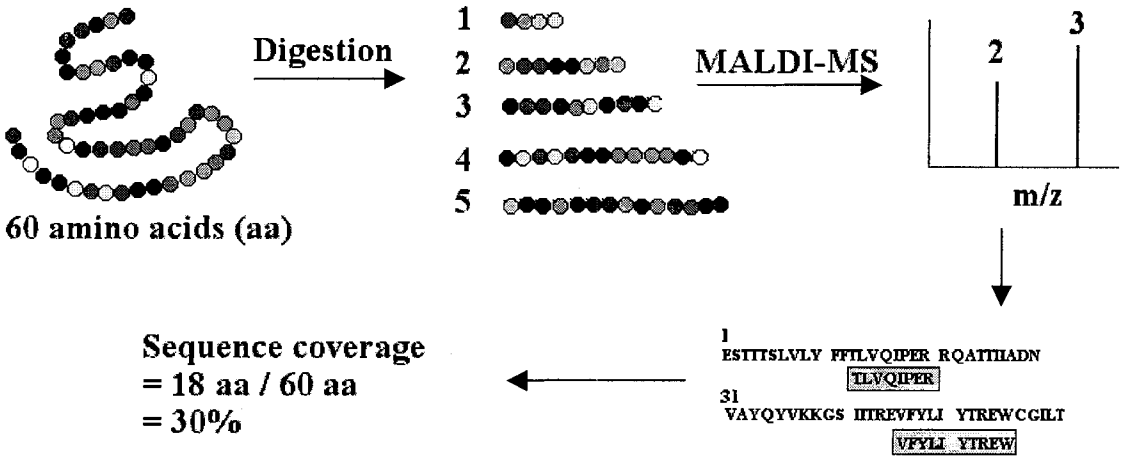

Figure 1.1 **A flowchart of the detection of peptides to generate a protein sequence coverage map using MALDI-MS. (Adapted from references).[11,16]**

1.3.2 Protein identification by peptide mass fingerprinting

Peptide mass fingerprinting (PMF) is a technique to identify an unknown protein by matching the observed fragment peptide masses to the theoretical peptide masses generated from a protein database.[13,17] The flowchart in Figure 1.2 introduces the basic concept of PMF.

The protein sequence databases include the National Center for Biotechnology Information (NCBInr) database and Swiss-prot database (Swiss-Prot). The search engines for protein identification are web accessible, such as Mascot (Matrix Science, London UK, http://www.matrixscience.com).[13]

There are many possible sources of error in protein identification using PMF, such as mass accuracy, mass shift caused by post-translational modifications and mass range restriction. The parameters used for protein database search include taxonomy, type of enzyme, number of missed cleavage and modifications.[13,17]

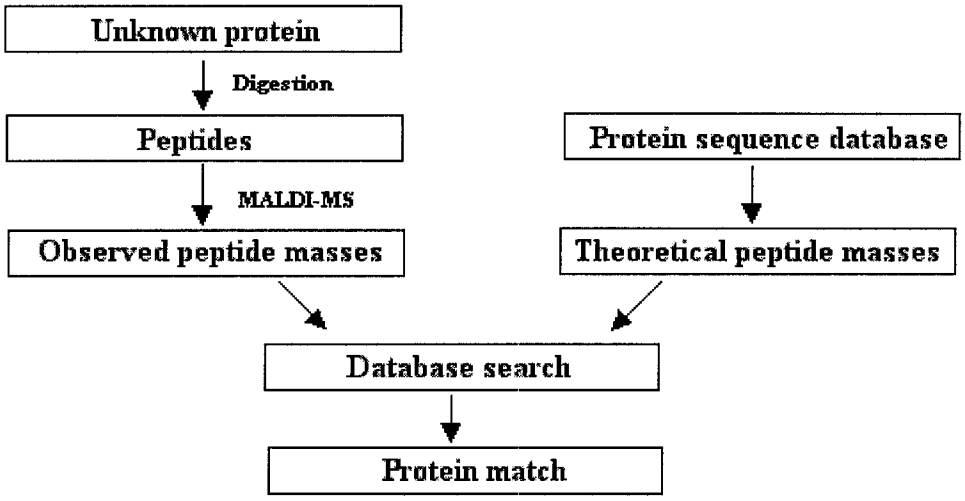

Figure 1.2 A flowchart of peptide mass fingerprinting (PMF). (Adapted from reference).[14]

1.3.3 Clarification of protein post-translational or chemical modifications

When a polypeptide chain is released from a ribosome, it is often not the last step in the formation of a protein. Various covalent modifications can occur, which are referred to as post-translational modifications (PTM).[18] Post-translational modifications alter the properties of a protein, and they change the biological functions of the protein. The most common PTMs include proteolytic processing, glycosylation, phosphorylation, prenylation and acylation.[19] Determination of the sites of PTM provides information concerning protein activity, conformation distribution, and spatial distribution in a cell.[19] An improved understanding of PTMs is believed to be very important in leading to the improved understanding of many diseases.

In synthetic modification of proteins, a chemical reagent is often added to a protein for the purpose of probing the structure-function relationships of a protein. For example, dansyl chloride is a fluorescent reagent. The dansylated proteins can be used to monitor protein functions, such as effect of pH change, by measuring fluorescence intensity.[20] Identification of the actual modification sites can improve the understanding of protein conformation.

Post-translational modification and chemical modification are both covalent reactions. Such covalent modifications cause mass shifts in an altered peptide, which can be measured using MALDI-MS. Most mass shifts increase the mass, but the formation of disulfide bonds cause mass decrease by 2 Da.[21] The modified peptide is identified by comparing the mass of peptides generated from an unmodified protein versus the peptides digested from a modified protein.[18,22] Figure 1.3 depicts the principle of the identification process.

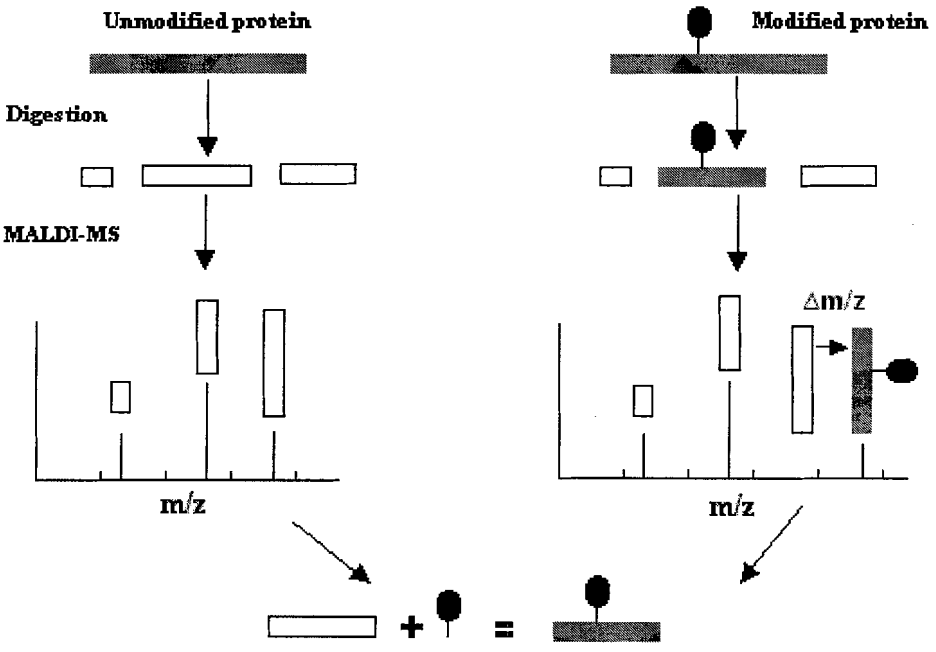

Figure 1.3 **Schematic diagram illustrate a general procedure to identify protein modification sites using MALDI-MS. The protein is shown as a solid bar, and modification is indicated by a black oval symbol. The unfilled rectangular represents peptides having no modification sites and the filled rectangular represents the peptide having a site of modification.**

1.3.4 Characterization of protein-protein interactions

Proteins rarely act alone in a cell. Most cellular processes are carried out by protein complexes. Proteins interact with other proteins to perform functions. The non-covalent interactions are forming and dissociating during a cell function. The forces include electrostatic forces, hydrogen bonds, van der waals forces and hydrophobic effects.[23-25]

Identification of the protein complexes, particularly under physiological conditions, has been fundamental to understanding their biological functions.[24,25] Gavin *et al.* applied tandem affinity purification and MALDI-MS to characterize protein complexes on a large scale in *Saccharomyces cerevisiae.*[25] The authors processed 1739

genes, purified 589 protein assemblies, defined 232 protein complexes, and proposed new functions for 344 proteins. Their analysis has provided an outline for a protein complex network. Of the 589 purified protein assemblies, 22% were not identified. These protein assemblies might not form sufficiently stable or soluble complexes.[25]

1.3.5 Elucidation of protein structure

The function of a protein is related to its structure. The primary structure of a protein is the peptide chain covalently linked amino acid residues, which can be described as the linear structure. The secondary structure consists of regions of repeating conformations of peptide chain, such as α helices and β sheets. Tertiary structure of a protein refers to the folding of a peptide chain into its native form. Some proteins possess quaternary structure, in which two or more peptide chains associate into a multisubunit protein.[26] Although the dominant information obtained from a MALDI mass spectrum is the molecular weight of the proteins, some structural information can also be derived, such as the quaternary structure of a protein through restricted digestions.[27,28]

In a recent study carried out in our group in collaboration with Dr. Rosemary B. Cornell at the Department of Molecular Biology and Biochemistry at SFU, a multi-domain protein, CTP: phosphocholine cytidylytransferase (CCT), was examined. Due to the cleavage sites dependence on the protein sequence and its native folding, characterization study of the limited proteolysis combined with MALDI-MS was applied in a tertiary structure of CCT. Data to support a quaternary structure based hypothesis regarding the reduced activity of the soluble form of CCT were generated.[28]

1.4 Objectives of research

(1) Characterization of the primary structure of a membrane protein

Detection of a large number of peptides increases the confidence of protein identification based on either peptide mass mapping or database searching. It is also a necessary requirement to enable mapping of the chemical and post-translational modifications on a protein.[9] Membrane proteins are embedded in a cell membrane. They perform several different functions in a cell including to form ion channels, which can transport ion and solute into a cell.[23,29] Analysis of membrane proteins using MALDI is a challenge, due to the hydrophobic properties of the membrane proteins. Membrane proteins tend to aggregate or precipitate in aqueous solution, and they also bind with container walls. Characterization of hydrophobic proteins using MALDI-MS is also a challenge due to solubility, co-crystallization and gas-phase basicity.[30] One major objective of my study was to increase the sequence coverage of a transmembrane protein. The commercially available protein, bacteriorhodopsin, was selected as a model integral membrane protein to study. Chapter 3 describes methodologies for the use of MALDI-MS to provide improved sequence coverage of bacteriorhodopsin.

(2) Investigation the wall-less sample preparation method in hydrophobic peptide detection

The sample preparation process is critical for detection of hydrophobic proteins or peptides. During the co-crystallization process of proteins or peptides with matrix, the hydrophobic proteins or peptides tended to segregate from matrix.[31] This segregation often results in poor analytical performance using MALDI-MS.[32,33] Our assumption was that the rapid evaporation could increase the number of hydrophobic proteins and

peptides in the co-crystallized solid by reducing the extent of hydrophobic protein and peptide segregation. The MALDI signal of hydrophobic proteins or peptides could then be detected or increased. Therefore, the sequence coverage of hydrophobic proteins could be improved.

For reference, the conventional dried-droplet sample preparation method requires several minutes to form a co-crystallized sample. The wall-less sample preparation method provides rapid co-crystallization within seconds. Therefore, we applied the wall-less sample preparation method in a study to increase the hydrophobic peptide detection using MALDI-MS. The results of primary sequence coverage for bacteriorhodopsin are discussed and presented in chapter 3.

(3) Identification of chemical modification sites on proteins

Chemical modification on proteins has been widely used to study protein function and structure. The identification of the modification sites is necessary to yield a better understanding of protein conformation changes.[34] Chapter 4 describes the process of characterizing and identifying chemical modification sites on two proteins, one is a hydrophilic protein, pheromone binding protein 2 (PBP2), and the other is a hydrophobic protein, cytochrome $P450_{cam}$ ($P450_{cam}$).

(4) Characterization of ion-channel protein-protein interaction

Identification of unknown proteins in a protein complex can provide information about protein-protein interactions.[25] Potassium voltage-gated ion channel Kv1.5 and its associated proteins from human embryonic cell (HEK293) were characterized by MALDI-MS in this thesis and discussed in chapter 5.

(5) Study of gas-phase cationization in MALDI

Gas-phase cationization is one type of secondary ionization in MALDI. A better understanding of cationization in MALDI could generate new strategies to improve analyte ion yield.[35] The objectives of this study were to (1) provide experimental evidence of the gas-phase cationization, (2) investigate the effect on cationization from the separation distance between neural molecule and cation, and (3) examine the potential application of a gas-phase cationization strategy to improve quantitative performance in MALDI-MS.

CHAPTER 2:PRINCIPLES OF METHODOLOGIES

2.1 Context

This chapter describes the methodologies used to study proteins and peptides in this thesis. These methodologies include matrix-assisted laser desorption/ionization (MALDI), time-of-flight (TOF) mass spectroscopy, and wall-less sample preparation method (WaSP).

2.2 Matrix-assisted laser desorption/ionization (MALDI)

MALDI was developed from the laser desorption ionization (LDI) technique. Since the 1960's, LDI has been used as one of the many possible ion sources for mass spectrometry.[36] This technique is not suitable for analysis of molecules that have low volatility, such as peptides, proteins or nucleic acids. The LDI technique causes fragmentation of such compounds, leading to spectra that are very difficult to interpret for sequence or structural information. In 1988, Japanese scientists Tanaka *et al.*[2] and German researchers Karas and Hillenkamp[37] independently developed a new technique, in which a compound termed a matrix was used to absorb energy from a laser pulse and assist the delivery of low volatility high molecular compounds to gas phase without excess fragmentation. This technique was named as matrix-assisted laser desorption/ionization (MALDI). It is one type of soft ionization technique.

2.2.1 MALDI matrices

MALDI uses a pulsed ultraviolet (UV) or infrared (IR) laser, and the compounds used as matrices are organic compounds with either high UV or IR absorbance, such as benzoic or cinnamic acid derivatives.[27,38,39] The pulsed laser is used to prevent formation of excess fragments of matrix and analyte.[40]

Matrices are essential in the MALDI process.[27] They have three major contributions in MALDI. First, matrices separate analytes from each other in order to minimize their aggregation. The mole ratio of analyte to matrix is about 1:100 to 1:50,000.[27]

Second, a common character of all matrices is their strong absorption at the laser wavelength.[41] The matrix absorbs energy from the laser and transfers it into the solid co-crystallized matrix and analytes. A small amount of matrix and analyte (some molecular layers on the surface of co-crystallized matrix and analyte) quickly change from solid phase into gas phase with laser irradiation.[42] A schematic diagram in Figure 2.1 illustrates some of the processes that take place, beginning with the laser pulse. This phase change of matrix and analyte is a very rapid, even explosive, solid-to-gas phase transition. It is known as MALDI laser induced plume.[43] After nanosecond laser pulses, significant expansion of the plume is observed for tens of nanoseconds.[44] In order to characterize the shape of MALDI laser induced plume, initial velocities of matrix and analyte, in the plume has been characterized using laser induced fluorescence (LIF).[43,45]

Third, matrices participate in the ionization process. The process is complex and discussed in the following section.

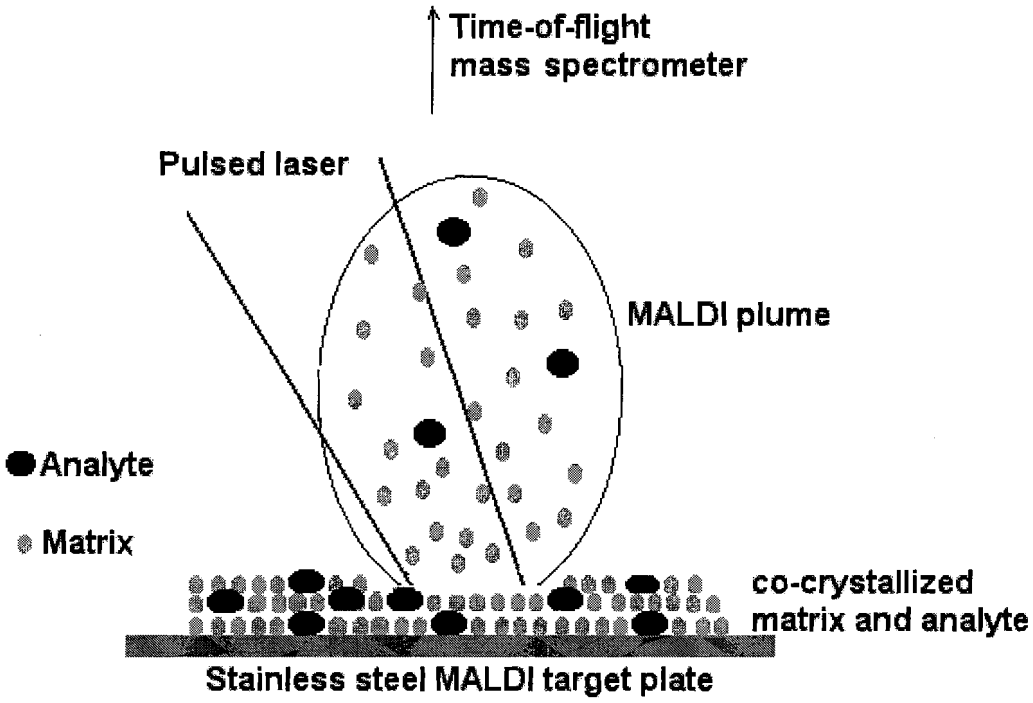

Figure 2.1 **Schematic diagram of MALDI. The co-crystallized matrix and analyte change to gas state from solid state upon laser irradiation.**

2.2.2 MALDI ionization

MALDI ionization has two mechanisms, primary ionization and secondary ionization. The primary ionization happens during the laser pulse. For example, the nitrogen UV laser pulsed width is 3-5 ns.[46] The secondary ionization is considered to be a gas-phase reaction, in the MALDI laser induced plume where the ions and neutral molecules collide. The expanded plume typically lasts on the order of tens of nanoseconds.[44,46]

2.2.2.1 Primary ionization

A proposed explanation of what is termed primary ionization is an excited-state proton transfer. The matrix molecule (M) absorbs one photon leading to the excited-state

(M*) (Equation 2.1). The excited matrix molecule (M*) transfers a labile proton in a collision to an analyte (A) before the excited molecule relaxes (Equation 2.2).[44]

$$M + hv \rightarrow M^* \qquad (2.1)$$

$$M^* + A \rightarrow (M-H)^- + AH^+ \qquad (2.2)$$

2.2.2.2 Secondary ionization

The secondary ionization takes place at the MALDI laser induced plume. The plume is an explosive solid-to-gas phase transition. Two major secondary ionisation reactions are gas-phase proton transfer and gas-phase cationization.[44,46,47]

(1) Gas-phase proton transfer

A protonated matrix molecule, formed at the primary ionization step, transfers a proton from matrix to an analyte molecule, such as a peptide or protein (Equation 2.3).[40,41,46] Proteins and peptides are detected predominantly in protonated form in MALDI.

$$MH^+ + A \rightarrow M + AH^+ \qquad (2.3)$$

(2) Gas-phase cationization

Cation adducts are often observed in MALDI, especially when the analytes are synthetic polymers. Cationized proteins or peptides are also observed in MALDI mass spectra.[27,48] The cation adducts of synthetic polymers are the dominant ion signals in

MALDI-MS, because their cation affinities are much higher than their proton affinities.[44,46,47] The synthetic polymers are favourable to form cation adducts rather than being protonated. The cations are typically sodium or potassium ions. These cations exist as impurities in sample, glassware and plastic ware and on MALDI target plates. Equations 2.4 and 2.5 show the cation reactions.

$$A + Na^+ \rightarrow (A + Na^+) \qquad (2.4)$$

$$A + K^+ \rightarrow (A + K^+) \qquad (2.5)$$

2.3 Time of flight mass spectrometer (TOF)

MALDI is normally combined with a time of flight (TOF) mass spectrometer, although other types of mass spectrometers can be interfaced to MALDI. The mass of an ion can be measured by using its flight time in TOF. Ions are accelerated to a fixed kinetic energy by an electric potential. The velocity of an ion is proportional to its $(m/z)^{-1/2}$, where m/z is the mass-to-charge ratio.[27] The ions pass through a field free flight tube, each travelling with a velocity characteristic of its mass to charge ratio. A detector at the end of the flight tube will produce a signal as an ion strikes at it. The arriving time of an individual ion at the detector is proportional to $(m/z)^{-1/2}$, and therefore accurate measurement of an ion's flight time can be used to calculate its mass to charge ratio.[27]

Two modes of time-of-flight mass spectrometers are in use, linear and reflectron (Figure 2.2).

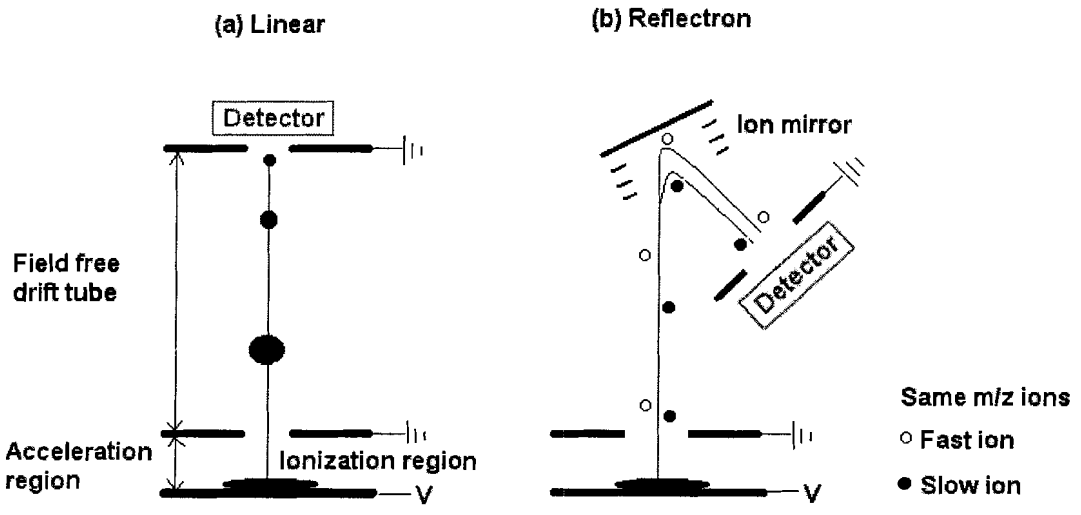

Figure 2.2 **(a) Linear and (b) reflectron time-of-flight mass analyzers coupled with MALDI. (Not drawn to scale and adapted from reference).[27]**

2.3.1 Linear time-of-flight mass spectrometer

A linear time-of-flight mass spectrometer is the least complex mass spectrometer. The ions are accelerated to a fixed kinetic energy by an electric potential, typically 1-30 kV (positive or negative polarity).[27] The length of the acceleration region is usually less than 1 cm.[27]

The accelerated ions enter a field-free drift tube and strike a detector at the end of the tube. The flight path ranges from 0.01 to 2 m in length.[27] Ions with different m/z travel with different velocities and arrive at the detector at different times. Typical flight times are between a few μs to several 100 μs.[42] Therefore, the mass of an ion can be determined through calculation of flight time of standard ions.[49]

Mass resolution (R) is an important parameter used to measure the instrument's capacity for signal separation between two similar masses, M_1 and M_2 (Equation 2.6).[27]

$$R = \frac{M}{\Delta m} \qquad (2.6)$$

Where M is the observed mass, Δm is the difference between two masses that can be separated.

The mass resolution can also be expressed by using full-width-at-half-maximum intensity (FWHM) as Δm.[49] The mass resolution is then expressed as Equation 2.7.

$$R = \frac{M}{FWHM} \qquad (2.7)$$

Another important parameter to measure the performance of the mass spectrometer is the mass accuracy. Mass accuracy is a measure of the error involved in assigning a mass to a given ion signal.[49] It is expressed as Equation 2.8.

$$accuracy = \frac{(M_o - M_t)}{M_t} \times 10^6 \qquad (2.8)$$

Where M_o is the mass observed, M_t is the theoretical mass. The mass accuracy is reported in parts per million (ppm).

A resolution of ~ 1,000 and a mass range up to 350 kDa are possible in linear TOF mass spectrometry.[12,50]

2.3.2 Reflectron time-of-flight mass spectrometer

One disadvantage of the linear mode of time-of-flight mass spectrometry is its relatively low mass resolution and mass accuracy. In order to distinguish the isotopic peaks of ions, higher mass resolution and mass accuracy are required. During the ionization process, the initial velocities and positions of the ions in the acceleration field are not the same, ions with the same mass to charge ratio (m/z) enter the field-free drift tube at different times with different velocities. This initial velocity distribution contributes directly to increaed peak width and decreased mass resolution of a single ion species.[27]

In order to improve the mass resolution, an ion mirror is added at the end of the flight tube (Figure 2.2b). The ions are stopped in the electric deceleration field and their flight direction is reversed. For ions with the same mass, the ones with higher velocity are travelling faster and enter the ion mirror sooner. Because of their higher velocity, they have higher energy and penetrate deeper into the ion mirror before they stop and turn around, so they spend more time within the ion mirror. The ions with lower velocity enter the ion mirror later, and do not penetrate as far as those with higher velocity, so they spend less time in the ion mirror. If the voltage of the ion mirror is adjusted properly, ions of the same mass travelling at different velocities will arrive at the detector at the same time. In other words, the initial velocity distribution can be corrected, which can reduce the peak width and increase the mass resolution.[27]

For example, the peptide angiotensin I (theoretical monoisotopic m/z = 1296.6833) is used to demonstrate the difference of mass resolution between linear and reflectron TOF mass spectrometers.

The MALDI-TOF-MS (Waters Corp., Milford, MA) in the Agnes laboratory was calibrated by using a mixture of three peptides, bradykinin fragments (2-9), renin and adrenocorticotropic hormone (ACTH) fragment 18-39 with their respective theoretical m/z of 904.4667, 1758.9303 and 2465.1949. Before calibration, the observed m/z value of agniotensin I was 1296.5895 with mass resolution of 5140 and mass accuracy of –72.3 ppm calculated by using Equation 2.7 and 2.8. Figure 2.3 is the mass spectra of angiotensin I obtained after calibration in the Agnes laboratory. Figure 2.3a is the linear time-of-flight mass spectrum of angiotensin I. Its isotopic peak distribution is not resolved. The monoisotopic peak of angiotensin I (m/z=1296.6802) is however very clearly separated from other isotopic peaks using the reflectron TOF mass spectrometer, its FWHM is 0.2469 (Figure 2.3b). In this specific example, the mass resolution increases 30 fold, from 171 using linear TOF, to 5250 using reflectron TOF. The mass accuracy of the monoisotopic peak of angiotensin I is –2.4 ppm in the reflectron TOF (Figure 2.3b).

The maximum resolution achieved in the reflectron TOF mass spectrometer is ~35,000 and the mass range up to 12 kDa.[27,50] All experiments in this thesis are performed using the reflectron mode TOF. And the typical mass resolution are 5,000 to 10,000 when the mass range (m/z) < 4000.

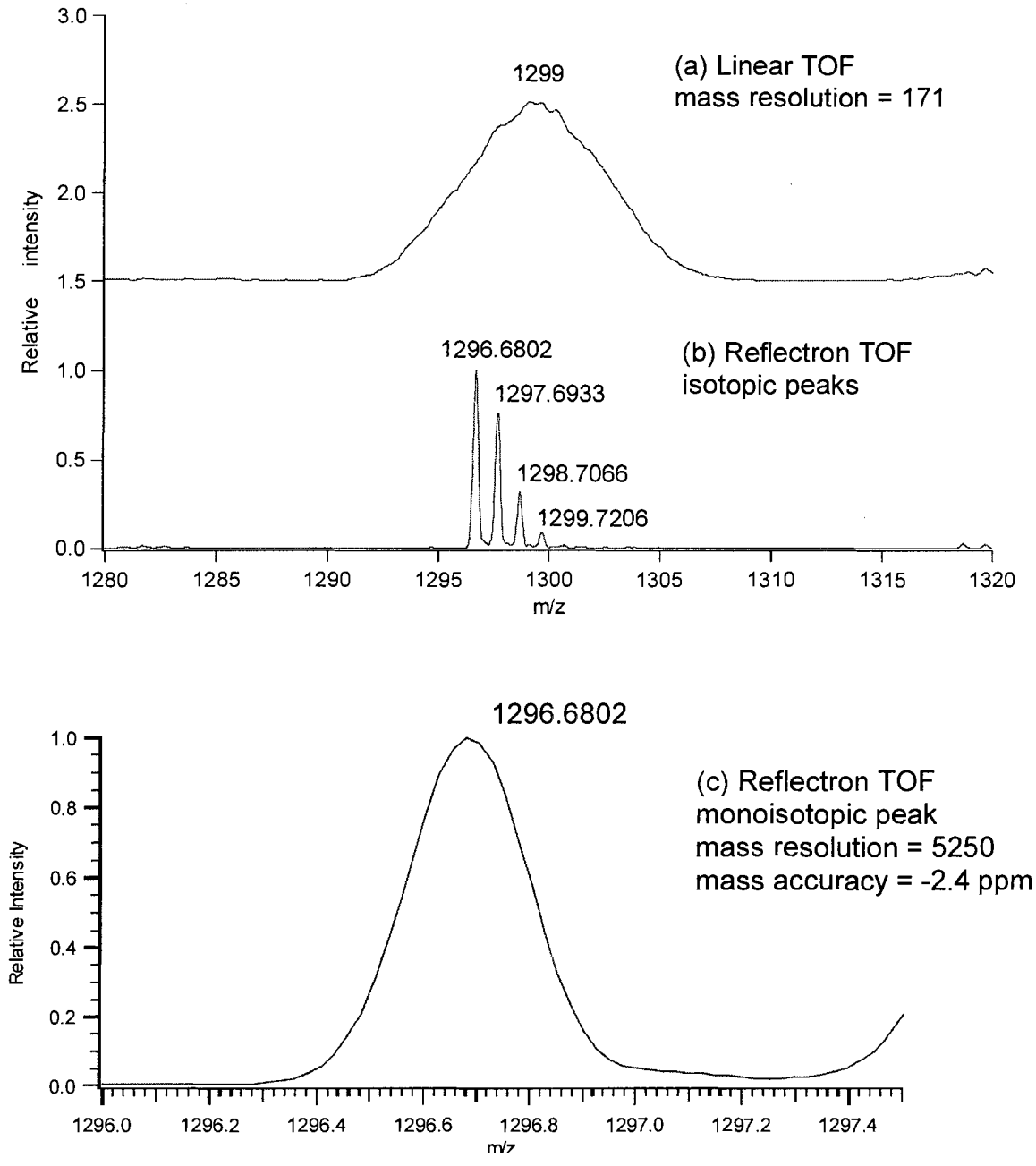

Figure 2.3 **MALDI mass spectra of peptide angiotensin I obtained in the Agnes laboratory. (a) using linear MALDI-TOF-MS, (b) using reflectron MALDI-TOF-MS and (c) the monoisotopic peak zoom in from (b) using reflectron mode.**

2.4 Wall-less sample preparation method (WaSP)

The methodology of the wall-less sample preparation (WaSP) has been developed and reported by our group.[51,52] The off-line sample preparation method has advantages

over the conventional MALDI sample preparation methods, such as the dried-droplet method. The dried-droplet method involves direct deposition of 1-2 μL of a solution containing analyte and matrix on a MALDI target plate using a pipette and allowing the "droplet of sample" to air-dry (several minutes) at room temperature.[37] This section provides an overview of the current status of the wall-less sample preparation method, and an introduction to how it was used in this thesis.

2.4.1 Apparatus of wall-less sample preparation

The main components of the wall-less sample preparation apparatus include an electrodynamic balance (EDB) positioned within a chamber and a piezoelectric droplet dispenser.[51,52] A schematic diagram of the wall-less sample preparation apparatus is presented in Figure 2.4. Droplets of an appropriate mass to net charge ratio can be levitated in the electrodynamic balance.

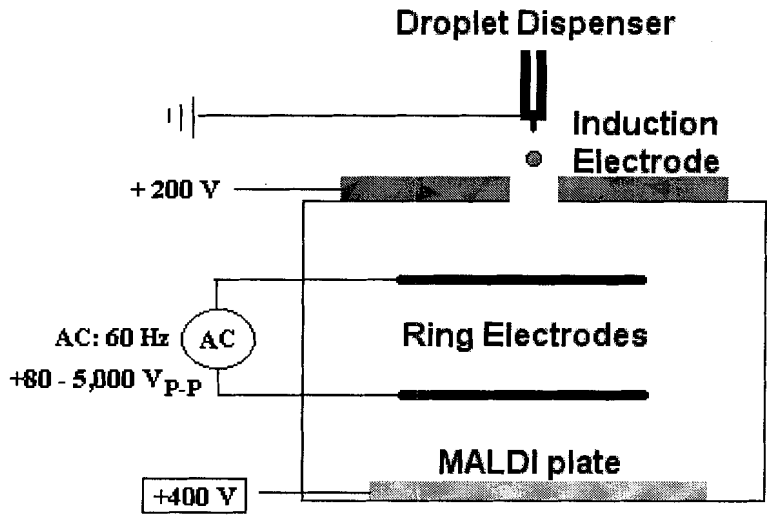

Figure 2.4 **Schematic diagram of wall-less sample preparation apparatus. The potential on MALDI plate is only shifted on when the droplets are deposited on plate. (Not drawn to scale).**

In brief, a piezoelectric droplet dispenser (model MJ-AB-01-40, Microfab Technology Ltd., Plano, TX) with a 40 μm diameter orifice was used to dispense the droplets. A DC potential of 200 V was applied to the induction electrode, which established a positive electrical field between the nozzle of dispenser and the induction electrode. The induction electrode has a 2 mm diameter hole that is aligned directly below the orifice of the droplet dispenser. Droplets were directed through the hole in the induction electrode and into the ring electrodes. Ring electrodes with 2 cm diameter were fabricated from copper wire. The two copper wire ring electrodes were mounted parallel at a separation distance of 6 mm. An AC potential (60 Hz, 80-5.000 V_{p-p}) was applied to the ring electrodes, which established an AC electric field necessary to levitate the charged droplets. Another DC potential of 400 V was applied to the MALDI target plate to effect droplet position. The induction electrode, the two ring electrodes and the

MALDI sample deposition plate are enclosed in a plexiglass chamber in order to minimize air convection currents. A 4 mW green HeNe laser (Uniphase model 1676, Manteca, CA) was used to illuminate the levitated droplets by light scattering.

2.4.2 Sample droplet levitation

An aliquot, ~10 μL, of a starting solution was loaded into the droplet dispenser. An example of a starting solution used in this thesis consisted of protein digestion, a MALDI matrix and 1% glycerol in acetronitrile. Droplets were created at 1 droplet per second from the droplet dispenser. The droplets passed through the hole in the induction electrode. A net negative charge was imparted onto each droplet during its formation by the electric field between the solution emerging from the nozzle at ground of the droplet dispenser orifice and the induction electrode, because a DC potential was applied to the induction electrode. The charged droplets flew toward the centre of the ring electrodes where they were trapped and levitated by the time dependent electrical field. For droplet deposition, the droplets were pulled down and deposited on the MALDI plate by applying a positive potential on the MALDI plate.

2.4.3 Features of wall-less sample preparation for MALDI-MS

Wall-less sample preparation methodology has been used to prepare MALDI-MS samples,[28,53-56] to enable the study of air particles effect on lung cells[57-59] and ion-induced nucleation.[60,61] This method has the following features: sample pre-concentration prior to deposition onto a MALDI plate,[52,54] femtomole detection limits,[54] reduced background ion signal in MALDI mass spectra[54] and an increased peptide signal-to-noise ratio (S/N) in MALDI.[56]

(1) Capable of preparing picoliter aliquots of sample material with deposition onto a substrate as μm- size sample spots.

The average initial volume of the droplets dispensed is nominally 300 ± 20 pL, which was determined using liquid scintillation.[56] Multiple droplets can be deposited one on top of another to increase sample loading. The detection limit for MALDI-MS from these sample spots was as low as the attomole range.[54]

(2) Sample preconcentration prior to deposition on the MALDI plate

The volume of each droplet was reduced before it was deposited onto the sample plate. This enables the concentration of analyte to be increased 10 to 1000 times relative to the dried-droplet method.[55] Table 2.1 summarizes the various analyte densities in sample spots using dried-droplet or wall-less sample preparation method.[55]

Table 2.1 Analyte densities for various MALDI sample preparation methods.[55]

Sample preparation	Volume consumed (μL)	Spot radius (μm)	Spot area (μm^2)	Analyte concentration (M)	# of molecules in spot	Analyte density (molecules/ μm^2)
Dried-droplet	1.00	1000	3.14×10^6	1×10^{-9}	6.02×10^8	192
WaSP 1 droplet	3×10^{-4}	10	314	1×10^{-9}	1.81×10^5	575
WaSP 50 droplets	0.015	50	7850	1×10^{-9}	9.03×10^6	1150
WaSP 100 droplets	0.030	50	7850	1×10^{-9}	1.81×10^7	2301

WaSP: wall-less sample preparation. Droplets were deposited one on top of another one.

The process of solvent evaporation from μL aliquot of solution on a MALDI plate typically required a few minutes by dried-droplet method. In the wall-less sample preparation method, the solvent evaporation in levitated droplets was already complete

within seconds.[56] This is attributed to surface area to volume ratio and the movement of levitated droplets within the electric field.

(3) Promotion of matrix CHCA and peptide co-crystallization

The ion signal-to-noise ratio of peptide adrenocorticotropic hormone fragment 18-39 (ACTH 18-39) increased in MALDI-MS relative to the dried-droplet sample preparation method.[56] Droplets with higher net charge were found to yield more matrix/peptide precipitates than droplets with lower or no net charge.[56]

CHAPTER 3:
TOWARDS IMPROVING MEMBRANE PROTEIN SEQUENCE COVERAGE

3.1 Context

This chapter describes some approaches for improving the sequence coverage of membrane proteins as measured using MALDI-MS. We chose to study a commercially available transmembrane protein, bacteriorhodopsin. Some common detergents, MALDI matrices and wall-less sample preparation were investigated for their influence on the detection of the peptides of bacteriorhodopsin generated by enzymatic digestion. Diem Ly Van, a graduate student in the Agnes group, and an undergraduate co-operative student, Teresita M. Cruz Sanchez, performed the wall-less sample preparation.

3.2 Abstract

Complete sequence coverage would be an ideal situation for protein identification, characterization of post-translational or chemical modifications. The objective of this study was to develop robust methods for improving membrane protein sequence coverage using common enzymes to digest the protein followed by peptide detection using MALDI-MS. Bacteriorhodopsin was used as a membrane protein study model. A detergent solution of sodium dodecyl sulfate (SDS) at a concentration of 0.08 mM was found to be compatible with MALDI-MS as indicated by an increased number of peptides detected. The relative less polar compounds α-cyano-4-hydroxycinnamic acid (CHCA) and sinapinic acid (SA) were used as matrices and higher sequence coverage of

bacteriorhodopsin was both observed relative to another hydrophilic matrix 2,5-dihydroxybenzoic acid (DHB). The wall-less sample preparation method combined with conventional dried-droplet method yielded a modest increase in sequence coverage to 89% from the conventional dried-droplet sample preparation of 81%. As we know, this is the first report on the sequence coverage of bacteriorhodopsin using MALDI-MS.

3.3 Introduction

3.3.1 Membrane protein

Membranes are essential to a cell. They provide a physical barrier between a cell and its environment. The membranes mainly consist of bi-layered lipids and embedded proteins. The outer surface of the membrane is hydrophilic, and the inner is hydrophobic. The integral membrane proteins are amphipathic with two hydrophilic regions on each side of the lipid bilayer, and hydrophobic transmembrane segments in the inner hydrophobic region of the membrane.[62]

Membrane proteins perform many functions in a cell, such as cell signalling (e.g. G protein coupled receptors), cell-cell interactions (integrins and adhesion proteins), intracellular compartmentalization (kinase-anchoring proteins), ion and solute transport (ion channels and porins), and energy generation (Adenosine Triphosphate (ATP) syntheses).[63,64] A number of diseases including diabetes and neurological disorders are directly attributed to abnormality of membrane proteins.[63] Currently membrane proteins account for ~70% of all pharmaceutical drug target studies.[64]

Membrane proteins are not soluble in aqueous solutions. It is more challenging to study membrane proteins compared with soluble proteins. For instance, more than 24,000

soluble proteins and their structure are known, while the structure of only ~80 membrane proteins are known.[63]

In this study, a transmembrane protein bacteriorhodopsin was chosen as a model protein for MALDI method development and comparison.

3.3.2 Bacteriorhodopsin

The integral membrane protein bacteriorhodopsin (BR) (molecular weight 26 kDa) is embedded in the purple membrane from *Halobacterium salinarium*.[65,66] Bacteriorhodopsin functions as a light-driven proton pump. A photosensitive pigment, retinal, is bound covalently to lysine residue (K216) of bacteriorhodopsin. When the bound retinal absorbs a photon, retinal isomerises from E to Z. An outcome of this process is that a proton is pumped from the cytosol of the cell to the extracellular environment. This process also results in a pH gradient in the membrane, leading to ion and molecule transportation and ATP generation.[62,67,68]

Bacteriorhodopsin is a very hydrophobic protein. It has low solubility in aqueous solution. Henderson and Unwin characterized its seven transmembrane α-helices by using electron microscopy with a resolution of 7 Å in 1975.[69] Figure 3.1 displays the crystal tertiary structure of bacteriorhodopsin as viewed from two different perspectives.[70]

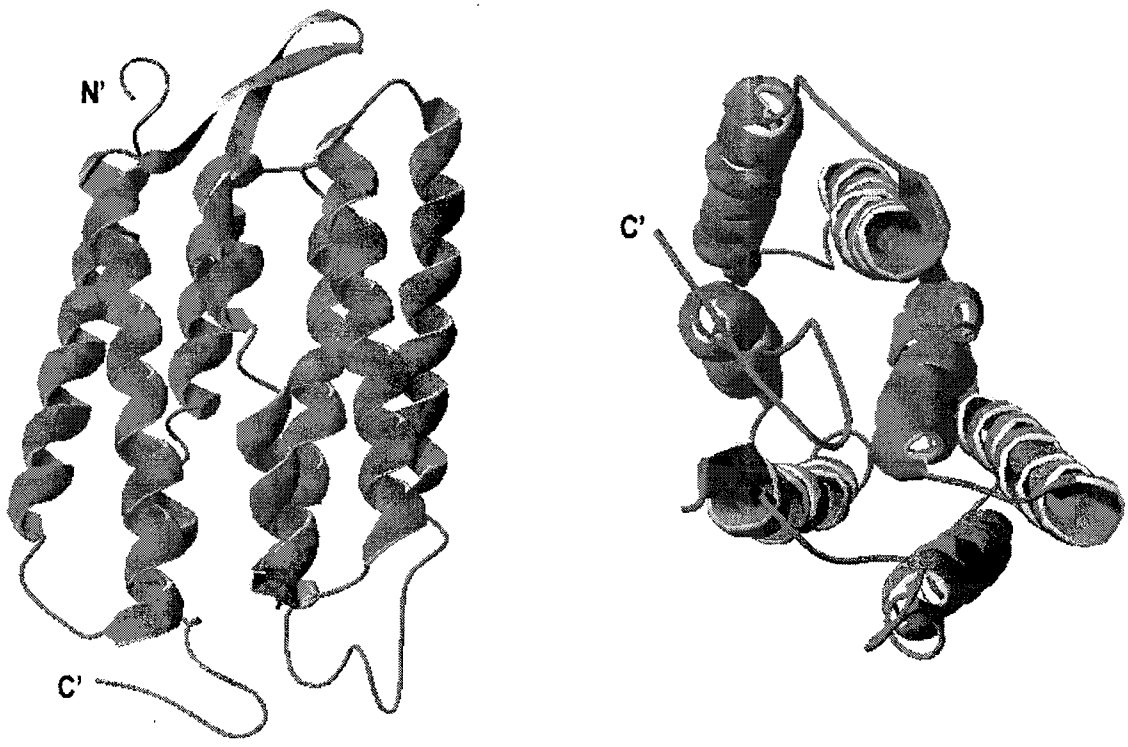

(a) Side View (b) Top view

Figure 3.1 **Crystal structure of bacteriorhodopsin.[70] (a) Side view, (b) top view. N' and C' stand for N-terminus and C-terminus respectively.**

3.3.3 Approaches to improving sequence coverage of bacteriorhodopsin

High sequence coverage is desired for reliable protein identification, good peptide mass mapping, and effective identification of post-translational or chemical modification sites. Besides bacteriorhodopsin, a soluble protein, myoglobin, was studied as an example of hydrophilic proteins. Hydrophilic proteins and peptides tend to be more readily detected by MALDI-MS. In our study, the complete sequence coverage (100%) of myoglobin was obtained in our laboratory.

The characterization of hydrophobic proteins, including membrane proteins, is problematic when using MALDI-TOF-MS. The membrane proteins are prone to

aggregate or precipitate in aqueous solution, they bind strongly to container walls, and they do not readily co-crystallize with the polar organic acid compounds commonly used as a matrix for MALDI.[30]

Recent MALDI-MS methodologies to improve the detection sensitivity of membrane proteins include: (1) fabricating a MALDI target plate that has a coating of a hydrophobic silicone polymer,[33] (2) digesting in-gel (SDS gel) with trypsin followed by cyanogen bromide (CNBr) cleavage,[71,72] (3) adding enzyme-friendly surfactants,[73,74] (4) applying common surfactant and utilizing a two-layer sample preparation strategy,[9] (5) using an organic solvent as a buffer,[75] (6) coupling liquid chromatography with mass spectrometry,[76,77] (7) manipulating temperature to improve solubility.[78] Most of this research was performed using bacteriorhodopsin as a model. A 97% sequence coverage of bacteriorhodospin was reported by Yu *et al.* when they combined the results together using MALDI-MS and using ESI-MS.[74] The sequence coverage of bacteriorhodopsin from MALDI was not clear in their paper. In addition, no sequence coverage obtained by MALDI-MS was reported in the above mentioned published papers, possibly due to the difficulty in obtaining high sequence coverage of bacteriorhodopsin by MALDI-MS.

The objective of our study was to develop a general method for characterizing the entire primary sequence of an integral membrane protein from a common enzyme digest. We believe that the sample preparation is critical for detection of hydrophobic peptides using MALDI. Factors including peptides solubility, evaporation rate of solvent and homogeneity of co-crystallized matrix and peptides were considered. The detergents and their compatibility with MALDI, polarity of MALDI matrices and a novel sample

preparation method termed as wall-less sample preparation method (WaSP) were investigated.

3.3.3.1 Detergents used to solubilize membrane proteins

One strategy to improve the solubility of hydrophobic proteins is through the addition of detergents. Detergents are used to solubilize hydrophobic proteins or peptides, reduce protein or peptide aggregation and minimize sample loss to containers. Detergents however can adversely affect the ion signal intensity of these proteins or peptides in MALDI-MS. Ionic detergents also can form ion adducts of analyte and matrices, leading to reduced analyte ion signals, lower mass resolution and mass accuracy.[9] The effect of detergents to MALDI depends not only on the type of detergents but also on the concentration of detergent. An anionic detergent, sodium dodecyl sulfate (SDS), and a non-ionic detergent, octyl-β-D-glucopyranoside (OG), were investigated at their 10% critical micelle concentration (CMC). CMC is the concentration of a detergent in solution at which the formation of micelles in the solution is initiated.[79] Table 3.1 summarized some of the properties of these two detergents.

The addition of detergent can have a negative impact on enzyme activity because the detergent can denature the enzyme.[74] The effect of detergent on protein digestion and on MALDI-MS, was performed by adding detergents before and after the digestion was allowed to proceed to completion.

Table 3.1 Detergents studied in this work and their critical micelle concentrations (CMC) in aqueous solution. [9]

Detergents	Type	Structure	CMC
Sodium dodecyl sulfate (SDS)	Anionic	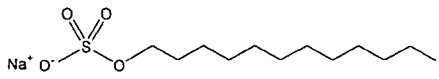	8 mM
Octyl-β-D-glucopyranoside (OG)	Non-ionic	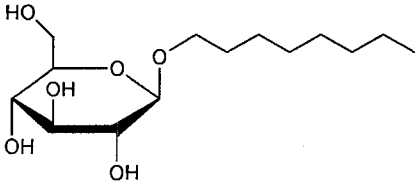	25 mM

3.3.3.2 Polarity of MALDI matrices

As described in chapter 2, matrices play a very important role in MALDI-MS. They isolate analyte in solution and in the solid phase by co-crystallization, absorb energy from laser and participate in the analyte ionization processes. The question in this study was whether the polarity of matrices is a factor in the detection of hydrophobic proteins and peptides using MALDI-MS. Our hypothesis is that matrices with lower polarity could be better suited for detection of hydrophobic proteins and peptides by MALDI-MS.

Three most commonly used matrices for proteins or peptides detection are α-cyano-4-hydroxycinnamic acid (CHCA), sinapinic acid (SA), and 2,5-dihydroxybenzoic acid (DHB). Their structure and some of their properties are presented in Table 3.2. Their influence on detection of hydrophobic peptides digested from bacteriorhodopsin were compared.

Hoteling and Owens have established a method to measure the relative polarity of compounds used as matrices by using a reverse-phase high-performance liquid

chromatography (HPLC) technique.[80] The authors used an HP1090 liquid chromatography with a YMC ODS-AQ (Waters Corp., Milford, MA) column (3.0 × 100 mm). A binary mobile phase was applied: mobile phase A is 0.1 M ammoniumacetate buffer (pH = 4.65) and mobile phase B is tetrahydrofuran. The gradient conditions started at 10% B, ramped to 100% B in 10 min, then held at 100% B for 1 min.[80] The HPLC separation of matrices was based on partitioning processes and the separation revealed the relative polarity character. The results showed that elution order of matrices was DHB first, followed by CHCA, then SA. This suggested that the polarity order was DHB > CHCA > SA.[80]

In this study, the sequence coverage of bacteriorhodopsin detected by different matrices was compared in order to find out whether the relative polarity of matrices contributed to improved sequence coverage of hydrophobic protein.

Table 3.2 **Matrices studied in this work.[27] *The HPLC retention time of matrices are from Hoteling and Owens method.[80] The circle in the photography is the sample well on a MALDI target plate. The diameter of the sample well is 3 mm.**

Name	Structure	Crystal morphology	HPLC retention times* (min)	Polarity
3,5-Dimethoxy-4-hydroxycinnamic Acid (Sinapinic Acid, SA)	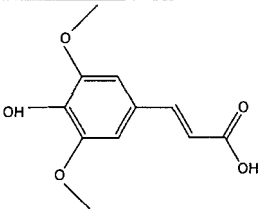	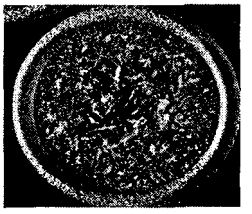	4.12	+
α-Cyano-4-hydroxycinnamic Acid (CHCA)	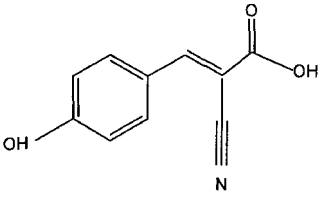	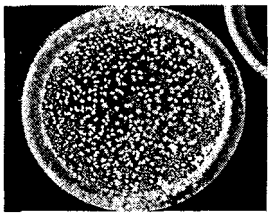	3.11	+
2,5-Dihydroxybenzoic Acid (DHB)	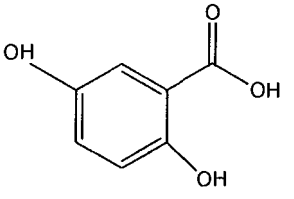	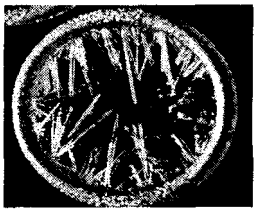	1.64	++

3.3.3.3 Wall-less sample preparation method

The hydrophobic proteins or peptides tend to segregate from the matrix during the co-crystallization process.[31] The segregation has been argued to be a reason for low ion intensity for hydrophobic peptides by MALDI-MS.[32,33] The solvent evaporation rate was assumed to be a factor related to the segregation of hydrophobic proteins or peptides. Fast solvent evaporation leads the hydrophobic proteins or peptides better co-crystallize with the matrix before allowing for segregation from the matrix.

The wall-less sample preparation method (WaSP) developed in the Agnes group has been shown to increase the ion signal intensity of a hydrophilic peptide, ACTH 18-39.[56] The solvent evaporation rate in the levitated droplets was estimated to be a few seconds.[55,56] We applied this WaSP method to study hydrophobic bacteriorhodopsin peptides, and then compared the results with that from the dried-droplet method, in which the solvent evaporation takes place within minutes.

We noted the wall-less sample preparation method is not applicable to DHB. The diameter of the orifice of the droplet dispenser was as small as 40 μm and DHB formed relatively large crystals rapidly that blocked the orifice of the droplet dispenser. Therefore the performance of DHB was not examined using wall-less sample preparation method.

3.4 Experimental section

3.4.1 Protein digestion

The transmembrane protein bacterorhodopsin was used as a model for a typical hydrophobic protein, and myoglobin was used as a typical hydrophobic protein myoglobin. Bacteriorhodopsin from *Halobacterium salinarium* (90% purity, Sigma), and myoglobin (90% purity, Sigma), were digested separately using the same procedure. One milligram of each protein was separately dissolved in 1000 μL buffer solution (100 mM NH_4HCO_3, 2 mM $CaCl_2$, pH=8). A 30 μL protein aliquot was heated at 95 °C for 3 min in order to thermally denature it. This protein solution was cooled to room temperature, and 3 μL chymotrypsin (Sigma) at concentration of 1 μg/μL in buffer solution (100 mM NH_4HCO_3, 2 mM $CaCl_2$, pH=8), was added. The molecular ratio of protein to

chymotrypsin was 10:1. The mixture of protein and chymotrypsin was incubated at 37 °C for 24 hours.

3.4.2 Addition of detergents

Two detergent solutions of 3 μL (8 mM SDS or 25 mM OG in water) were separately added to one mixture of protein and chymotrypsin prior to digestion, and in another sample the surfactant was added after the digestion completed. The final concentration of surfactant in these solutions was about 0.8 mM for SDS or 2.5 mM for OG, which is 10% of their CMC.

3.4.3 Preparation of matrix solutions

Three common used matrices, CHCA, SA and DHB were examined for their influence on detection of chymotryptic bacteriorhodopsin peptides. Saturated CHCA solution was prepared in a solution of acetonitrile and methanol (v/v = 1:1). Saturated SA solution was dissolved in methanol and 0.1% trifluoroacetic acid TFA solution (v/v = 2:3). DHB solution was 10 mg/mL in methanol and 0.1% TFA solution (v/v = 2:3).

3.4.4 Dried-droplet sample preparation

(1) One microliter of intact protein bacteriorhodopsin solution (1 μg /μL) was mixed with 1 μL of matrix solution (CHCA, SA or DHB) and deposited on a stainless steel MALDI target plate using a 2 μL handheld micropipette. Samples were prepared in duplicate.

(2) One microliter of protein digestion, bacteriorhodopsin or myoglobin, was mixed with 1 μL of matrix solution (CHCA, SA or DHB) and deposited on the MALDI target plate. Samples were analysed in duplicate.

3.4.5 Wall-less sample preparation

A solution of bacteriorhodopsin used for wall-less sample preparation was prepared by mixing 2.5 μL of a digest of bacteriorhodopsin, 25 μL of matrix solution (CHCA or SA), 37.5 μL acetonitrile, 5 μL of 20% glycerol in H_2O, 20 μL H_2O, and 10 μL acetone. An aliquot of the resulting solution was loaded into the droplet dispenser by using a 10 μL pipette. A DC potential of 30 V was applied on the piezoelectric dispenser. The droplets were dispensed at 1 droplet per second. A DC potential of 200 V was used on the induction electrode, AC waveform of 80-5,000 V_{P-P} and 60 Hz was applied on the ring electrodes. The droplets were levitated in the ring electrodes, then deposited on the MALDI plate by applying a potential of 400 V on the plate.

3.4.6 MALDI mass spectrometry

MALDI-MS was performed on a Micromass MALDI time-of-flight mass spectrometer (Waters Corporation, Milford, MA, USA) equipped with a nitrogen UV laser (337 nm, pulse width 2 ns) and a 2.3 m flight path in the reflectron mode, and controlled by MassLynx software vision 3.5 (Waters). The standard operation condition for peptide detection included an accelerating voltage of 15 kV and the ion extraction pulse voltage of 2450 V. All data were acquired using a positive ion reflectron mode.

A stock solution of consisting standard peptide mixture angiotensin I, renin and ACTH 18-39 at a concentration of 1 pmol/ μL was used as the external standard to calibrate the ion flight time in TOF-MS before sample analysis. Chymotrypsin autolysis peaks were used to perform the internal calibration in the mass spectrum.

The mass spectra of peptides were acquired in mass range 700-4000 (m/z), and it is from the sum of 200 random laser shots over sample surface for each sample.

3.5 Results and discussion

3.5.1 Detection of protein bacteriorhodopsin

As a control experiment, the intact protein bacteriorhodopsin was examined, and failed to be detected with any matrix by MALDI-MS. The possible reason is the length of hydrophobic protein is a major factor for detection by MALDI-MS.[15] MALDI-MS is more favourable for lower masses (m/z < 10,000). Increase of molecular weight of a protein or peptide leads to more difficulty in being detected by MALDI-MS.[16] Bacteriorhodopsin has a molecular weight of 26 kDa, and it was not detected using MALDI-MS.

3.5.2 Effects of detergents on sequence coverage

Two commonly used detergents, SDS and OG, were investigated their performance on solubilzing bacteriorhodopsin and effect on MALDI-MS detection. Figure 3.2 shows representative MALDI mass spectra of chymotrypsin digests of bacteriorhodopsin with matrix CHCA using the dried-droplet sample preparation method.

Chymotrypic bacteriorhodospin peptides were observed in all mass spectra using different samples (Figure 3.2). Some peaks, such as m/z= 890.4, 986.6, 1125.6, 1468.7 and 1738.9, appeared at every mass spectrum. But the number of detected bacteriorhodopsin peptides varied with the different sample-handling conditions. The number are respectively 6, 10, 7, 10 and 7 under the conditions of (a), (b), (c), (d) and (e).

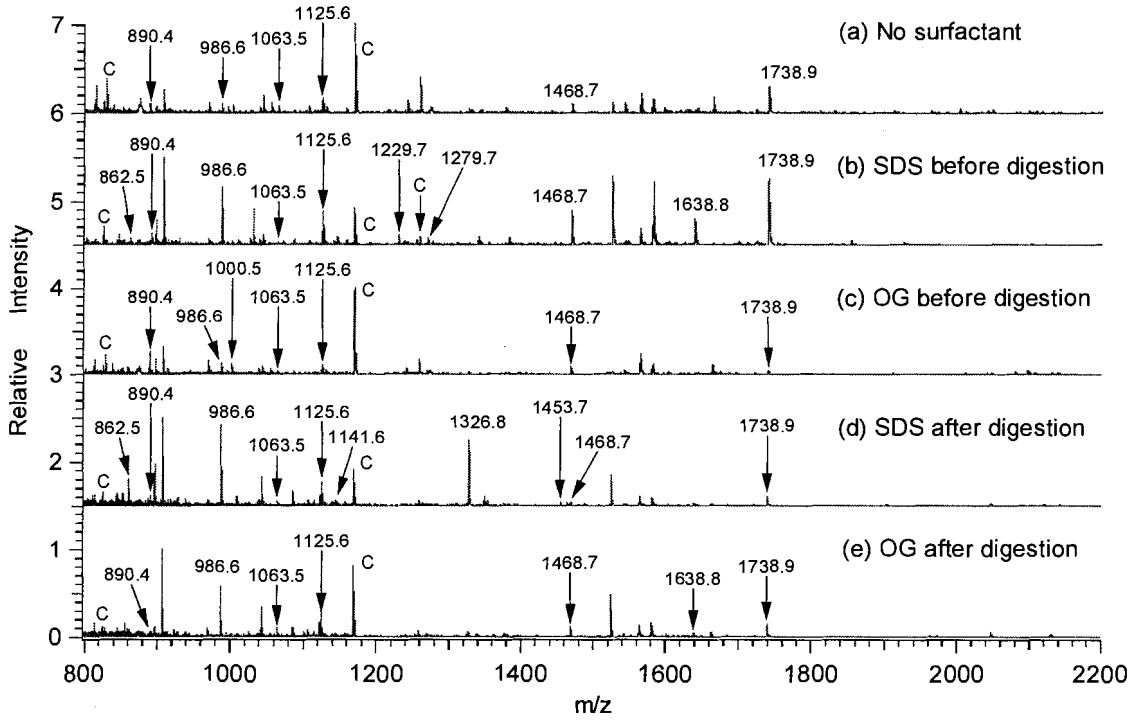

Figure 3.2 **MALDI mass spectra of bacteriorhodopsin chymotrypic peptides using matrix SA and dried-droplet method. (a) no surfactant, (b) SDS added before digestion, (c) OG added before digestion, (d) SDS added after digestion (e) OG added after digestion. Letter C indicates the peak from chymotrypsin autolysis.**

The highest coverage of bacteriohodopsin was 59% with matrix SA, when SDS was added before digestion. Under the same condition, 100% sequence coverage of myoglobin was obtained with SA. The sequence coverage of proteins with matrix SA was summarized in Table 3.3, when detergents added before or after digestion.

Table 3.3 **Summary of sequence coverage of proteins with different detergents using the dried-droplet sample preparation method with matrix SA. BR is bacteriorhodopsin.**

Protein	(a) No detergent	(b) SDS before digest	(c) OG before digest	(d) SDS after digest	(e) OG after digest	(f) Combination of (a)(b)(c)(d)(e)
BR	42%	59%	29%	49%	41%	80%
Myoglobin	73%	100%	81%	90%	81%	100%

The sequence coverage of bacteriorhodopsin containing SDS increased to 59% for adding SDS before digestion from the 42% sequence coverage without SDS. The SDS-containing samples (SDS added before digestion and SDS added after digestion) showed they had higher sequence coverage of bacteriorhodopsin than samples not containing SDS. SDS is an anionic detergent, its hydrophobic tail interacted with protein by hydrophobic interaction, the anionic head of SDS reduced the surface tension of protein, protein then became soluble in water.[79] Therefore, SDS improved the solubility of bacteriorhodopsin and its peptides.

OG is a non-ionic mild detergent,[9] the OG-containing samples did not increase the sequence coverage of bacteriorhodopsin. The possible reason was that OG at low concentration was not strong to solublize this very hydrophobic transmembrane protein bacteriorhodopsin or its peptides.

The total sequence coverage of bacteriorhodopsin using the dried- droplet sample preparation method from the digest containing or not containing detergents was 81%.

As an example for hydrophilic protein, myoglobin was studied. Its sequence coverage improved to 100% at SDS-containing sample from 73% without detergent. This suggested SDS contributed to improved hydrophilic protein sequence coverage. The result is better than that from Zhang and Li, they obtained 96% sequence coverage of myoglobin using trypsin as enzyme. [9]

The full sequence of bacteriorhodopsin, and its detected peptide regions by MALDI-MS from each condition were mapped in Figure 3.3. Each detected bacteriorhodopsin peptide in MALDI mass spectrum was traced back to find out its position in the full sequence of bacteriorhodopsin. For example, the peak with m/z value

of 1738.9 in Figure 3.2 was in the sequence from amino acid position 27 to 42 (FLVKGMGVSDPDAKKF) in Figure 3.3. Mapping the positions from all detected peptides together manually, the detected peptide regions were obtained and shown in Figure 3.3. Some common regions, such as position of 27-42, 55-61, and 67-80, were detected under five different conditions. Some regions, such as position of 16-25, 81-86 and 231-248, were only detected when SDS was added after digestion completion, which indicated that the sequence coverage of bacteriorhodopsin increased in the SDS-containing bacteriorhodopsin sample.

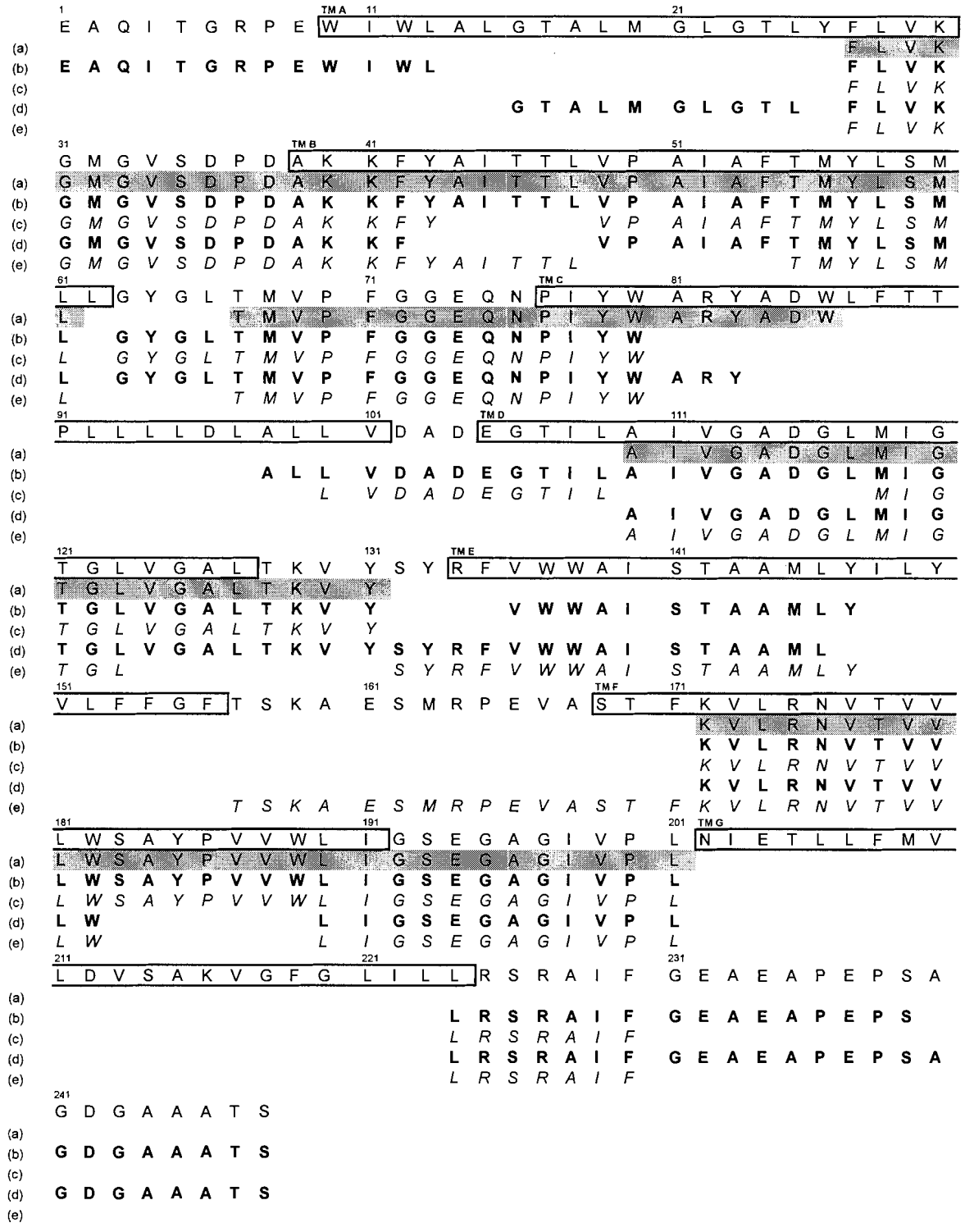

Figure 3.3 **Bacteriorhodopsin sequence[81] and its detected peptide regions with different detergents using dried-droplet sample preparation method. The first row is the full sequence of bacteriorhodopsin with its transmembrane regions (TM) indicated by the rectangular box. Row (a) no detergent, highlighted by grey background. (b) SDS added before digestion, letters in bold. (c) OG added before digestion, letters in italic. (d) SDS added**

after digestion letters in bold. (e) OG added after digestion, letters in italic. (Mapping from using three matrices).

3.5.3 Effects of matrices on sequence coverage

The commonly used matrices CHCA, SA and DHB were examined with the chymotrypic digests of bacteriorhodopsin by using the dried-droplet sample preparation method (Figure 3.4). Common peaks, such as m/z=1063.5, 1738.9, were detected by using any one of the three matrices. The detected peptide number by using matrix SA, CHCA and DHB were respectively 8, 4 and 3.

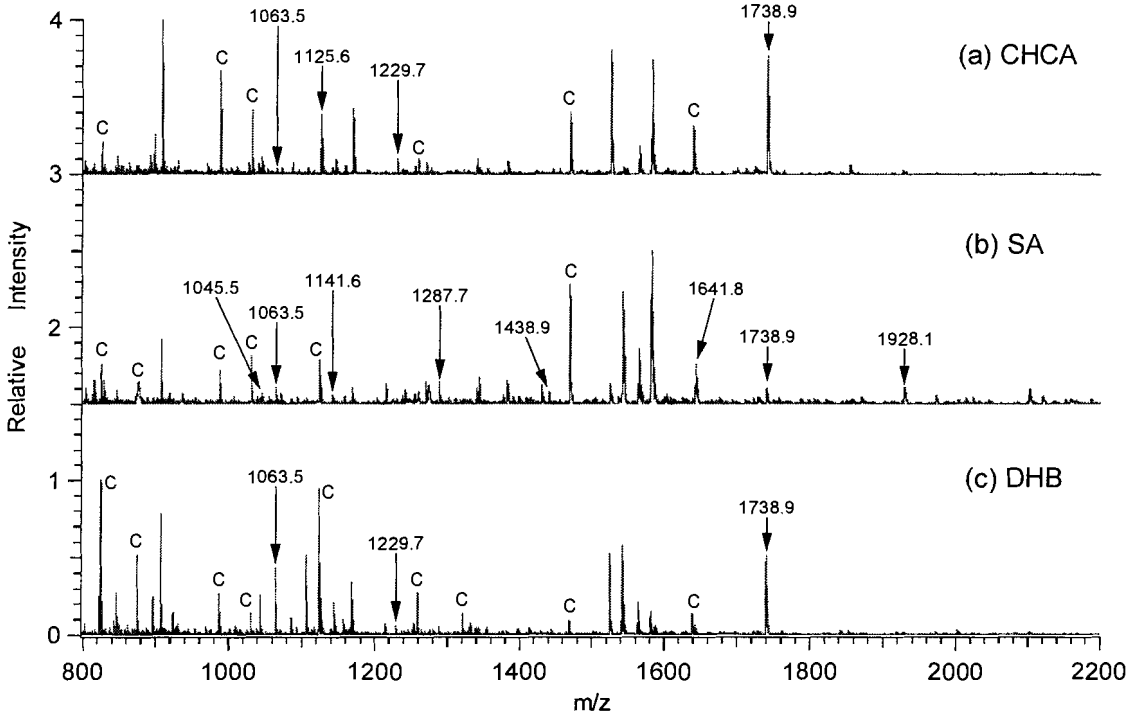

Figure 3.4 **MALDI mass spectra of bacteriorhodopsin chymotrypic peptides using dried-droplet sample preparation method when SDS was added before digestion. (a) using matrix CHCA, (b) using SA, (c) using DHB. Letter "C" indicates the autolysis peak of chymotrypsin.**

Table 3.4 Summary of peptide sequence coverage of proteins with different matrices using dried-droplet sample preparation method when SDS was added before digestion.

Protein	(a) CHCA	(b) SA	(c) DHB	(d) combination of (a) (b) (c)
Bacteriorhodopsin	38%	59%	31%	67%
Myoglobin	79%	100%	86%	100%

Table 3.4 showed the sequence coverage of bacteriorhodopsin detected by MALDI-MS using different matrices. The sequence coverage of bacteriorhodopsin detected by MALDI-MS with matrix SA was 59%. It was higher than that with matrices CHCA (38%) and DHB (31%). The order of the sequence coverage was consistent with the reverse order of polarity of matrices (SA<CHCA<DHB). In other words, the use of the least polar matrix SA obtained the highest sequence coverage, while the most hydrophilic matrix DHB yielded the lowest sequence coverage. The results suggest that the hydrophobic interaction between matrix and peptides is a possible factor for detection of hydrophobic peptides. This interaction between matrix and analytes is consistent with the results from Hoteling and Owens's research on hydrophilic peptides and synthetic polymers.[80,82] They found that the matching the polarity of matrix and a peptide or polymer produced the best MALDI signal intensity. [80,82]

In our study, the least polar matrix SA was found to give highest sequence coverage of hydrophobic protein bacteriorhodopsin. The detected peptides with matrices were presented in Figure 3.5. We found the detected peptide region of bacteriorhodopsin from using matrix DHB was covered by that from using matrix SA. In addition, matrix CHCA only detected three more amino acids at position 59-61 comparing to the detected regions from using SA as matrix.

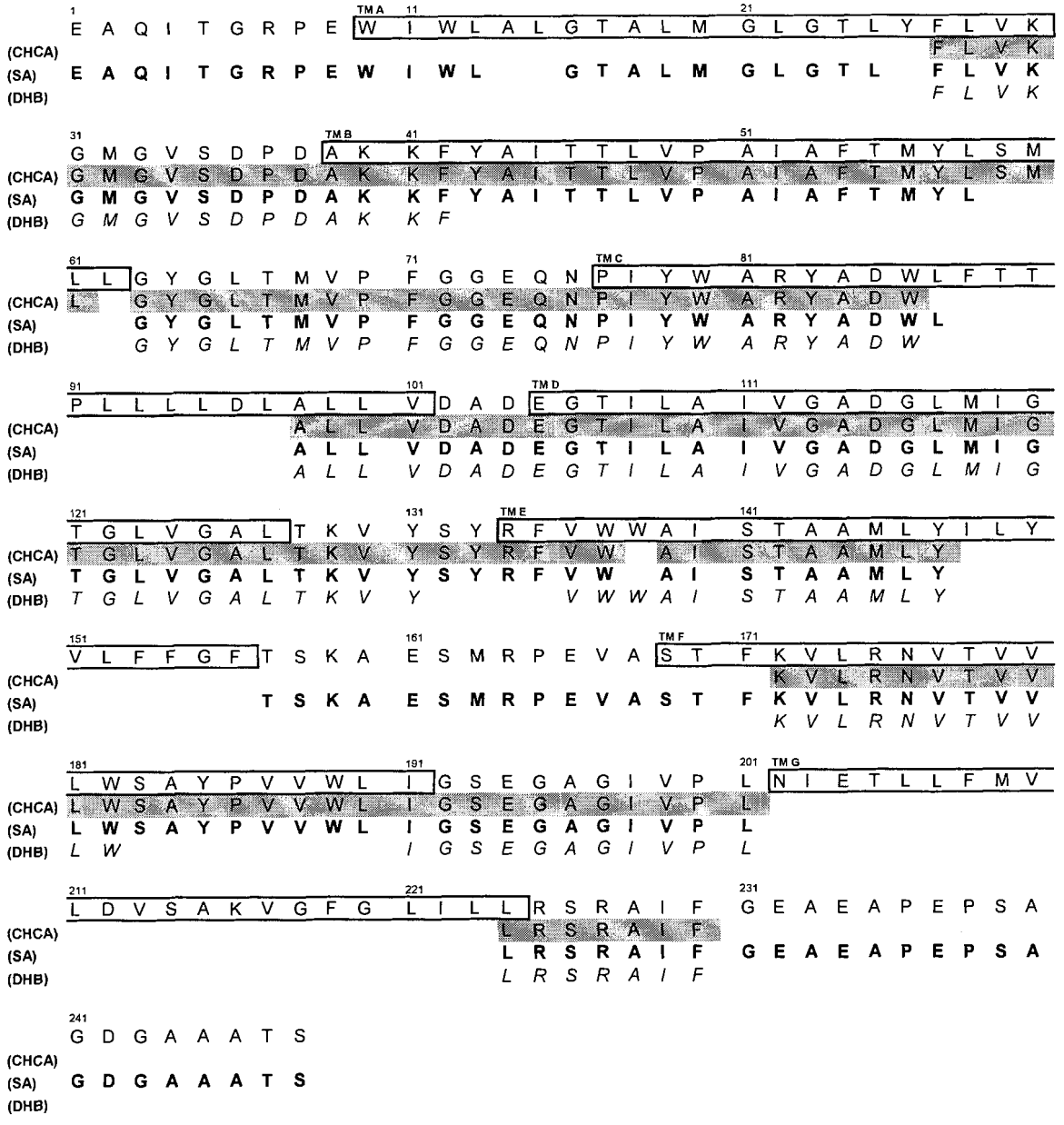

Figure 3.5 **Bacteriorhodopsin sequence and its detected peptide regions with different matrices using dried-droplet method. The first row is the full sequence of bacteriorhodopsin with the transmembrane regions (TM) written with the rectangular box. The second row is using matrix CHCA, highlighted in grey background. The third row is using SA, written in bold. The forth row is using DHB, written in italic.**

The sequence coverage of myoglobin with SA was 100%, higher than that with CHCA or DHB (90%). Myoglobin is a hydrophilic protein, but its polarity is uncertain.

Since SA is a polar matrix, one possible explaination is that the relative polarity of myoglobin and SA are similar.

3.5.4 Effects of wall-less sample preparation method on sequence coverage

The MALDI mass spectra of chymotrypic peptides of bacteriorhodopsin using two sample preparation methods, dried-droplet sample preparation method and wall-less sample preparation method, were obtained in Figure 3.6. Some common peaks, such as: m/z= 1012.5, 1063.5 and 1125.6, were detected by two methods.

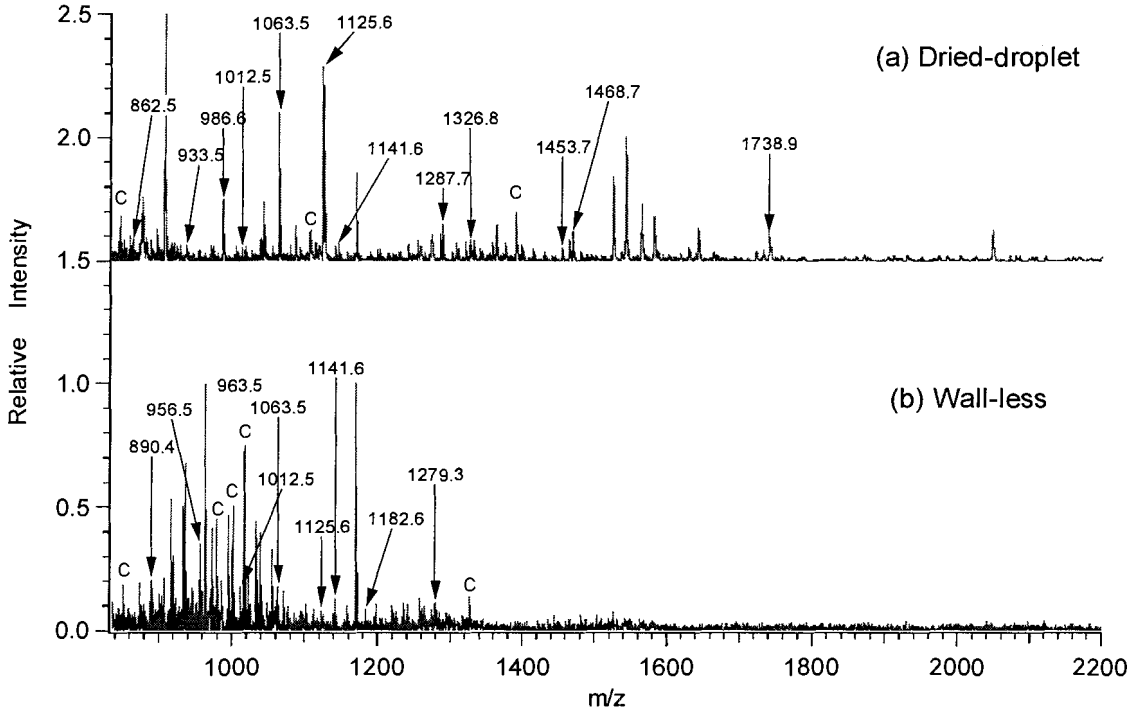

Figure 3.6 MALDI mass spectra of bacteriorhodopsin chymotrypic peptides using different sample preparation methods when matrix SA was used and SDS was added after digestion completation. (a) dried-droplet sample preparation method (b) wall-less sample preparation method. Letter "C" indicates the autolysis peaks of chymotrypsin.

In addition, the dried-droplet sample preparation method detected some peptide peaks such as m/z = 1453.7, 1468.7 and 1738.9, which were not detected by the wall-less

sample preparation method. Meanwhile the wall-less sample preparation method detected some peptide peaks, for example m/z = 890.4, 956.5 and 963.5, which were not detected by dried-droplet sample preparation method. This suggested these two methods are complementary.

The sequence coverage from different sample preparation is summarized in Table 3.5. The dried-droplet sample preparation method obtained 81% sequence coverage. The wall-less sample preparation method contributed to detect new peptides and the combination of two methods improved the sequence coverage to 89%.

Table 3.5 Summary of peptide sequence coverage of bacteriorhodopsin from different sample preparation methods (Matrices CHCA and SA, from all conditions).

Protein	(a) Dried-droplet method	(b) Wall-less method	(C) Combination of (a) (b)
Bacteriorhodopsin	81%	65%	89%

In order to better display the contribution of wall-less sample preparation method on improved sequence coverage, the detected peptide regions from two methods were mapped in Figure 3.7. The transmembrane region G with amino acid position 202 to 223 (NIETLLFMVLDVSAKVGFGLILLL) was not detected by the dried-droplet sample preparation, but part of it (MVLDVSAKVGFGLILLL) was detected by the wall-less sample preparation method. This detection of hydrophobic peptide was probably due to solvent fast evaporation in levitated droplets. The hydrophobic peptides did not have enough time to segregate from matrix in the levitated droplets before co-crystallization. It

shows that the wall-less sample preparation and dried-droplet method are complementary sample preparation methods to improve the sequence coverage of bacteriorhodopsin.

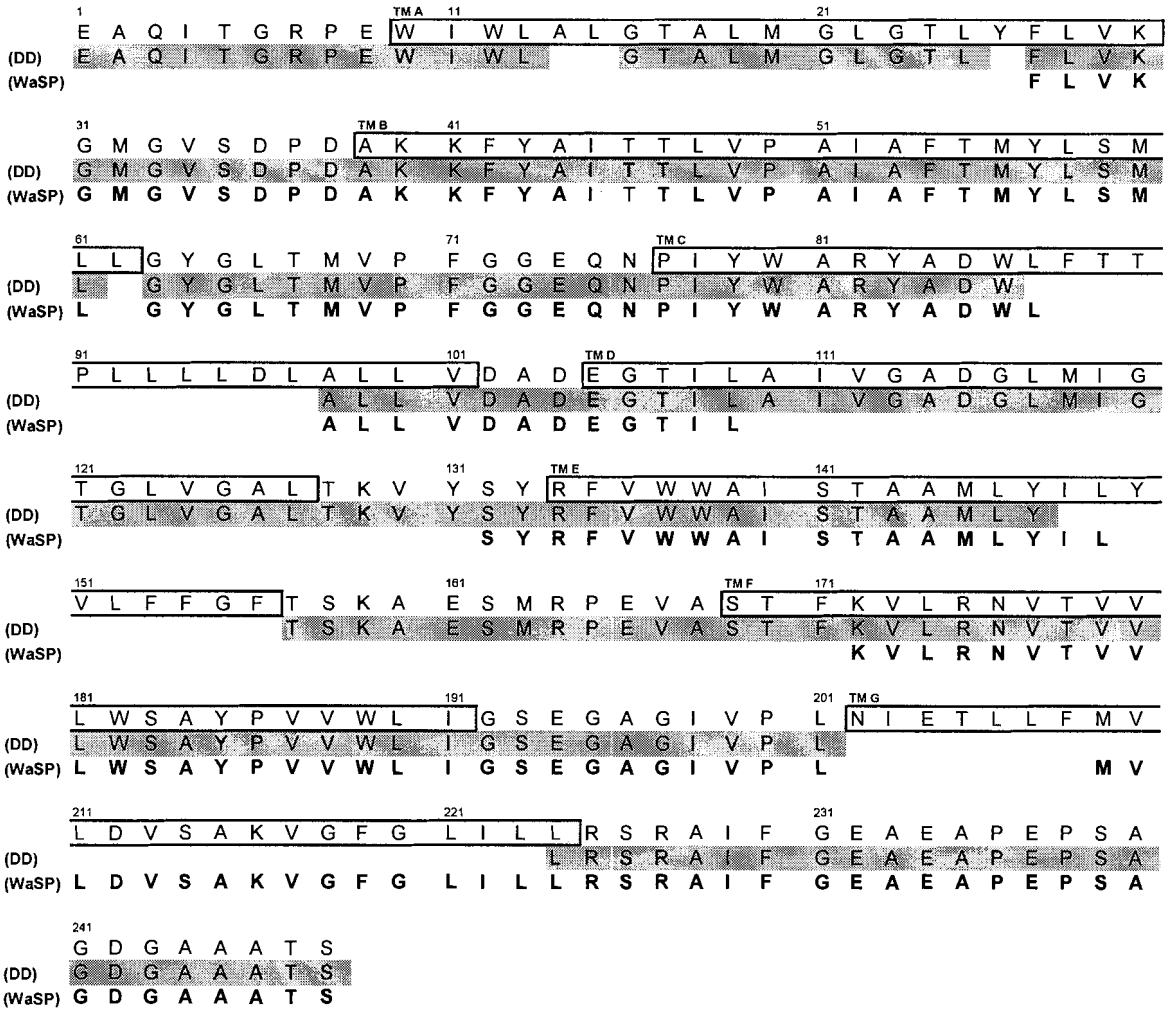

Figure 3.7 **Bacteriorhodopsin sequence and its detected peptide regions using different sample preparation methods. The first row is the full sequence of bacteriorhodopsin with transmembrane regions indicated with the rectangular box. The second row (DD) is the detected peptides using dried-droplet sample preparation with highlighting by the grey background. The third row of (WaSP) is the detected peptides using wall-less sample preparation method indicated in bold.**

3.5.5 Discussion of undetected peptides of bacteriorhodopsin

A total three major peptide regions in bacteriorhodopsin sequence were not detected in Figure 3.7. These peptide regions, position 88-97, 150-156 and 202-208, were very hydrophobic from the transmembrane regions. Their grand average of

hydropathicity, abbreviated as GRAVY, was calculated by using web accessible ProtParam program (http://kr.expasy.org/tools/protparam.html). ProtParam is running by the Expert Protein Analysis System (ExPASy) proteomics server of the Swiss Institute of Bioinformatics (SIB). ProtParam is a tool to compute various physical and chemical parameters for a user entered sequence or for a given protein stored in protein databases, e.g, Swiss-Prot. These parameters include GRAVY, pKa, and theoretical isoelectric point.

The GRAVY was calculated by using the Kyte and Doolittle scale.[83] Each amino acid is given a hydrophobocity score between –4.5 to 4.5. A score of –4.5 is the most hydrophilic, while a score of 4.5 is the most hydrophobic. The GRAVY score is the linear combination score for all the amino acids in a peptide or protein. The positive value of GRAVY means the peptide or protein is hydrophobic.[83] The Kyte and Doolittle scale can also be used to predict the potential transmembrane region by Kyte and Doolittle plot.[83] Table 3.6 summarized some properties of the undetected peptides of bacteriorhodopsin.

Table 3.6 Undetected peptides of bacteriorhodopsin.

#	Peptide sequence	Position	Missed cleavage	Monoisotopic mass [$M+H^+$]	GRAVY
(1)	FTTPLLLLDL	88-97	4	1144.6713	1.530
(2)	YVLFFGF	150-156	3	891.4507	2.100
(3)	NIETLLF	202-208	2	848.4652	1.029

The missed cleavage sites of the potential peptides #1 and #2 were 4 and 3, respectively. Thus, these peptides were likely cleaved by chymotrypsin into peptides of mass < 800 Da. The Peptide Cutter from the ExPASy was used to predict the potential cleavage sites of these peptides. (http://au.expasy.org/tools/peptidecutter/). This prediction was based on a user entered sequence. Figure 3.8 shows the potential cleavage sites with possibility of cleavage. Chymotrypsin cleaves at the C-terminal side of phenylalanine (F), tyrosine (Y), tryptophan (W) and leucine (L) (when they are not before proline (P)).

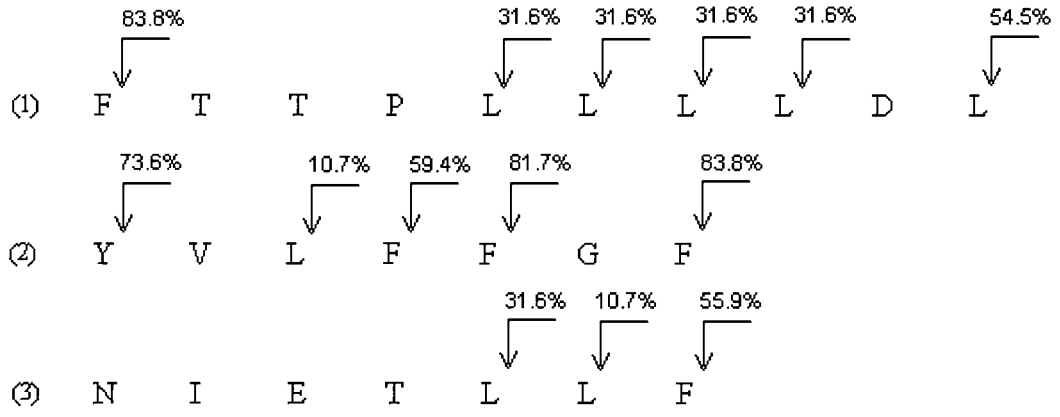

Figure 3.8 Undetected peptides of bacteriorhodopsin and their potential chymotrypsin cleavage sites indicating with arrows. The number of percentage shows the possibility of cleavage.

If the digestion went to completion, and the missed cleavage sites entered into the protein search algorithm ≤ 2, as predicted in Figure 3.8, the mass of their smaller peptides, e.g. TTPL from the potential peptide (1) in Figure 3.8, is at or below 700 Da. Due to the matrix cluster suppression of analyte ion signal,[84] the MALDI mass range (m/z) was set at 800-4000 for bacteriorhodopsin peptide detection in this study. Therefore these smaller peptides were not detected due to their m/z being outside of the detection

window examined. One exception was peptide (3) (NIETLLF) in Figure 3.8 failing to be detected. Its m/z value is 848.4652 with 2 missed cleavage sites.

3.6 Conclusion

This chapter described approaches to study the primary structure of a membrane protein, bacteriorhodopsin, and strategies to improve its sequence coverage as measured using MALDI-MS. (1) The addition of a low concentration anionic detergent SDS improved the solubilization of the hydrophobic protein, which lead to an increased sequence coverage. (2) Of the common MALDI matrices used, the least polar matrix SA gave the best sequence coverage of bacteriorhodopsin. It was probably due to more favourable intermolecular interactions between less polar matrix and hydrophobic peptides, which suggested the hydrophobic interaction is a possible factor for detection of hydrophobic peptides or proteins. (3) The wall-less sample preparation method was shown to be a complementary sample preparation method to the traditional dried-droplet method. These approaches are good starting points for future studies of membrane proteins on their primary structure and identification through their high sequence coverage by using MALDI-MS.

Table 3.7 **Summary of detected bacteriorhodopsin chymotrypic peptides. The check marks (✔) indicate using dried-droplet method. The solid circles (●) show using wall-less sample preparation method.**

Peptide	Position	No surfactant			SDS in digestion			OG in digestion			SDS after digestion			OG after digestion		
(m/z)		CHCA	SA	DHB	CHCA	SA	DHB	CHCA	SA	DHB	CHCA	SA	DHB	CHCA	SA	DHB
857.4310	132-137										✔	✔			●	
862.4708	224-230				✔ ●	✔ ●	✔			✔	✔	✔		●	✔	
874.4054	55-61														●	
877.4056	72-79		●		●			●	●		●			●	●	
890.4004	55-61	✔			✔			✔			✔	●		✔		
894.4474	81-87	●									●			●		
933.5079	16-25											✔				
940.4814	139-147						✔		●				✔	✔	✔ ●	
956.4763	139-147		●									●				
963.4974	138-146		●			●						●				
967.4426	80-86	✔	✔	✔												
979.4923	138-146		●						●						●	
984.4865	63-71		●													
986.5787	175-182	✔ ●	✔	✔	✔ ●	✔ ●	✔	✔	✔	✔	✔ ●	✔	✔	✔	✔	✔
992.5417	212-221							●								
1000.4814	63-71				✔	✔	✔	✔	✔	✔			✔			
1007.4991	182-189	✔	✔ ●													
1012.5178	191-201										●	✔ ●	✔			✔

Peptide	Position	No surfactant			SDS in digestion			OG in digestion			SDS after digestion			OG after digestion		
(m/z)		CHCA	SA	DHB	CHCA	SA	DHB	CHCA	SA	DHB	CHCA	SA	DHB	CHCA	SA	DHB
1028.5127	49-57	✔ ●	✔					●			●			●		
1045.5417	100-109					✔	✔		✔		●			●		
1063.4849	72-80	✔ ●	✔ ●	✔	✔	✔	✔	✔	✔	✔	✔ ●	✔ ●	✔	✔	✔	✔
1088.6944	222-230				●				●		●			●	●	
1116.6669	44-54	✔	✔													
1120.5831	182-190	✔	✔ ●						✔						●	
1125.6018	190-201	✔	✔		✔			✔			✔	✔ ●		✔	✔	
1140.7469	172-181	✔ ●	✔ ●	✔		✔				✔	✔					
1141.5967	49-58					✔ ●		✔				✔ ●				
1166.6495	139-149		●													
1182.6444	139-149				●							●				
1218.7098	212-223		●						●						●	
1229.6629	98-109				✔	✔	✔					●				
1264.6400	136-146						✔						✔			
1279.7302	43-54	●	✔		✔							●				
1287.6982	110-123	✔	✔			✔						✔	✔		✔	
1326.8262	172-182				✔	✔	✔				✔ ●	✔	✔			
1335.7346	209-221											●				
1438.7980	118-131	✔	✔	✔		✔			✔	✔			✔			
1453.6864	72-83										✔	✔				
1468.6782	67-79	✔	✔	✔	✔ ●	✔ ●	✔	✔	✔	✔	✔	✔	✔	✔	✔	✔

Peptide	Position	No surfactant			SDS in digestion			OG in digestion			SDS after digestion			OG after digestion		
(m/z)		CHCA	SA	DHB	CHCA	SA	DHB	CHCA	SA	DHB	CHCA	SA	DHB	CHCA	SA	DHB
1494.7626	29-42					✔			✔			✔				
1587.6774	231-248					✔					●	✔				
1598.8331	1-13					✔										
1607.8467	28-42					✔	✔									
1638.7626	67-80				✔ ●	✔ ●			●		✔ ●	✔		✔		
1641.8311	29-43	✔	✔			✔			✔							
1738.9202	27-42	✔ ●	✔ ●	✔	✔ ●	✔ ●	✔	✔			✔ ●	✔	✔	✔		✔
1928.0533	183-201					✔										
1997.0378	157-174														✔	
2157.1266	29-48														✔	

Table 3.8 Detected myoglobin chymotrypic peptides using dried-droplet sample preparation.

Peptides	Position	No detergent			SDS in digestion			OG in digestion			SDS after digestion			OG after digestion		
(m/z)		CHCA	SA	DHB	CHCA	SA	DHB	CHCA	SA	DHB	CHCA	SA	DHB	CHCA	SA	DHB
754.3735	34-40	✔	✔	✔	✔	✔	✔	✔	✔	✔	✔	✔	✔	✔	✔	✔
763.3263	1-7			✔			✔			✔			✔			✔
778.4099	147-153		✔	✔		✔	✔		✔	✔		✔	✔		✔	✔
787.4466	44-49	✔	✔	✔	✔	✔	✔	✔	✔	✔	✔	✔	✔	✔	✔	✔
813.4147	41-46	✔	✔	✔	✔	✔	✔	✔	✔	✔	✔	✔	✔	✔	✔	✔
881.5573	62-69	✔	✔		✔	✔	✔	✔				✔	✔	✔	✔	
886.4787	8-14					✔	✔					✔	✔			
901.4420	33-40	✔			✔	✔		✔	✔	✔	✔			✔		✔
924.4328	116-123	✔	✔	✔	✔	✔	✔	✔	✔	✔	✔	✔	✔	✔	✔	✔
950.5060	139-146	✔	✔	✔	✔	✔	✔	✔	✔	✔	✔	✔	✔	✔	✔	✔
980.5781	107-115		✔	✔	✔	✔	✔	✔	✔	✔	✔					
1097.5744	138-146	✔	✔			✔										
1158.5795	34-43	✔	✔	✔	✔	✔	✔	✔	✔	✔	✔	✔	✔	✔	✔	✔
1176.6489	77-86				✔	✔										
1231.5959	1-11	✔	✔	✔		✔	✔		✔	✔	✔	✔				✔
1256.6891	105-115	✔	✔	✔	✔	✔	✔			✔	✔	✔				✔
1320.7276	139-149	✔	✔				✔	✔				✔			✔	✔
1339.7010	136-146		✔		✔				✔		✔					
1351.6415	50-61					✔	✔				✔	✔	✔			
1369.7731	104-115	✔	✔	✔	✔	✔	✔				✔	✔			✔	✔

Peptides	Position	No detergent			SDS in digestion			OG in digestion			SDS after digestion			OG after digestion		
(m/z)		CHCA	SA	DHB	CHCA	SA	DHB	CHCA	SA	DHB	CHCA	SA	DHB	CHCA	SA	DHB
1375.6891	124-137	✔					✔		✔		✔				✔	
1391.6841	124-137				✔	✔										
1506.9372	62-76				✔	✔		✔	✔		✔	✔				
1514.8807	77-89				✔	✔		✔						✔		
1522.7865	15-29	✔	✔	✔	✔	✔	✔	✔	✔	✔	✔	✔	✔	✔	✔	✔
1548.7698	34-46	✔	✔	✔	✔	✔	✔	✔	✔		✔	✔			✔	
1671.8859	138-151													✔		
1855.0918	73-89	✔	✔	✔	✔	✔	✔	✔	✔	✔	✔	✔	✔	✔	✔	✔
1921.9772	12-29	✔	✔	✔	✔	✔	✔	✔	✔	✔	✔	✔	✔	✔	✔	✔
1960.1496	87-103					✔						✔				
2136.0647	44-61	✔			✔	✔		✔		✔		✔		✔	✔	
2451.3149	12-33		✔	✔	✔	✔		✔	✔			✔	✔		✔	

CHAPTER 4:
IDENTIFICATION OF CHEMICAL MODIFICATION SITES ON PROTEINS

4.1 Context

This chapter describes the identification of the chemical modification sites on proteins. The chemical modifications were performed to facilitate experiments designed to improve understanding of protein native topology. This is an inter-department collaborative project with Dr. Erika Plettner at the Department of Chemistry at SFU. Two proteins, pheromone binding protein 2 (PBP2) from the Gypsy Moth *Lymantria dispar,* and cytochrome $P450_{cam}$ ($P450_{cam}$) from *Pseudomonas putida*, were investigated. Doctoral candidates, Yongmei Gong and Adina Rojubally from Dr. Plettner's research group, performed the covalent protein modifications. I performed MALDI-TOF-MS on the modified proteins followed by data analysis. Our work to identify sites of chemical modification allows studies of the native topology of these two proteins.

4.2 Abstract

MALDI-TOF-MS was used to identify sites of covalent chemical modification on two proteins. Yongmei Gong reacted dansyl chloride (DNS-Cl) with pheromone binding protein 2 (PBP2) to form modified protein DNS-PBP2. The dansyl chloride was expected to add at sterically accessible lysine (Lys or K) residues. The experimental results showed that the modification was at the lysine residues K31 and K38 of DNS-PBP2. This finding enables further studies of the modified proteins that would be designed to elucidate new

information regarding the structure-function and protein-ligand interactions of PBP2. Adina Rojubally produced, isolated and modified another protein cytochrome $P450_{cam}$ ($P450_{cam}$) with two thiol-reactive probes, 5'-(4-Bromo-heptyl)-5-methyl-[2,2']bipyridinyl (7C-BIPY) and 5-((2-iodoacetamido)ethyl amino)naphthalene-1-sulfonic acid (IAEDANS). 7C-BIPY and IAEDANS were separately added to wild type $P450_{cam}$ and $P450_{cam}$ containing a histidine tag. The reactions were at cysteine (Cys or C) residues. The modification sites were identified using MALDI-TOF-MS. The experimental results showed that 7C-BIPY modified $P450_{cam}$ at C285 and C334, while IAEDANS only modified $P450_{cam}$ containing a histidine tag at site C334. This work provided mass spectral evidence that selective chemical modifications of $P450_{cam}$ were achieved.

4.3 Introduction

MALDI-MS has been used for identification of covalent and post-translational modifications of proteins, as well as to monitor the protein chemical reactions. The latter can be used to characterize the surface topology and binding sites of a protein or protein complex.[28,85-87] The digested peptides from the unmodified protein were compared to that generated from the chemically modified protein. The covalent modification sites were identified by mass shift in the MALDI-MS spectra.

4.3.1 Pheromone binding protein 2 (PBP2)

PBP2 is a 16-kDa protein that was isolated from the gypsy moth, *Lymantria dispar*.[88,89] Dansyl chloride (1-dimethylnaphthalin-5-sulfonyl chloride, DNS-Cl) is a fluorescent detection reagent, and it is a lysine site-specific reactant at $pH \geq 9.0$. This site-specific reaction is shown in Equation 4.1. Dansyl chloride gave highly fluorescent

dansylated residues on PBP2, because of the rigid extended π system in the resultant dansyl sulfonamide.[34] The technique of fluorescence spectroscopy was used to study the conformational properties of the PBP2-ligand complex.[90]

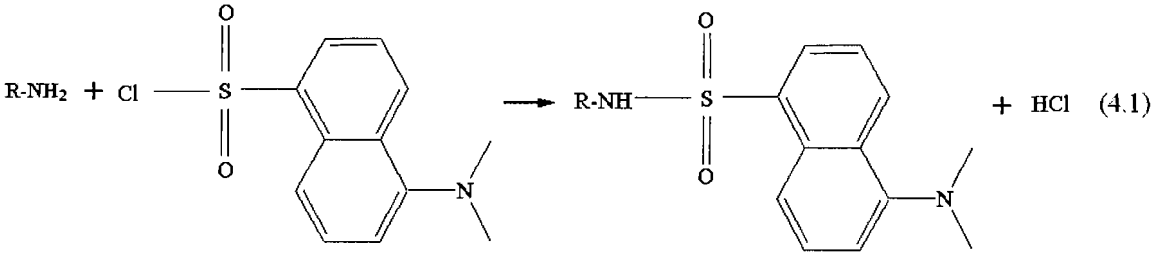

Dansyl chloride

The mass of PBP2 is changed after modification. The monoisotopic mass of the modified peptide increases by n times of 233.0510 Da, due to the mass shift. Here n is the number of modified lysine residues in the peptide. Therefore comparing the peptide mass of PBP2 and DNS-PBP2, the modified peptides and the related lysine residues in DNS-PBP2 would be identified.

PBP2 has 11 lysine residues in its peptide chain at locations of K2, K11, K14, K17, K31, K38, K44, K58, K78, K121 and K126. From a model of PBP2 (Figure 4.1), three lysine residues, K14, K38 and K44, are located on PBP2 loops, the remaining eight lysine residues are on α-helices. Three out of eleven lysine residues are the most surface exposed. K38 is located on an exposed loop. K31 and K126 are at the outside of helices. These positions suggest that K38, K31 and K126 are the most likely sites for reaction with dansyl chloride. The model of PBP2 was created by "threading" the sequence of PBP2 onto the crystal structure of the PBP from silk moth, *Bombyx mori.*[91]

The tryptophan (Trp or W) residue contains an aromatic side chain. If it is close to DNS, tryptophan could enhance the fluorescence of DNS due to the potential energy transfer. Two tryptophan residues, W37 and W129, are in the PBP2 sequence. W129 is not close to any lysine residue. W37 is next to K38. W37 would enhance the fluorescent signal of dansyl chloride, when W37 is excited at wavelength $\lambda = 295$ nm.

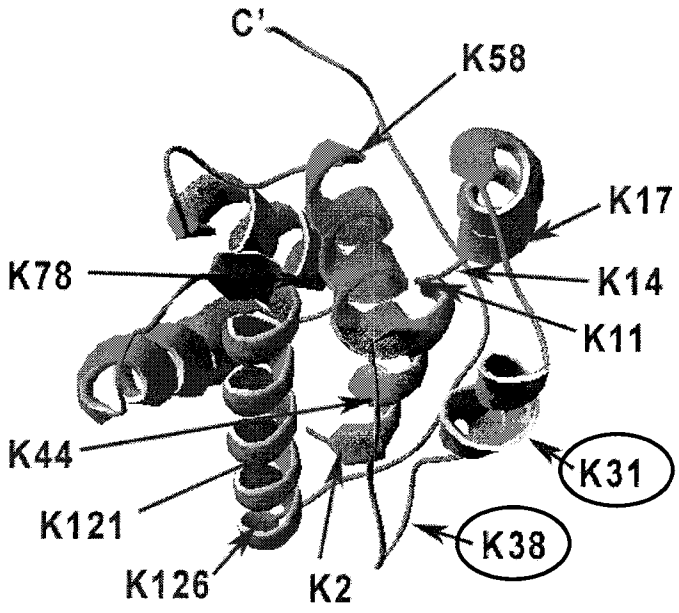

Figure 4.1 **Crystal structure of PBP2 and its lysine residues labelled. This model was created by "threading" the sequence of PBP2 onto the crystal structure of the PBP from silk moth, *Bombyx moli.*[91] The circles show the modification sites identified in this work.**

Cyanogen bromide (CNBr) and chymotrypsin were separately used to digest PBP2 and DNS-PBP2, due to they do not cleavage at lysine residues of the primary sequence of a protein. CNBr cleaves protein at methionine (M). Chymotrypsin cleaves at the C-terminal side of phenylalanine (F), tyrosine (Y), tryptophan (W) and leucine (L)

(when they are not before proline (P)). None of these cleavage sites are potential modification lysine (K) residues (Figure 4.2).

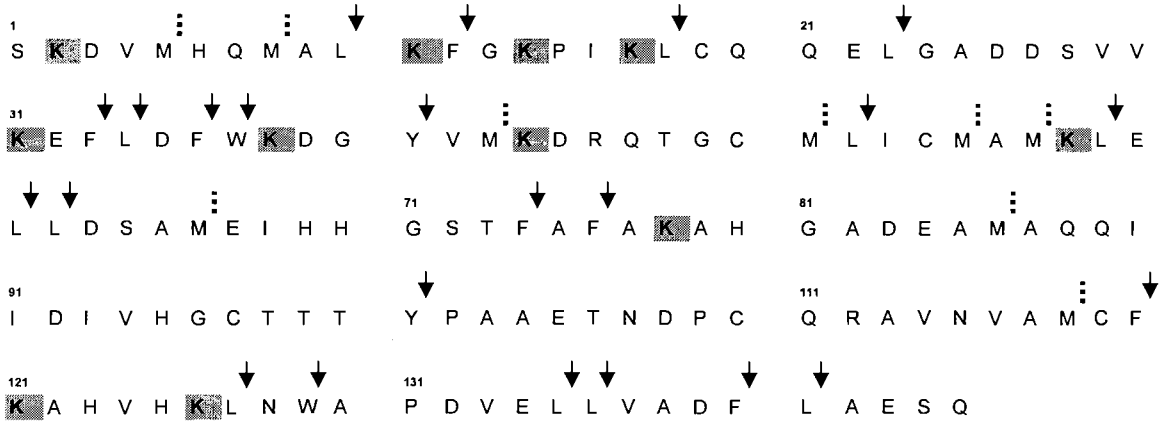

Figure 4.2 PBP2 sequence.[92] Its lysine residues are written in bold and highlighted with grey background. Chymotrypsin cleavage sites are indicated by the arrows. The dashed lines show CNBr cleavage sites.

4.3.2 Cytochrome $P450_{cam}$ ($P450_{cam}$)

Cytochrome $P450_{cam}$ is a hydrophobic protein. The detection of hydrophobic proteins and peptides is a challenge for MALDI-MS as discussed in chapter 3. Hydrophobic proteins and peptides are not soluble in aqueous solution, and they are prone to sample loss on the walls of containers. Furthermore they have low ionization efficiency in the process of desorption/ionization in MALDI. We applied the approaches learned in chapter 3 to study $P450_{cam}$ modification sites. The detergent SDS was used to solubilize $P450_{cam}$ and its peptides generated by digestion. The relative weak polar matrix SA was used to detect the hydrophobic peptides.

Since its discovery in the late of 1950's,[93-95] the structure and function of cytochrome P450 has been widely studied using chemical, physical and biochemical techniques, including X-ray crystallography, optical spectroscopy (UV, NMR, IR, CD), and site-directed mutagenesis.[96] $P450_{cam}$ is cytochrome P450 that is bound to its substrate camphor. Camphor is bound at the substrate site above the iron porphyrin of $P450_{cam}$.

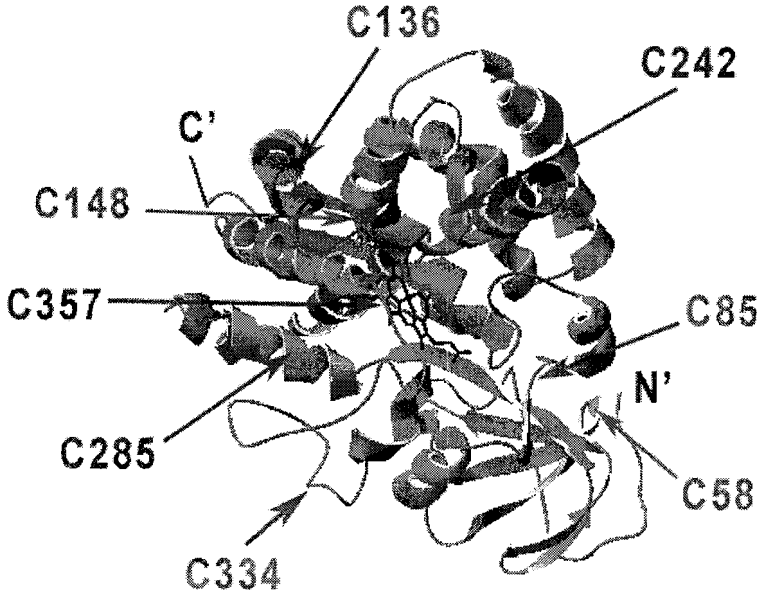

Figure 4.3 Crystal structure of wild type $P450_{cam}$ with the cysteine residues labelled.[97]

Wild type $P450_{cam}$ was isolated and purified from *Pseudomonas putida*. It contains 428 amino acid residues, including 8 cysteine residues.[98,99] In its native conformation, a heme is embedded in a hydrophobic region of $P450_{cam}$. $P450_{cam}$ is an interesting template for chemical selective modification, due to the eight cysteine residues that are classified into three sub-groups. A) Surface-exposed, C58, C85, C136, C148 and C334; B) substrate access channel, C242 and C285, which are relatively buried

by helices; C) inaccessible in the interior, C357, which is coordinated to the iron atom of the heme. Of all the cysteine residues, C334 is the most surface exposed and was anticipated to be the most probably modification site (Figure 4.3).

Figure 4.4 shows the sequence of wild type $P450_{cam}$[100] and its trypisn and chymotrypsin cleavage sites. None of the cleavage sites are at the potential modification cysteine residues.

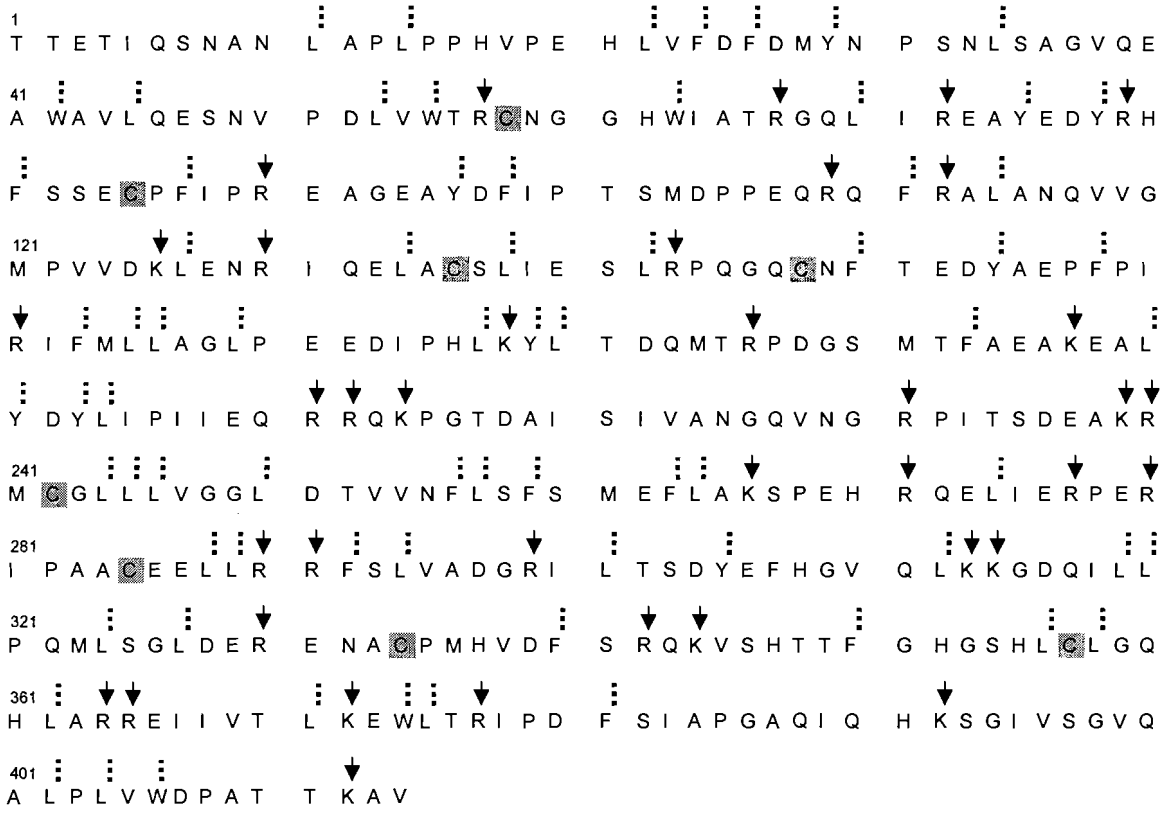

Figure 4.4 The sequence of wild type $P450_{cam.}$[100] And its cysteine residues are in bold and highlighted with grey background.[16] Trypsin cleavage sites are indicated by arrows. The dashed lines indicate the chymotrpsin cleavage sites.

Wild type $P450_{cam}$ was modified by 5'-(4-Bromo-heptyl)-5-methyl-[2,2']bipyridinyl (7C-BIPY), and formed BIPY-WTP450. 7C-BIPY is used as a cross-

linker to attach another protein with $P450_{cam}$. The reaction is cysteine specific at pH values between 8 and 9 (Equation 4.2).[99,101]

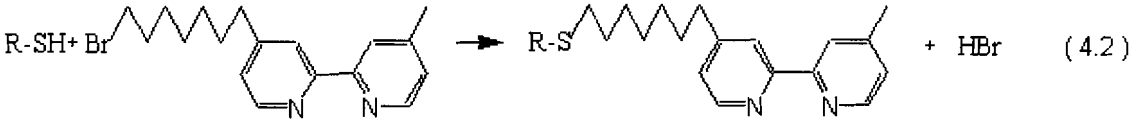

(4.2)

7C-BIPY

The native conformation of $P450_{cam}$ may change, when a histidine tag (His-tag) was attached at its C-terminal site. The His-tag contained 14 amino acid residues (EKLASALEHHHHHH). It likely coordinated with the active substrate access channel, and "blocked" the reaction pathway during the modification process.

The amino acid sequence of $P450_{cam}$ containing a His-tag and its trypsin and chymotrypsin cleavage sites are shown in Figure 4.5.

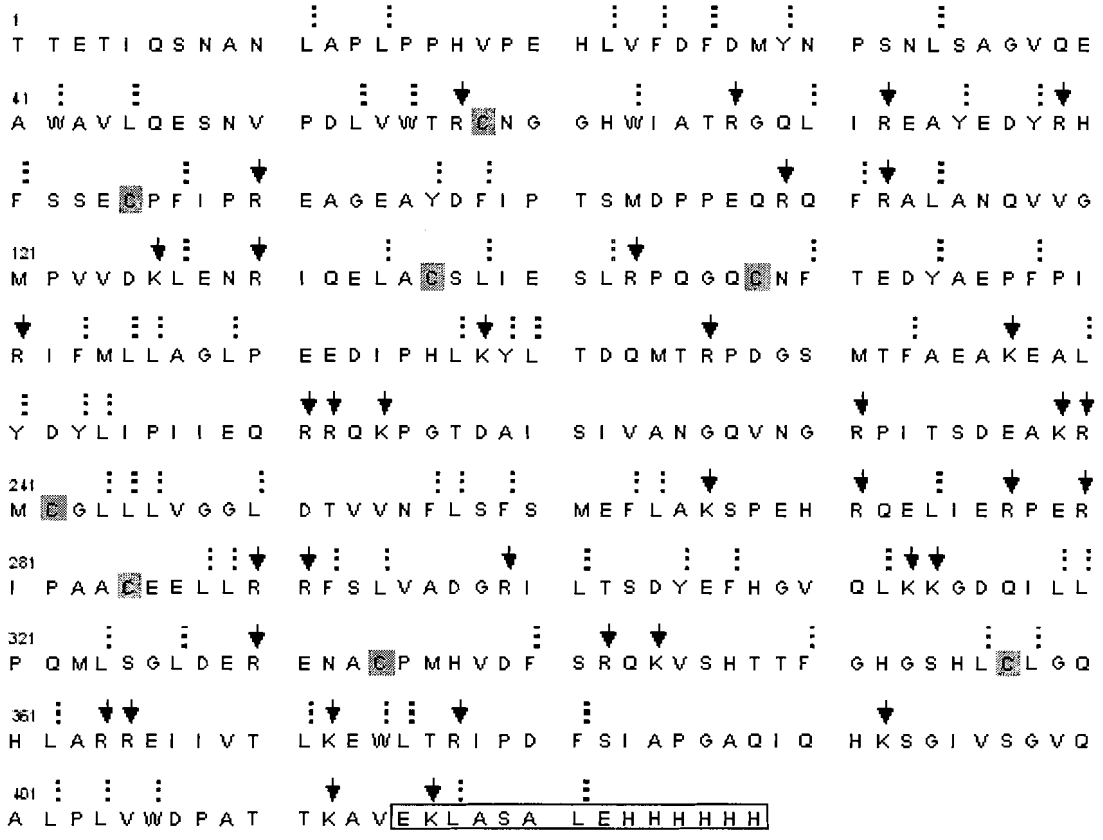

Figure 4.5 **The sequence of $P450_{cam}$ containing a His-tag. Trypsin cleavage sites are indicated by the arrows. The dash lines indicate the chymotrpsin cleavage sites. The cysteine residues are in bold and highlighted by the grey background. The His-tag is indicated with a rectangular box.**

The fluorescent reagent 5-((2-iodoacetamido)ethyl amino)naphthalene-1-sulfonic acid (IAEDANS) was reacted with His-tag $P450_{cam}$ to form IAEDANS-P450. Some of the cysteine residues of His-tag $P450_{cam}$ were modified by a process indicated by

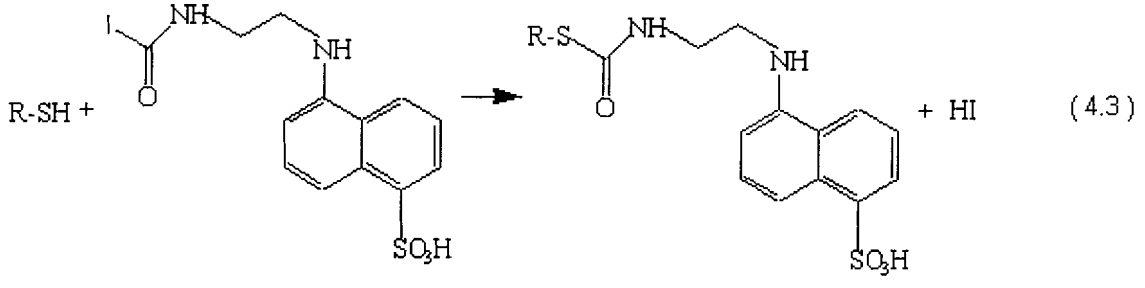

Equation 4.3 IAEDANS

As indicated by Equations 4.2 and 4.3, the mass of modified protein $P450_{cam}$ would shift as a result of a covalent addition of a compound to $P450_{cam}$. The theoretical monoisotopic peptide mass of modified BIPY-WTP450 and IAEDANS-P450His-tag increased by 266.1782 Da and 306.0673 Da, respectively. Through comparing the mass shift, the modified peptides would be identified and the positions of cysteine bound with either BIPY or IAEDANS would be discovered.

4.4 Experimental section

4.4.1 Sample preparation of PBP2

Yongmei Gong performed protein modifications of PBP2 and CNBr digestion. I performed the chymotrypsin digestion of PBP2 and MALDI-MS analysis of the peptides from both digests.

4.4.1.1 PBP2 modification

To a solution of PBP2 10 mL (50 μM PBP2 in 20 mM $NaHCO_3$, pH=10.3), 0.02 mL dansyl chloride (50 mM in ethanol) was added three times with 30 min separation between additions. A total of 0.06 mL dansyl chloride was added to the PBP2 solution. This reaction was allowed to proceed at room temperature for a total of 1.5 h.

4.4.1.2 PBP2 digestion

(1) CNBr digestion

One milligram of sample of PBP2 and DNS-PBP2 were separately dissolved in a 200 μL solution of 70% trifluoroacetic acid (TFA) in water (v/v). Two small white crystals of CNBr (~1 mg) were directly added in the protein solution. CNBr was about 15

fold molar excess over methionyl residues in PBP2. The mixture was sealed in a tube and incubated at room temperature. *Since CNBr is a highly toxic reagent, proper care was taken. It was handled only in a fume hood, and the chemist wore gloves and a mask.* After a 24 h incubation period, the tube was opened and left in a fume hood for 3 hours before using the vacuum centrifuge ("Speedvac"). To terminate the reaction, the solution was evaporated to dryness in fume hood. The dry peptides were dissolved in a 100 μL solution of 0.1% TFA in water (v/v) and stored in the freezer (~10 °C) for MALDI-MS analysis.

(2) Chymotrypsin digestion

Two microliters of chymotrypsin (5 μg / μL in 100mM NH_4HCO_3, 2mM $CaCl_2$, pH=8 buffer) was added to 50 μL PBP2 or DNS-PBP2 solution (1 μg/ μL in 100mM NH_4HCO_3, 2mM $CaCl_2$, pH=8), and incubated at 37°C for 24 hours. Immersing the mixture in liquid nitrogen terminated the digestion, and the digest solution was stored in the freezer (-10 °C) for MALDI-MS analysis.

4.4.1.3 Sample preparation for MALDI-MS

The MALDI matrix SA was saturated in 50% acetonitrile / water containing 0.1% TFA. One microliter of digest solution was mixed with 1 μL solution of SA, and deposited on MALDI target plate by using a pipette. Samples were analysed in duplicate.

4.4.2 Sample preparation of $P450_{cam}$

Adina Rojubally performed the chemical modifications of $P450_{cam}$ with BIPY and IAEDANS, and the subsequent purification steps. I performed the protein digestion by using trypsin and chymotrypsin, and MALDI-MS analysis.

4.4.2.1 Reduction of disulfide bonds on $P450_{cam}$

After protein modification and isolation, any unmodified cysteine residues would most likely reform disulfide bonds. Therefore, the reducing agent dithiothreitol (DTT) 5 μL (10 mM) was added to 20 μL protein solution (1 μg/ μL). This mixture was then stored at room temperature for 2 h before digestion. The reaction is shown in Equation 4.4.

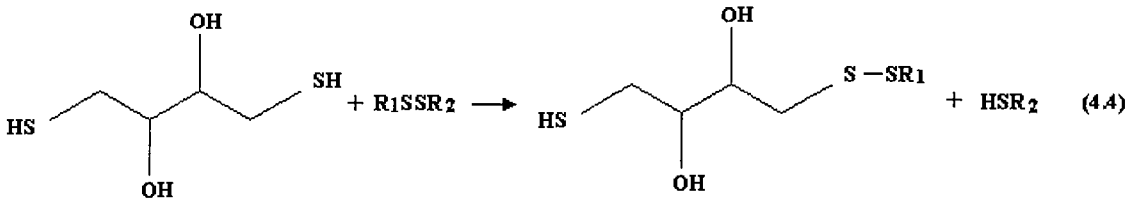

DTT

4.4.2.2 $P450_{cam}$ digestion

Trypsin (sequence grade, Promega, Madison, WI, USA) and chymotrypsin (Sigma, USA) were separately used to digest $P450_{cam}$ and its modified proteins (BIPY-WTP450 and IAEDANS-P450). In order to denature the protein, 20 μL of reduced protein (1 μg/ μL in 100 mM NH_4HCO_3, 2 mM $CaCl_2$, pH=8) were heated at 95 ˚C for 3 min, and cooled to room temperature. Two microliter of SDS solution (8 mM in 100 mM NH_4HCO_3, 2 mM $CaCl_2$, pH=8) was added to protein solution, and 3 μL of trypsin or chymotrypsin (2 μg/ μL in 100 mM NH_4HCO_3, 2 mM $CaCl_2$, pH=8) was then added. This mixture was incubated at 37˚C for 24 hours. Immersion of the mixture into liquid nitrogen terminated the protein digestion, and the solution of protein digestion was stored in the freezer for MALDI-MS analysis.

4.4.2.3 MALDI-MS Sample preparation

The weak polar MALDI matrix SA was used. One microliter of the solution of digested protein was mixed with 1 μL of saturated SA solution (ACN / 0.1% TFA, v/v = 2:3). This mixture was deposited on a MALDI target plate by using a pipette. Samples were analysed in duplicate.

4.5 Results and discussion

4.5.1 Identification of modification sites on PBP2

A representative mass spectrum of peptides generated from unmodified protein PBP2 is shown in Figure 4.6a. Peptides containing all eleven unmodified lysine residues were detected from PBP2, nine from chymotrypic digestion and two from CNBr digestion (Table 4.1). A PBP2 sequence coverage of 78% was obtained.

MALDI mass spectrum (Figure 4.6b) showed that three modified chymotryptic peptides of DNS-PBP2 were detected, m/z=1276.8391 (fragment 34-41, K38), 1675.2621 (24-36, K31) and 1861.4426 (24-37, K31). Their respective unmodified peptides, m/z=1043.5764, 1442.0824, 1628.2544, were detected as well. The difference of the mass was 233.2627, 233.1797 and 233.1882 Da respectively due to the addition of dansyl residue. No other modified peptides were detected (Table 4.2).

These three modified peptides were detected. One contained K38, the other two peptides both contained K31. This suggested the dansyl chloride modified PBP2 at K31 and K38 (Figure 4.1).

Modified K31 and K38 are likely the most surface exposed lysine residues. K38 is next to W37, the potential fluorescence energy transfer between DNS and W37 could be

monitored and provide information about PBP2 conformational changes. The potential energy transfer could be developed as a potential method to investigate the protein-ligand interaction.

Table 4.1 Detected unmodified PBP2 peptides containing lysine residues from chymotrypsin or CNBr digestion. An asterisk * denotes the peptides from CNBr digestion.

Peptide Position	**Lysine Position**	**Unmodified Theoretical** $[M+H]^+$	**Unmodified Observed** $[M+H]^+$	**Mass Accuracy** (ppm)
34 – 41	K38	1043.4838	1043.5100	25
24 – 36	K31	1441.6851	1441.9824	206
24 – 37	K31	1627.7644	1628.1437	233
121–127	K121, 126	832.5157	832.8712	427
53 – 61	K58	1122.5725	1122.7478	156
121–129	K121, 126	1132.6380	1133.0921	401
1 – 12	K2, 11	1466.7136	1465.9584	-515
11 – 23	K11, 14, 17	1602.9042	1602.0740	-518
42 – 61	K44, 58	2504.1877	2503.8274	-144
*58 – 66	K58	971.5413	971.0537	-502
*67 – 86	K78	2078.9684	2078.9395	-14

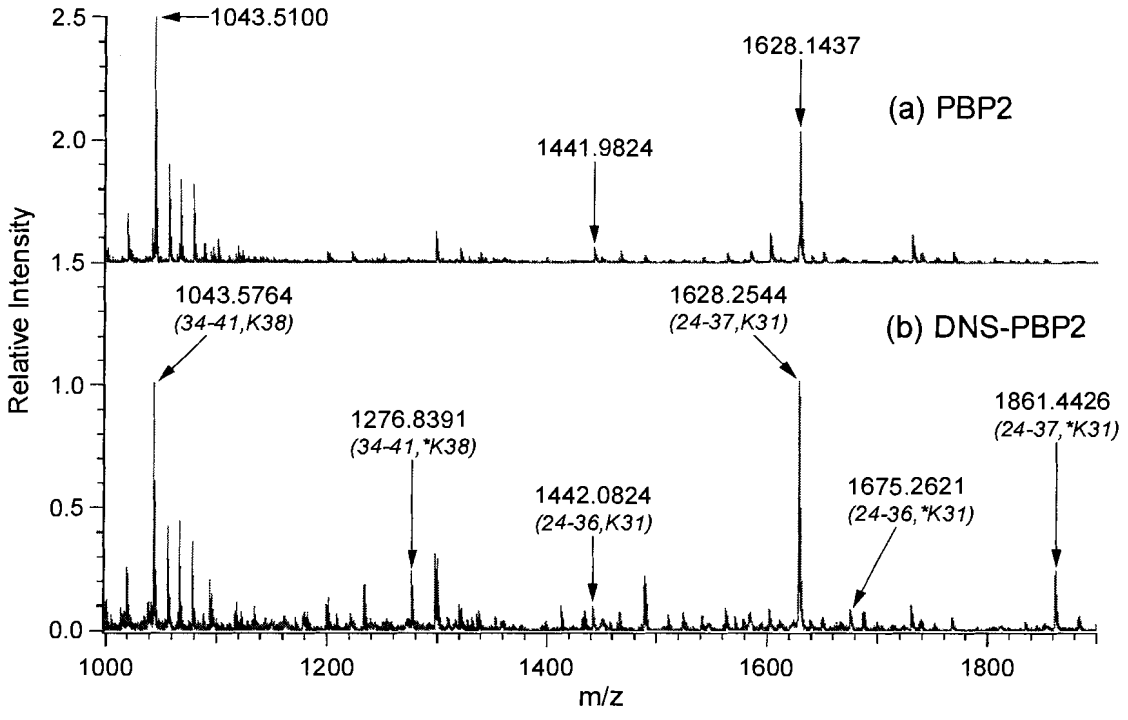

Figure 4.6 **MALDI mass spectra of PBP2 and DNS-PBP2 chymotrypic peptides containing lysine. (a) PBP2 peptides. (b) DNS-PBP2 peptides . An asterisk denotes the modified peptides.**

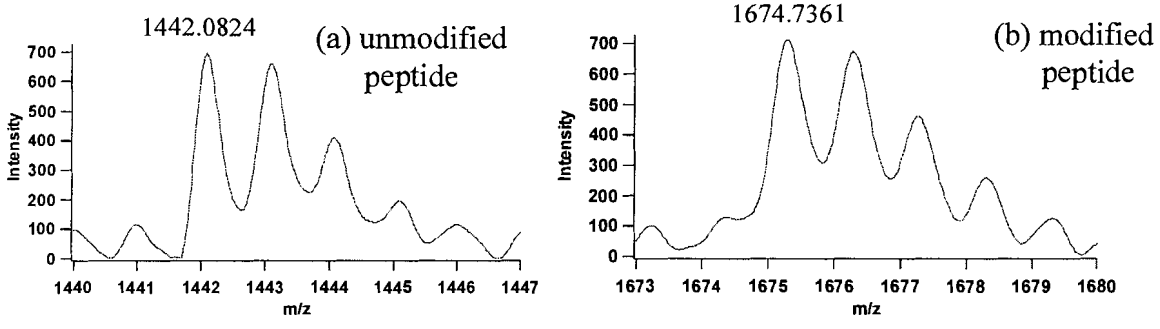

Figure 4.7 **(a) and (b) are x-axis zoom in showing the unmodified and modified peptide containing K31 in Figure 4.6b.**

Table 4.2 **Detected DNS-PBP2 peptides containing lysine residues from chymotrypsin or CNBr digestion. An asterisk * denotes the peptides from CNBr digestion. A (-) indicates no peptide detected.**

Peptide Position	Lysine In peptide	Unmodified Theoretical $[M+H]^+$	Unmodified Observed $[M+H]^+$	Modified Theoretical $[M+H]^+$	Modified Observed $[M+H]^+$	DNS Modified Lysine
34 – 41	K38	1043.4838	1043.5764	1276.5348	1276.8391	K38
24 – 36	K31	1441.6851	1442.0824	1674.7361	1675.2621	K31
24 – 37	K31	1627.7644	1628.2544	1860.8154	1861.4426	K31
121–127	K121,126	832.5157	832.9108	1065.5667	-	-
				1299.6177	-	-
53 – 61	K58	1122.5725	1122.5869	1355.6235	-	-
121–129	K121,126	1132.6380	1133.4921	1365.6890	-	-
				1598.7400	-	-
1 – 12	K2,11	1466.7136	1466.1423	1699.7646	-	-
				1932.8156	-	-
11 – 23	K11,14,17	1602.9042	1602.0189	1835.9552	-	-
				2069.0062	-	-
				2302.0572	-	-
42 – 61	K44,58	2504.1877	2503.4990	2737.2387	-	-
				2970.2897	-	-
*58 – 66	K58	971.5413	971.0178	1204.5923	-	-
*67 – 86	K78	2078.9684	2078.5017	2312.0194	-	-

4.5.2 Identification of modification sites on $P450_{cam}$

Unmodified peptides containing all eight cysteine residues were detected (Table 4.3). The wild type unmodified $P450_{cam}$ sequence coverage of 80% was obtained.

For modified protein BIPY-WTP450, two tryptic modified peptides containing C334 and C285 respective were detected by MALDI-MS, m/z=1742.9551 (331-342, C334) and 1607.3766 (281-291, C285) (Figure 4.8). No other modified peptides were detected. Table 4.4 summarized the detected peptides of BIPY-WTP450. This result indicated that 7C-BIPY modified the wild type of $P450_{cam}$ at C334 and C285.

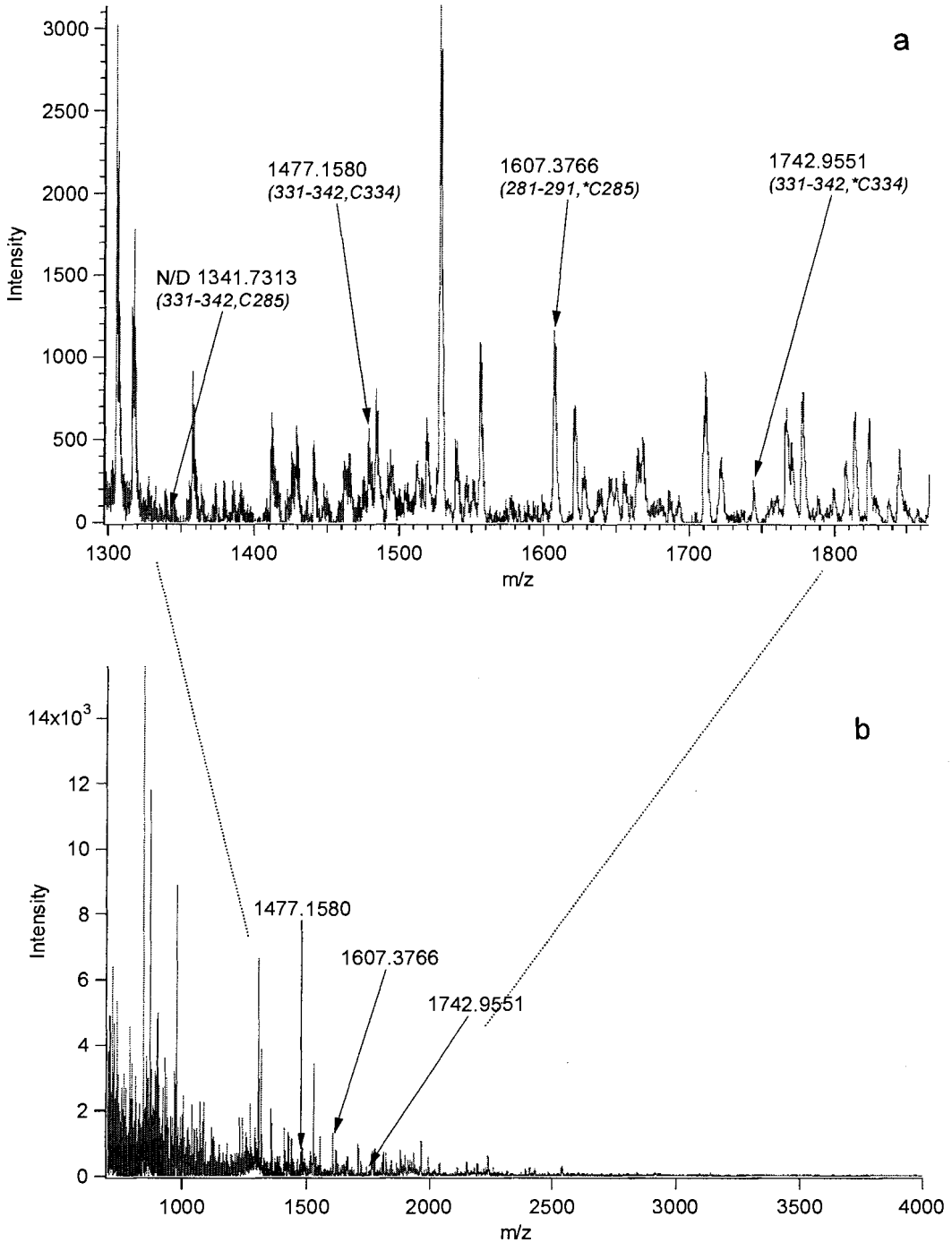

Figure 4.8 **MALDI mass spectra of tryptic BIPY-P450 peptides. An asterisk denotes the modified peptides. (a) is x-axis zoom in on the modified peptides from (b). N/D: not detected.**

Table 4.3 **Detected unmodified $P450_{cam}$ peptides containing cysteine residues from trypsin or chymotrypsin digestion. An asterisk * denotes the peptides digested using chymotrypsin.**

Peptide Position	Cysteine In peptide	Unmodified Theoretical $[M+H]^+$	Unmodified Observed $[M+H]^+$	Mass Accuracy (ppm)
331 – 342	C334	1476.6364	1477.0812	-301
331 – 344	C334	1732.7899	1732.8019	-7
281 – 291	C285	1341.7313	1342.0118	-209
241 – 266	C242	2875.4812	2876.3912	-316
*56 – 70	C58	1740.8716	1740.0755	457
*82 – 87	C85	740.2925	740.0825	284
*135 – 142	C136	906.4606	906.7918	-365
*139 – 150	C148	1462.7113	1462.9891	-190
*139 – 154	C148	1970.8918	1970.7153	90
*351 – 362	C357	1329.6486	1329.2709	284

Table 4.4 **Detected BIPY-WTP450 peptides containing cysteine residues from trypsin or chymotrypsin digestion. An asterisk * denotes the peptides digested using chymotrypsin. A (-) indicates no peptides detected.**

Peptide Position	Cysteine In peptide	Unmodified Theoretical $[M+H]^+$	Unmodified Observed $[M+H]^+$	Modified Theoretical $[M+H]^+$	Modified Observed $[M+H]^+$	BIPY Modified cysteine
331 – 342	C334	1476.6364	1477.1580	1742.8146	1742.9551	C334
281 – 291	C285	1341.7313	-	1607.9095	1607.3766	C285
241 – 266	C242	2875.4812	2876.3912	3141.6594	-	-
*56 – 70	C58	1740.8716	1740.8214	2007.0498	-	-
*82 – 87	C85	740.2925	740.3658	1006.4707	-	-
*135 –142	C136	906.4606	906.8752	1172.6388	-	-
*139 –150	C148	1462.7113	1463.0287	1728.8895	-	-
*139 –154	C148	1970.8918	1970.3505	2237.0700	-	-
*139 –154	C148	1970.8918	1970.3505	2237.0700	-	-
*351 –362	C357	1329.6486	1329.9965	1595.8268	-	-

For another modified protein IAEDANS-P450, two modified tryptic peptides both containing C334 were detected, m/z=1782.4518 (331-342, C334) and 2038.2134 (331-344, C334). A MALDI mass spectrum shows these modified peptides in Figure 4.9. No other modified peptides were detected. The summary of detected peptides is listed in Table 4.5. The results show that IAEDANS reacted with $P450_{cam}$ at C334 only, when $P450_{cam}$ contained a His-tag.

Table 4.5 **Detected IAEDANS-P450 peptides containing cysteine residues from trypsin or chymotrypsin digestion. An asterisk * denotes the chymotrypic peptides. A (-) indicates no peptides detected.**

Peptide Position	Cysteine In peptide	Unmodified Theoretical $[M+H]^+$	Unmodified Observed $[M+H]^+$	Modified Theoretical $[M+H]^+$	Modified Observed $[M+H]^+$	IAEDANS Modified cysteine
331 – 342	C334	1476.6364	1476.8965	1782.7037	1782.4518	C334
331 – 344	C334	1732.7899	1732.2822	2038.8572	2038.2134	C334
281 – 291	C285	1341.7313	1342.1118	1647.7986	-	-
241 – 266	C242	2875.4812	2876.0021	3181.5485	-	-
*56 – 70	C58	1740.8716	1740.0769	2046.9389	-	-
*82 – 87	C85	740.2925	740.3318	1046.3598	-	-
*135 – 142	C136	906.4606	906.6683	1212.5279	-	-
*139 – 150	C148	1462.7113	1462.9500	1768.7786	-	-
*139 – 154	C148	1970.8918	1970.3505	2276.9591	-	-
*351 – 362	C357	1329.6486	1330.2717	1635.7159	-	-

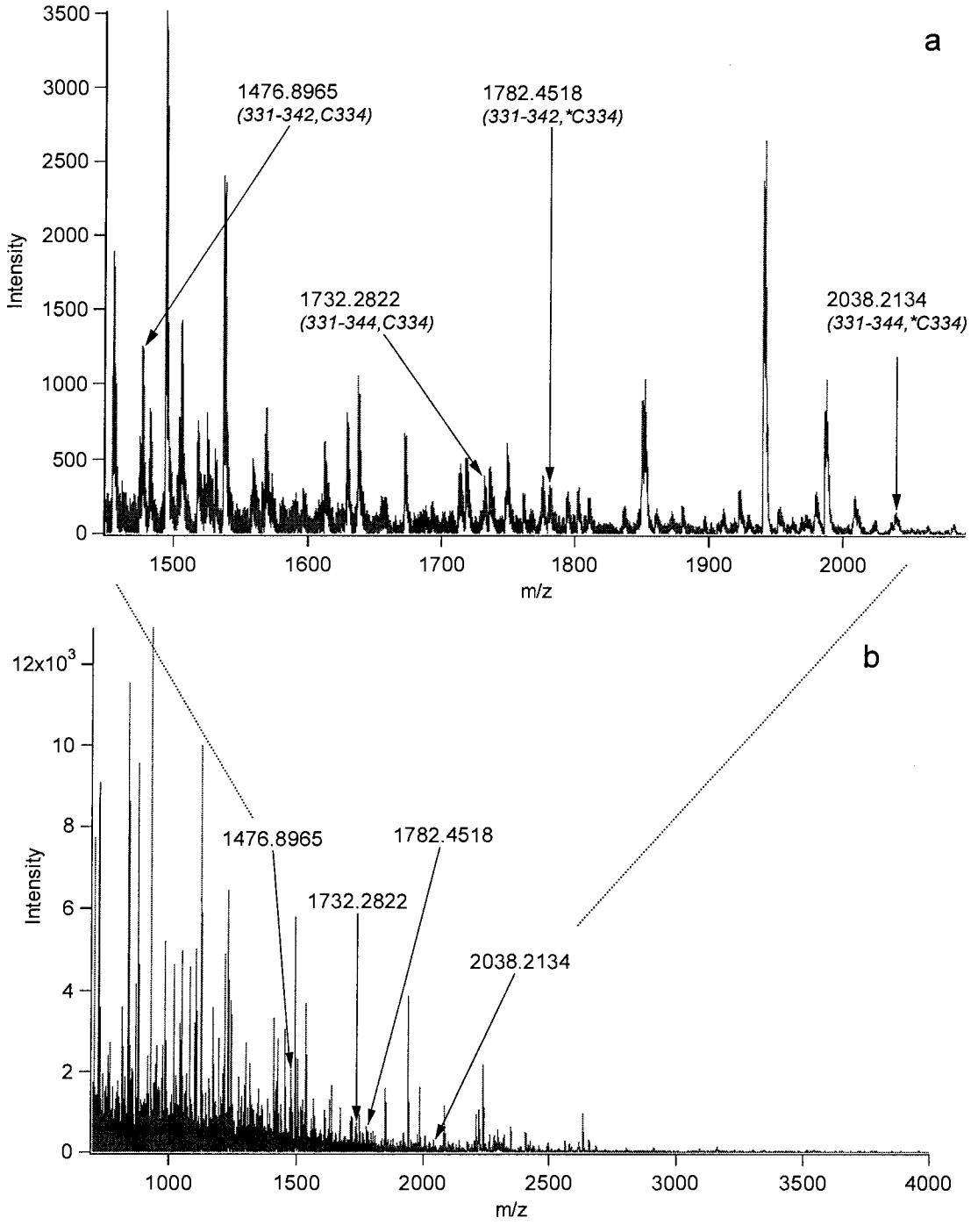

Figure 4.9 **MALDI mass spectra of tryptic IAEDANS-P450 peptides. An asterisk * denotes the modified peptide. (a) is x-axis zoom in on the modified peptide from (b).**

As discussed in the introduction, the conformation may be different between wild type $P450_{cam}$ and His-tag $P450_{cam}$. 7C-BIPY reacted with the wild type $P450_{cam}$ at the most surface exposed C334 and one cysteine residue C285 in the active access channel. IAEDANS only reacted at C334 on His-tag $P450_{cam}$ (Figure 4.10). The possible reason was that the His-tag interacted with the access channel and prevented C285 from reacting with reagent IAEDANS. The selective chemical modification sites suggested $P450_{cam}$ conformation change due to the addition of a His-tag.

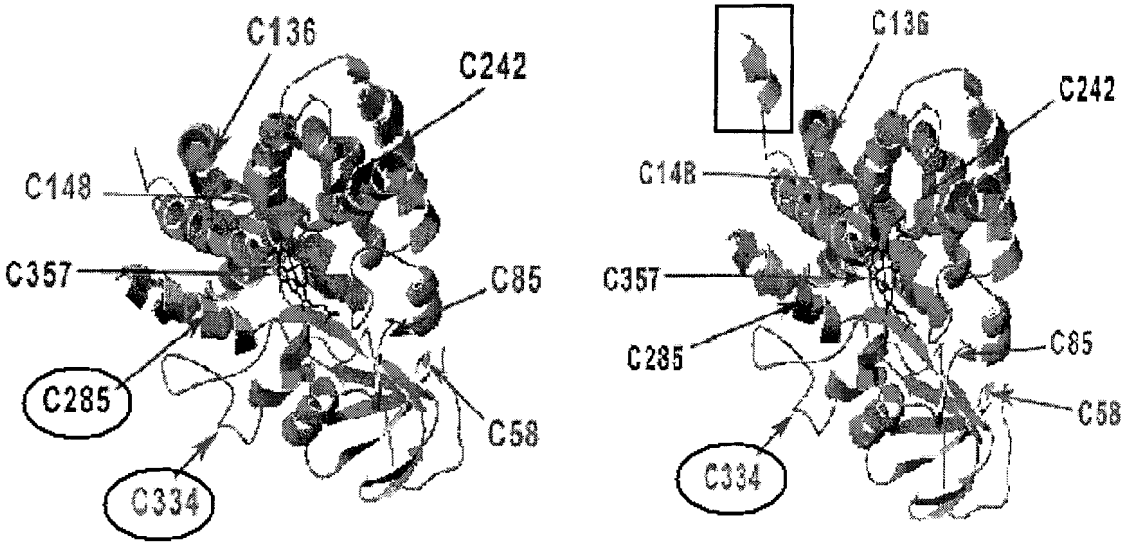

(a) Wild type P450cam

(b) P450cam containing a histidine tag

Figure 4.10 (a) Crystal structure of wild type $P450_{cam}$.[97] Its modified cysteine residues, C285 and C334 indicated by circles. (b) crystal structure of P450cam containing a histidine tag shown in rectangular, and modified cysteine residue C334 indicated by circle.

4.6 Conclusion

Two proteins, PBP2 and $P450_{cam}$, were characterized by MALDI-MS. Their chemical covalent modification sites were identified. The results showed that DNS

modified PBP2 at its lysine residues K31 and K38. The finding confirmed that the K31 and K38 were the most surface exposed lysine residues of PBP2, which was correlated with the structure analysis. This work has enabled further study of protein structure-function and protein-ligand interaction of PBP2.Wild type $P450_{cam}$ was modified by 7C-BIPY at cysteine residue C334 and C285. When a His-tag was attached to the wild type $P450_{cam}$, IAEDANS modification sites of $P450_{cam}$ were identified at C334 only. This selective modification suggested a conformational change of $P450_{cam}$.

CHAPTER 5: CHARACTERIZATION OF ION CHANNEL PROTEIN-PROTEIN INTERACTIONS

5.1 Context

This chapter describes identification of potassium voltage-gated ion channel Kv1.5 and its associated proteins by using MALDI-TOF-MS combined with co-immunoprecipitation. The aim of this study was to identify proteins that interact with Kv1.5 under physiological conditions. This was a collaborative project with Dr. David Fedida's group from the Department of Cellular and Physiological Sciences at the University of British Columbia. A Ph. D. candidate, Jodene Eldstrom, in his group performed the co-immunoprecipitation on Kv1.5, gel separation and protein trypsin digestion. I performed all MALDI-MS work and interpretation of the mass spectra data.

5.2 Abstract

Kv1.5 and its associated proteins were co-immuniprecipitated by antibodies. The mixture of proteins were separated through sodium dodecyl sulfate polyacrylamide gel electrophoresis (SDS-PAGE), followed by in-gel trypsin digestion on each gel band. The peptides recovered from the digested protein in gel bands were characterized using MALDI-MS and the masses of detected peptides were submitted to the database Mascot for peptide mass fingerprinting (PMF) search. The computer output of the peptide mass fingerprint (PMF) search suggests that synapse-associated protein (SAP97) was found from the gel co-immunoprecipitated with Kv1.5. This work provided the first mass spectral evidence of protein-protein interaction between Kv1.5 and SAP97.

5.3 Introduction

Transmembrane protein Kv1.5 is a potassium voltage-gated channel subfamily A member 5. It has six transmembrane regions. Its sequence is shown in Figure 5.1. The protein Kv1.5 in myocardium opens in response to depolarisation of potentials and shuttles positive potassium ions out of the cell. The cardiac potassium channel effects the contractility of the human heart, the propagation of the impulse and the cause of arrhythmias, which makes Kv1.5 a target for antiarrhythmic drugs.[102,103]

A family of anchoring proteins named Membrane-Associated Guanylate Kinases (MAGUK) are PDZ domain proteins that have been proposed to be involved in the localization of ion channels.[104] PDZ is named after three proteins, postsynaptic density protein (PSD-95), discs-large protein (Dlg) and zonula occludens-1 (ZO-1).[105] A PDZ domain is about 90 amino acid residues.

The synapse-associated protein (SAP97) is a PDZ domain protein, has three PDZ domains, an Src homology 3 (SH3) region and a guanylate kinase-like domain (GUK).[106] A short peptide at the C-terminal of Kv1.5 binds to the PDZ domain of SAP97 (Figure 5.2).[107] The binding has been determined by Western blot, confocal imaging of green fluorescent protein-tagged proteins and the patch clamp technique.[105,108]

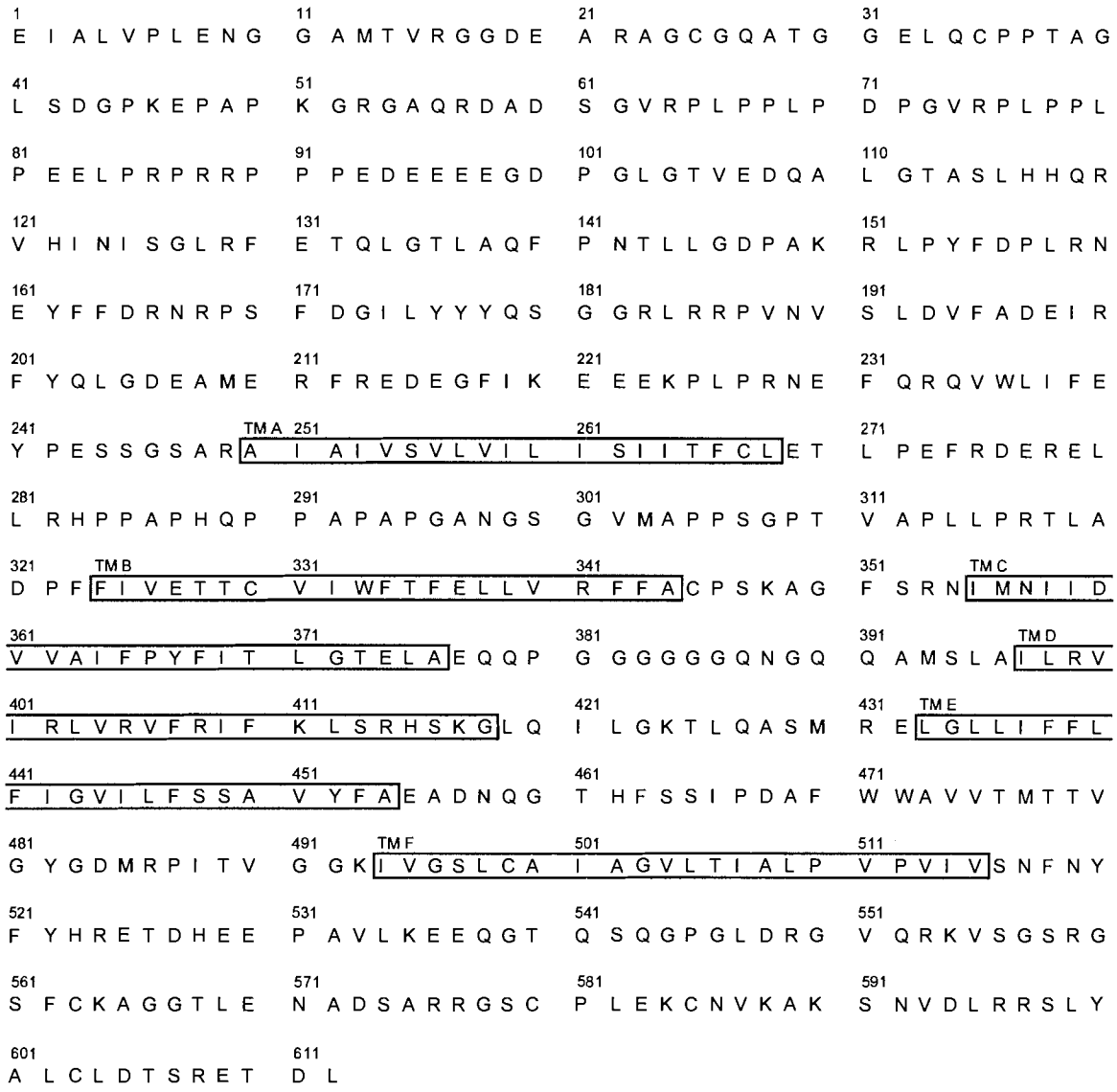

Figure 5.1 Kv1.5 sequence. The amino acid sequence that are transmembrane helices (TM) are within the rectangular boxes.

Dr. Fedida's group did not find direct evidence to support the interaction of Kv1.5 and SAP97.[103] In this collaborative project MALDI-TOF-MS was applied to identify proteins non-covalently interacting with Kv1.5.

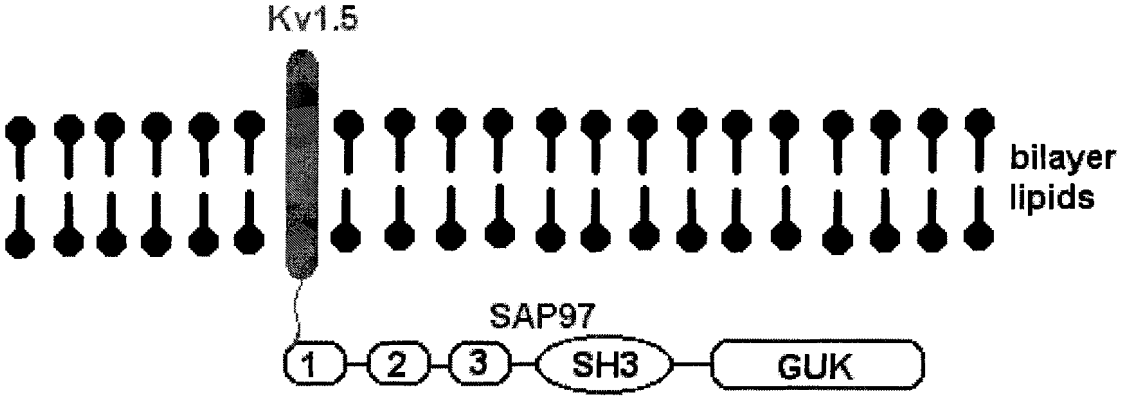

Figure 5.2 **Schematic diagram of Kv1.5 and SAP97. The circles with numbers indicate PDZ domains of SAP97. (Adapted from references).[107,109]**

Protein separation using one-dimensional (1D) or two-dimensional (2D) gel electrophoresis, followed by the MALDI peptide mass fingerprinting (PMF) has become a very popular technique for protein identification.[110]

MALDI yields the best results for an individual hydrophilic peptide relative to a hydrophobic peptide, or a peptide mixture. In this study, an antibody was used as a "bait" to "fish" out the proteins associated with Kv1.5. The protein identification was conducted by PMF using the web based search engine Mascot (Matrix Science, London UK, http://www.matrixscience.com). The strategy is summarized in Figure 5.3.

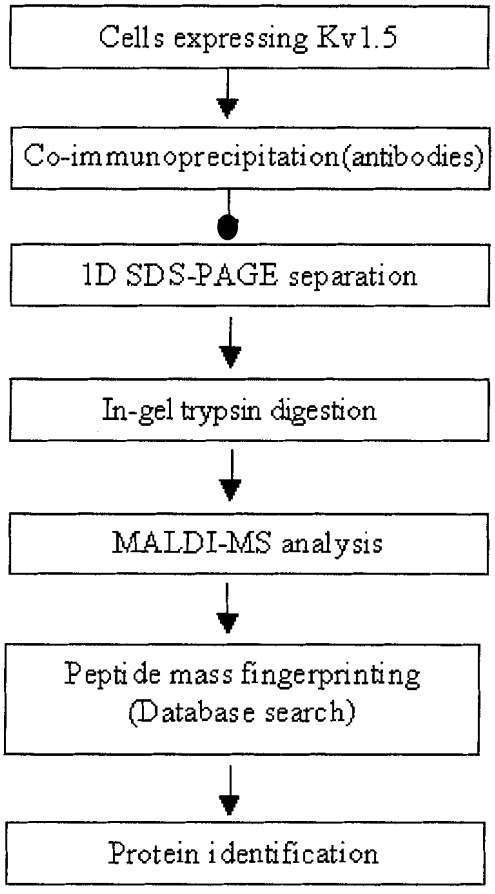

Figure 5.3 Strategy for protein identification by MALDI-MS peptide mass fingerprinting.

5.4 Experimental section

5.4.1 Kv1.5 expression in cell and co-immunoprecipitation

Jodene Eldstrom performed Kv1.5 expression in human embryonic cell line (HEK293), co-immunoprecipitation, SDS-PAGE separation and in-gel trypsin digestion. The procedure was described in detail in previous publications from Dr. Fedida's group.[102,103] Once the Kv1.5 had been immunoprecipitated, any protein in the co-immunoprecipitated complex was separated from other proteins in the cell.[111] Three antibodies, mouse anti-PDZ, rabbit C-term anti-Kv1.5 and mouse T7 tagged anti-Kv1.5

performed the immunoprecipitation. SDS-PAGE was applied to separate the protein mixture followed by in-gel trypsin digestion.

5.4.2 Sample preparation for MALDI-MS

Commercially available $ZipTip_{C18}$ (Millipore, Billerica, MA, USA) were used to desalt and concentrate the peptide samples from the solution of gel electrophoresis bands provided by Jodene Eldstrom. $ZipTip_{C18}$ is a trade name for a 10 μL pipette tip that has a 0.6 μL bed of reverse phase chromatography media fixed at the narrow end of the tip. One microliter of saturated solution of matrix CHCA in methanol and acetonitrile (v/v = 1:1) was mixed with 1 μL desalted peptide solution and deposited onto a MALDI target plate by using a pipette, and the sample was allowed to co-crystallized on the plate. Samples were analysed in duplicate.

5.4.3 Protein database search

Protein identification by peptide fingerprinting was conducted on Mascot (Matrix Science, London UK, http://www.matrixscience.com). Two protein databases were used, the National Center for Biotechnology Information (NCBInr) database and Swiss-port database. The MH^+ value of the monoisotopic peaks were submitted to Mascot protein search, and the top 20 possible proteins were reported by Mascot. The parameters in Table 5.1 were used for a typical protein search.

Table 5.1 **Parameters used in peptide mass fingerprinting database search at Mascot.**

Parameters	Value
Database	NCBInr / Swissport
Taxonomy	Homo sapiens (human)
Enzyme	Trypsin
Allow missed cleavages	2
Fixed modification	None
Variable modification	Oxidation (Methionine)
Protein mass	No specific range
Peptide tolerance	±1 Da

5.5 Results and discussion

5.5.1 SDS gel

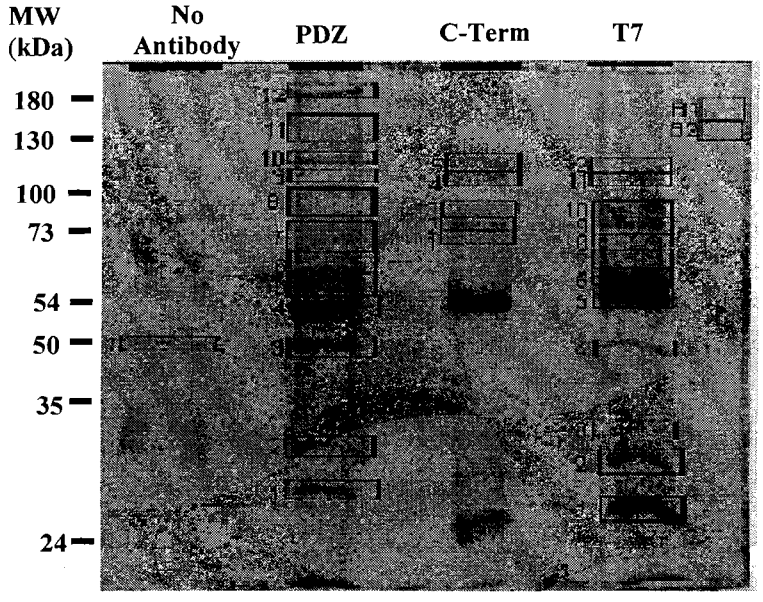

Figure 5.4 **SDS gels of Kv1.5 and its co-immunoprecipitated proteins. "MW" was the molecular mass marker, from 24 kDa to 180 kDa. The column indicated as "No Ab" was protein without using any antibody. The column of "PDZ" indicated the proteins extracted from cell with mouse anti-PDZ antibody. The "C-Term" and "T7" columns were respectively proteins extracted from rabbit C-term anti-Kv1.5 and mouse T7 tagged anti-Kv1.5 antibodies respectively. Gel bands B1 and B2 were blank gel bands. (Gel was performed by Jodene Eldstrom).**

SDS gel was used to separate the co-immunoprecipitaed proteins with Kv1.5. In Figure 5.4, antibody anti-PDZ recognized the PDZ proteins, which were under the column labelled with "PDZ", and C-term anti-Kv1.5 extracted Kv1.5 and its associate proteins, which were listed under " C-Term", the third antibody T7 tagged anti-Kv1.5 labelled as "T7" was used to extract Kv1.5 at its N-terminal site along with its associated proteins. Each gel band was exercised and performed in-gel trypsin digestion.

5.5.2 MALDI-MS analysis

Figure 5.5 is one representative MALDI mass spectrum obtained from gel band PDZ#8 in Figure 5.4. Four peaks of trypsin autolysis peptides were used as the internal standard. A total of 23 remaining peaks value (m/z) were submitted to Mascot. A representative MALDI mass spectrum of gel band T7 #10 is also presented in Figure 5.6. Four trypsin autolysis peptides were detected. The remaining 49 detected peaks were submitted to Mascot research.

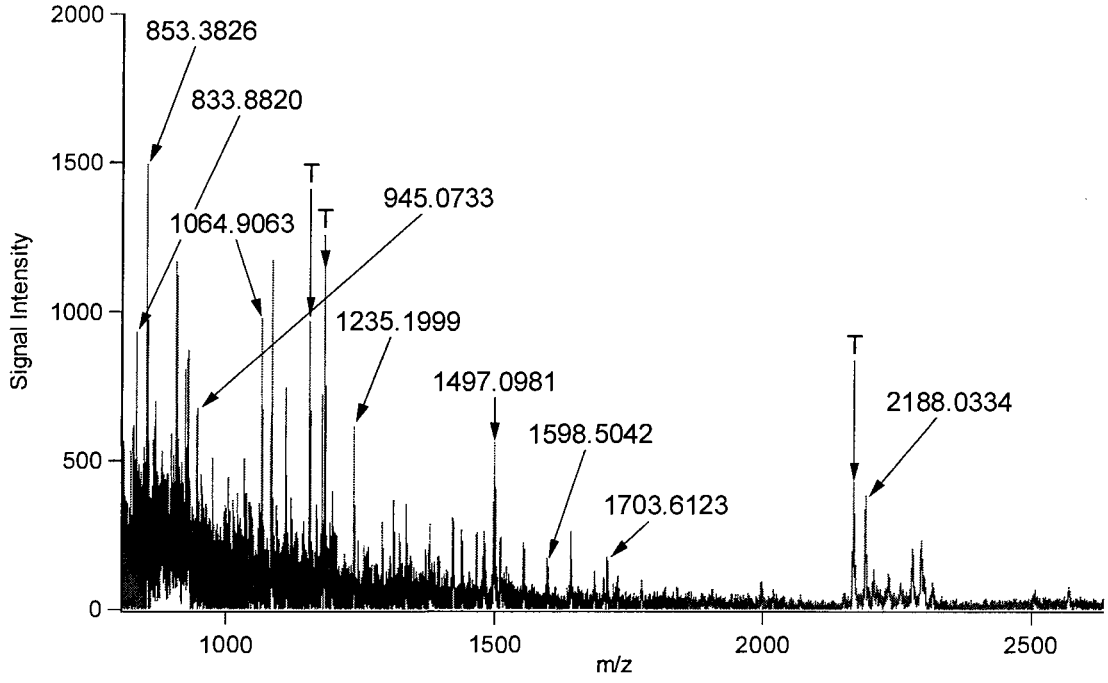

Figure 5.5 **A MALDI mass spectrum of gel band PDZ #8. The letter "T" indicates the trypsin autolysis peaks.**

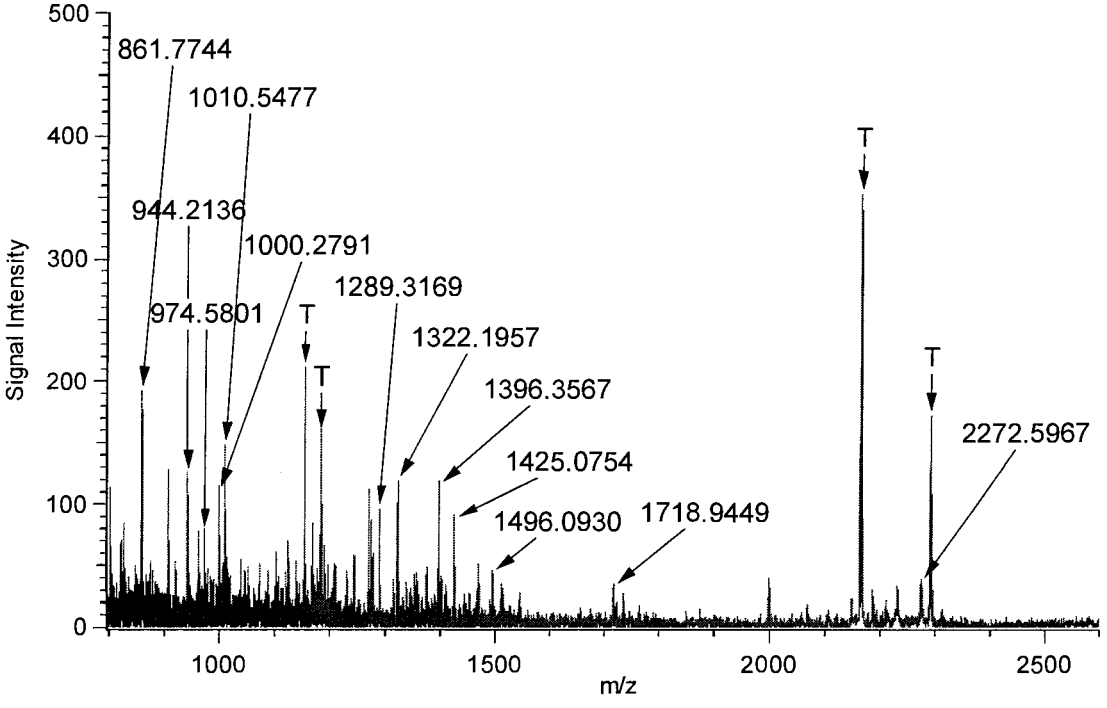

Figure 5.6 **A MALDI mass spectrum of gel band T7 #10. Letter "T" indicates the trypsin autolysis peak.**

5.5.3 Protein identification

The peaks obtained from MALDI mass spectra were manually submitted to Mascot for peptide mass fingerprinting search (Table 5.3 and 5.4). Two databases, the National Center for Biotechnology Information database (NCBInr) and Swiss-prot database (Swiss-prot), were used in the protein search. The probability for the observed match between the experimental data and each database was calculated. The match with the lowest probability is reported as the best match. The probability for a good match is a small number. The Mascot score is $-10\text{Log}_{10}(P)$, where P is the probability. [112] The best match is the one with the highest score, and a significant match is a score of the order of 70.[112]

The results from the two databases, NCBInr and Swiss-prot, were consistent. A protein "Synapse-associated protein 97 (SAP97)" was identified in gel band PDZ#8 and T7#10 with Mascot scores of 66 and 99 respective. Table 5.2 summarizes the results from the Mascot search. SAP97 has a mass of 103158 Da. The mass of PDZ #8 and T7 #10 was ~100 kDa in gel (Figure 5.4).

Table 5.2 Summary of the Mascot search results of gel band PDZ#8 and T7#10.

Gel band	Identified protein	Mascot score (NCBInr / Swiss-Prot)	Molecular weight (Da)	Number of peptides matching	Number of peptides submitted	Sequence coverage
PDZ#8	SAP97	66 / 66	103158	18	23	18%
T7#10	SAP97	99 / 99	103158	34	49	27%

5.5.4 Protein-protein interaction site

Three antibodies, mouse anti-PDZ, mouse T7 tagged anti-Kv1.5 and rabbit C-terminus anti-Kv1.5, were used to co-immunoprecipitate Kv1.5 and its associated proteins in cell HEK923.

The mouse Anti-PDZ antibody recognized PDZ domain proteins including SAP97. The MALDI-MS results showed that one gel band, PDZ#8, was identified as SAP97, which suggested that SAP97 was interacting with Kv1.5 in the human embryonic cell line (HEK293).

The mouse T7 tagged anti-Kv1.5 recognized Kv1.5 at its N-terminus. SAP97 was also found in one of its gel bands, T7#10. When Kv1.5 was immunoprecipitated with anti-Kv1.5, its associated proteins were co-immunoprecipitated, which suggested that Kv1.5 had strong interactions with SAP97. In addition, this interaction was not at the N-term of Kv1.5.

The rabbit C-terminus anti-Kv1.5 was bound with Kv1.5 at its C-terminus. When the C-terminus anti-Kv1.5 recognized Kv1.5 at its C-termininus, the interaction between Kv1.5 and its associated proteins at C-terminal side of Kv1.5 was destroyed. Therefore, the proteins binding to Kv1.5 at its C-terminal side were not co-immunoprecipitated with Kv1.5. SAP97 was not identified by MALDI-MS in the gel bands co-immunoprecipitated with C-term anti-Kv1.5 antibody.

The results from interaction sites of three antibodies and the corresponding Mascot protein searches indicated that SAP97 interacted with Kv1.5 at its C-terminus.

5.6 Conclusion

Co-immunoprecipitation following by MALDI-TOF-MS was used to investigate the ion channel Kv1.5 and its associated proteins. The results showed that SAP97 interacted with Kv1.5 at its C-terminus. This is the first mass spectral evidence in support of the protein-protein interaction between Kv1.5 and SAP97. This work demonstrated that MALDI-MS has great potential to identify membrane proteins and providing mass spectral evidence of protein-protein interaction in complex "real" cells.

Table 5.3 Identification of peptides from gel band PDZ #8.

Identity	Peptide position	Theoretical $[M+H]^+$	Observed $[M+H]^+$	Mass accuracy (ppm)
SAP97	10-27	2188.1361	2188.2092	33
	21-30	1245.6551	1244.8430	-652
	297-307	1234.7159	1235.1999	392
	304-309	834.5313	833.8820	-778
	316-323	1003.6225	1004.0015	378
	452-465	1598.8501	1598.5042	-216
	561-576	1702.7376	1703.6123	514
	577-586	1237.7016	1236.9929	-573
	654-662	1064.6467	1064.9063	244
	665-673	1038.4856	1038.8179	320
	665-674	1194.5867	1195.0844	417
	682-687	829.4612	828.7425	-866
	773-779	853.3691	853.3826	16
	780-792	1685.7593	1685.5509	-124
	855-872	2210.0367	2210.8247	357
	866-873	974.5270	974.5843	59
	874-880	898.4456	897.8409	-673
	907-925	2218.1759	2218.0334	-64
Trypsin	126-136	1153.5741	1153.6007	23
	208-216	1182.5981	1182.6112	11
	50-69	2163.0570	2163.0823	12
	70-89	2289.1549	2289.2478	41
Unidentified			945.0733	
			1322.0657	
			1497.0981	
			2166.2539	
			2203.2732	

Table 5.4 Identification of peptides from gel band T7 #10.

Identity	Peptide position	Theoretical $[M+H]^+$	Observed $[M+H]^+$	Mass accuracy (ppm)
SAP97	10-27	2188.1361	2188.2092	33
	21-30	1245.6551	1244.8430	-652
	297-307	1234.7159	1235.1999	392
	304-309	834.5313	833.8820	-778
	316-323	1003.6225	1004.0015	378
	452-465	1598.8501	1598.5042	-216
	561-576	1702.7376	1703.6123	514
	577-586	1237.7016	1236.9929	-573
	654-662	1064.6467	1064.9063	244
	665-673	1038.4856	1038.8179	320
	665-674	1194.5867	1195.0844	417
	682-687	829.4612	828.7425	-866
	773-779	853.3691	853.3826	16
	780-792	1685.7593	1685.5509	-124
	855-872	2210.0367	2210.8247	357
	866-873	974.5270	974.5843	59
	874-880	898.4456	897.8409	-673
	907-925	2218.1759	2218.0334	-64
Trypsin	126-136	1153.5741	1153.6007	23
	208-216	1182.5981	1182.6112	11
	50-69	2163.0570	2163.0823	12
	70-89	2289.1549	2289.2478	41
Unidentified			945.0733	
			1322.0657	
			1497.0981	
			2166.2539	
			2203.2732	

CHAPTER 6: A STUDY OF GAS-PHASE CATIONIZATION IN MALDI-MS

6.1 Context

This chapter describes a study of gas phase cationization in MALDI. The objectives of this study are: (1) to provide experimental results of the gas-phase cationization by using a single laser simultaneously irradiating two adjacent samples, (2) to investigate the effect of separation distance on cationization, (3) to examine the potential application of quantitative measurement.

6.2 Abstract

Gas-phase cationization is often observed with synthetic polymers in MALDI mass spectra. To better understand this type of ionization process in MALDI, a very simple two-plate method was developed. Polyethylene glycol (PEG) and cation reagents were separately deposited on two adjacent plates. A single laser irradiated both samples simultaneously. The cation adducts of PEG were observed in the MALDI mass spectrum. The relative extent of cationization based on relative signal intensity depended on the separation distance of PEG and cation reagents and the type of cation. These experimental results support the gas-phase cationization mechanism. The two-plate method was also investigated with respect to its potential to perform quantitative analysis. A linear response using the two-plate method was observed over 2 decades of analyte concentration with the correlation coefficient R^2 value of 0.9657.

6.3 Introduction

Cation adducts of synthetic polymers are often observed in MALDI mass spectrum.[113] A better understanding of the cationization process in MALDI could lead to improved ion yields, determine polymer molecular weight distribution, and increase sensitivity. To better understand the cationization process, several questions need to be addressed. Where and when do the detected analyte ions form? Are the ions formed in the mixture of molecule and cation (solution or solid state)? Or are they formed in the gas phase from ion-molecule reaction?

6.3.1 MALDI laser induced plume

The plume generated by MALDI laser is considered to be a pulsed jet expansion, transformation from solid state to gas state, where the matrix molecules, analyte molecules, and cation ions collide in the plumes. The image of the plume has been obtained using laser induced fluorescence (LIF).[43,45]

The results of recent studies show that the plume induced by UV laser irritation lasts about 35-70 ns with a plume velocity of 500-1000 m/s.[46,47,114] The jet expansion causes the radial component of the velocity to be considerably smaller than the axial velocity.[40,45,115] The "axial" direction is towards the time-of-flight mass spectrometer. The direction of "radial" is perpendicular to the axial direction. The plume density is up to 10% of the pre-desorption solid.[46,47]

6.3.2 Preview study on gas-phase cationization in our group

Our group studied the cationization by using the wall-less sample preparation method.[52,53] The electrodynamic balance (EDB) was used to deposit two different

samples on two adjacent sample spots. One of the samples was polyethylene glycol with an average molecular weight of 1000 (PEG1000) with a matrix of CHCA, Another sample was cation reagent CsCl with CHCA. A single laser irradiated the two adjacent sample spots simultaneously. Two MALDI laser induced plumes formed containing neutral molecules PEG1000 and Cs^+ respectively. When the separation distance was close enough that the two plumes overlapped, PEG 1000 collided with Cs^+, cesium adducts of PEG formed and detected by MALDI-MS (Figure 6.1). The experimental results provided evidence of gas-phase cationization.[53]

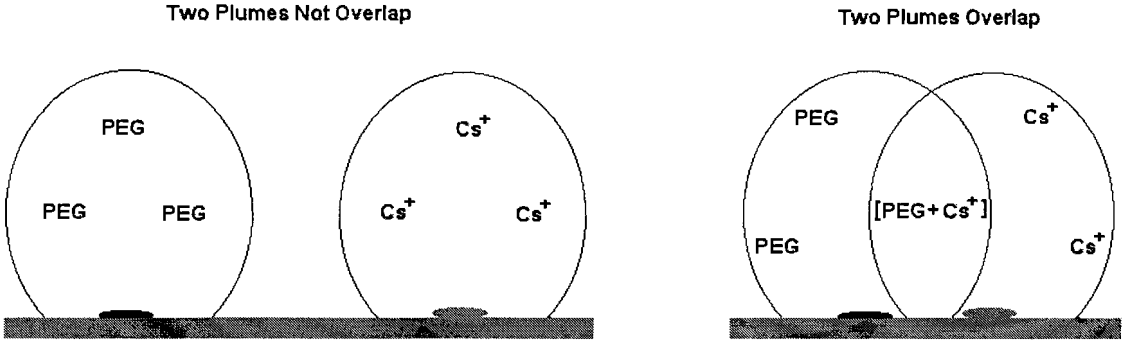

Figure 6.1 Schematic diagram of the gas-phase cationization (Adapted from reference)[53].

6.4 Experimental section

6.4.1 Two-plate method

We developed a very simple two-plate method based on the two spots method to further analyze the gas-phase cationization. Two laboratory made stainless steel plates were used as the two sample plates, which could be fixed on a plate holder with electrically conductive tape. The distance between the two sample plates was 0-100 μm. A laser simultaneously irradiated the two sample plates.

The advantages of the two-plate method include: (1) providing exclusive secondary pathway; (2) applying a simple sample preparation method, (3) analyzing samples under normal MALDI conditions, and (4) requiring no extra experimental apparatus.

The two sample plates and plate holder were made of stainless steel, which are chemically stable under laser irradiation. A standard MALDI plate was machined to hold two sample plates (55 mm × 41 mm × 2 mm) with a depth of recessed region (40 mm × 30 mm × 1 mm) in the centre. The dimension of each sample plate was (28 mm × 18 mm × 1 mm) (Figure 6.2a). When the sample plates were placed into the recessed region of the plate holder, the top side of the sample plates was the same height as the edge of the holder plate.

Using the same heights for the plates ensured there were no obstacles in loading or unloading of the samples from the MALDI vacuum chamber. These conditions also minimized that as a source of error in the maintained the same flight length for the analyte ions. Otherwise the mass accuracy would be degraded.

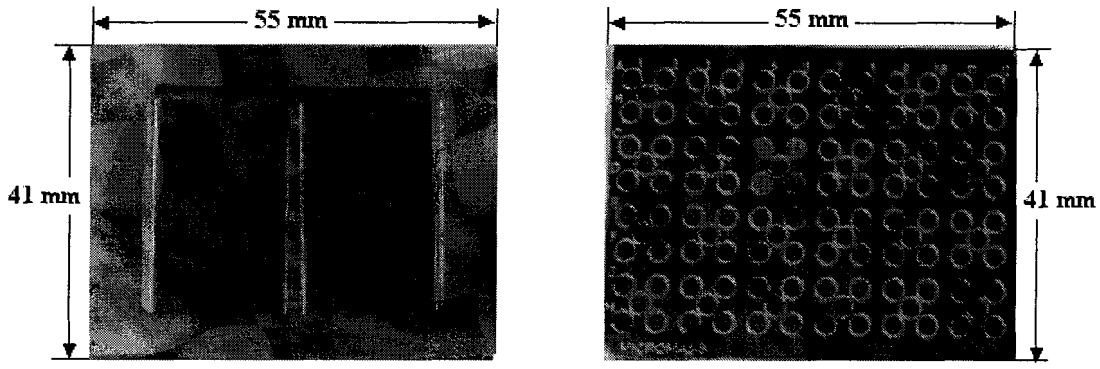

(a) a two-plate mode (b) a standard MALDI target plate

Figure 6.2 Photographs of the two-plate and a standard MALDI target plate. (a) Two sample plates on top of the plate holder, (b) a standard MALDI target plate, the circles are sample wells with diameter 3.0mm.

PEG1000 was used as the neutral molecule source, and CsCl and KCl were used as the cation reagents. Equations 6.1 and 6.2 express the gas-phase cationization process.

$$EO_X + Cs^+ \rightarrow [EO_X + Cs^+] \qquad (6.1)$$

$$EO_X + K^+ \rightarrow [EO_X + K^+] \qquad (6.2)$$

Where EO is an ethylene oxide unit of polyethylene glycol, and x is the degree of polymerisation.

6.4.2 Sample preparation on two sample plates

PEG1000 was dissolved in methanol aqueous solution (0.1 mM, methanol: water=1:1, v/v). Matrix CHCA was saturated in methanol. A 1 μL PEG1000 solution was

mixed with 9 μL CHCA solution. Then the mixture of PEG and CHCA was deposited on the edge of one sample plate.

One microliter of a CsCl or KCl solution (2 M in water) was mixed with 9 μL of the CHCA solution and deposited onto the other sample plate. After the samples co-crystallized and were completely dry, the two sample plates were placed side-by-side on the plate holder, and fixed with electrically conductive tapes. The two prepared plates were investigated using an optical microscope (Motic, B5 Professional, Richmond, BC, Canada). Their separation distance ranged from 0 to 60 μm. The gas-phase cationization was examined as a function of the separation distance of PEG and cation reagents. A single nitrogen UV laser (beam spot 650 μm × 450 μm) irradiated both samples simultaneously.

6.4.3 Sample preparation for quantitative study

Instrument limitations of detection, such as detector saturation from analyte or standard ion signal peaks, lead to sub-optimal dynamic range.[116,117] Another problem for quantitative measurement is the signal suppression of the less concentrated component (analyte or standard) by the more concentrated component.[117] The range of linear response and the correlation coefficient of analyte were examined.

Peptides angiotensin I (theoretical m/z =1296.6833) and bradykinin (fragment 2-9) (theoretical m/z =904.4667) were used as the standard and analyte respectively. Matrix CHCA was saturated in a solution of acetonitrile and methanol (v/v=1:1).

Five microliters of an angiotensin I (1 μM) was mixed with 5 μL of CHCA solution and deposited on one sample plate to form a sample spot area of 10 mm ×

2.5mm. Analyte bradykinin (2-9) at concentrations from 0.01 to 6 μM was studied. A 5 μL of bradykinin (2-9) solution was mixed with 5 μL of a CHCA solution and deposited on the other plate. The spot of co-crystallized bradykinin and CHCA was about the same size of angiotensin I sample spot. The laser irradiated both sample spots simultaneously. The laser beam spot is 650 μm × 450 μm. The separation distance between the two plates was 40 μm.

The conventional quantitative method by using an internal standard was studied in order to compare the two-plate quantitation method. A mixture solution consisted of 2.5 μL angiotensin I solution (2 μM, internal standard), 2.5 μL bradykinin solution (concentration ranged from 0.02 to 12 μM) and 5 μL CHCA solution was deposited on the sample plate. The MALDI mass spectra were collected under the same condition as the two-plate method.

6.5 Results and discussion

6.5.1 Evidence of gas-phase Cs^+ reaction with PEG1000

Co-crystallized CsCl and CHCA was on the one sample plate (Figure 6.3a), PEG1000 and CHCA were co-crystallized on other sample plate (Figure 6.3b). The separation distance was 8 μm. A single laser irradiated three different positions.

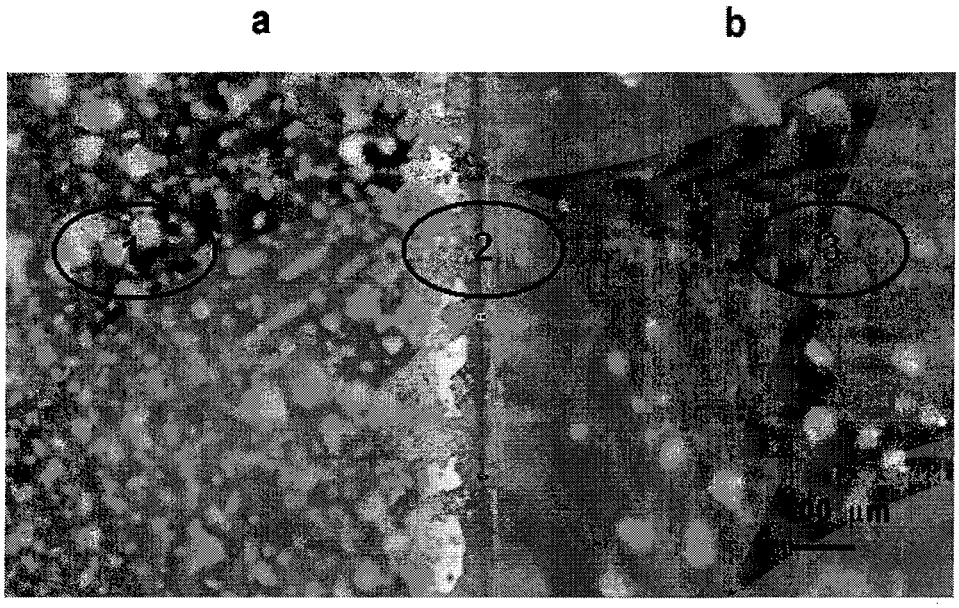

Figure 6.3 **A microscope image of two plates covered by co-crystallized analytes with matrix CHCA. (a) CsCl co-crystallized with CHCA. (b) PEG1000 co-crystallized with CHCA. The circles with number indicate the position of laser irradiations. Position 1, where laser irradiated CsCl. Position 2, where laser irradiated simultaneously at both samples, CsCl and PEG1000. Position 3, where laser irradiated PEG1000.**

The MALDI mass spectrum (Figure 6.4a) showed that the Cs^+ ion was detected when laser irradiated position 1. Ion signal from matrix ions and clusters was not observed in the spectrum due to suppression by Cs^+. When the laser irradiated at position 3, the MALDI mass spectrum (Figure 6.4b) showed no cesium adducts of PEG were detected. At position 2, the laser irradiated both samples, the cesium adducts of PEG were observed as the dominant signal in the mass spectrum (Figure 6.4c).

The detected cesium adducts of PEG in MALDI mass spectrum indicated that the cationization took place in the gas phase.

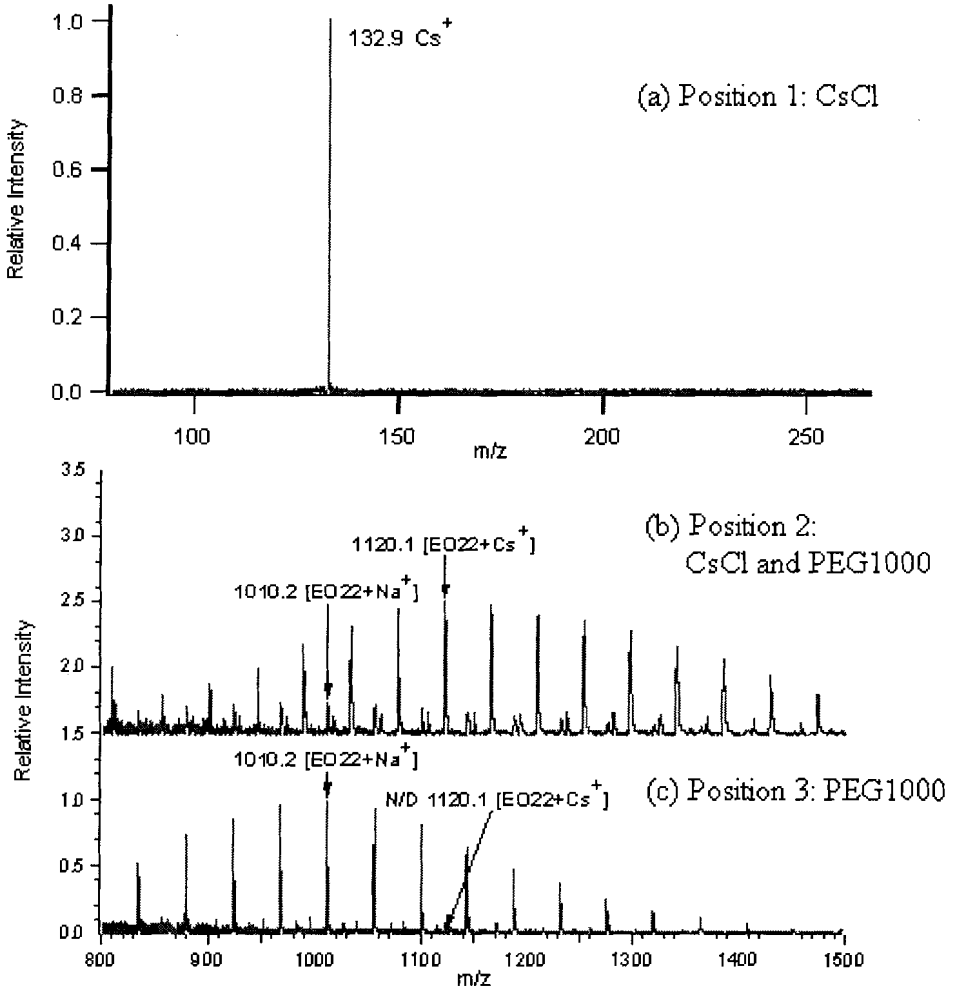

Figure 6.4 **MALDI mass spectra with laser irradiation different positions 1, 2, 3, in Figure 6.3. (a) Mass spectrum from laser irradiate position 1, where was the co-crystallization of CsCl and CHCA, (b) mass spectrum from laser irradiate position 2, where was CsCl and PEG1000 simultaneously, (c) mass spectrum from laser irradiate position 3, where was co-crystallized PEG1000 and CHCA. N/D: not detected.**

6.5.2 The effect of cation and separation distance on gas-phase cationization

(1) Cs^+ reaction with PEG1000 in gas-phase

Sodium and potassium impurities in the PEG sample and glassware were difficult to remove. Sodium adducts of PEG were used as an internal standard. The intensity ratio of cesium adducts of PEG verse sodium adducts of PEG were used to investigate Cs^+

reaction with PEG in gas phase. The cationization of PEG (EO19, EO22 and EO23) were examined. Here EO was the ethylene oxide unit of PEG, the number X was the degree of polymerization. Their average ratio was plotted in Figure 6.5.

The average intensity ratio was decreased as the separation distance between PEG and CsCl increased (Figure 6.5). No cesium adducts of PEG were observed when the separation distance was greater than 20 ± 2 μm.

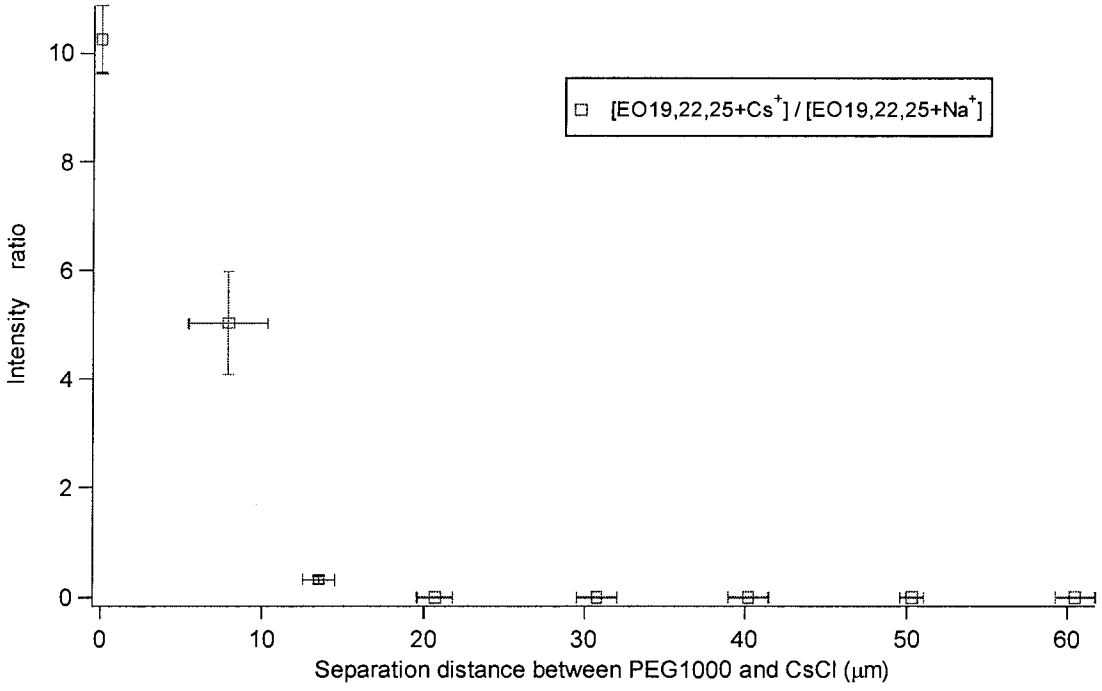

Figure 6.5 Separation distance effect on gas-phase cesium reaction with PEG1000.

(2) K^+ reaction with PEG1000 in gas-phase

The gas-phase cationization of PEG by KCl was also studied. The intensity ratio of potassium adducts of PEG to sodium adducts of PEG was used to investigate K^+ reaction with PEG in gas phase. The level of impurity K^+ in PEG1000 and glassware was measured to be 0.078, and that intensity ratio of potassium adducts of PEG to sodium

adducts of PEG in PEG sample was considered as background signal. Therefore a value of 0.078 was subtracted from the intensity ratio of potassium adducts to sodium adducts measured from the gas-phase cationization.

The intensity ratio dropped as the separation distance between PEG and KCl increased (Figure 6.6). When the separation distance was equal to or greater than 40 μm, the detected intensity of sodium adducts of PEG became the same as that detected in the PEG sample only.

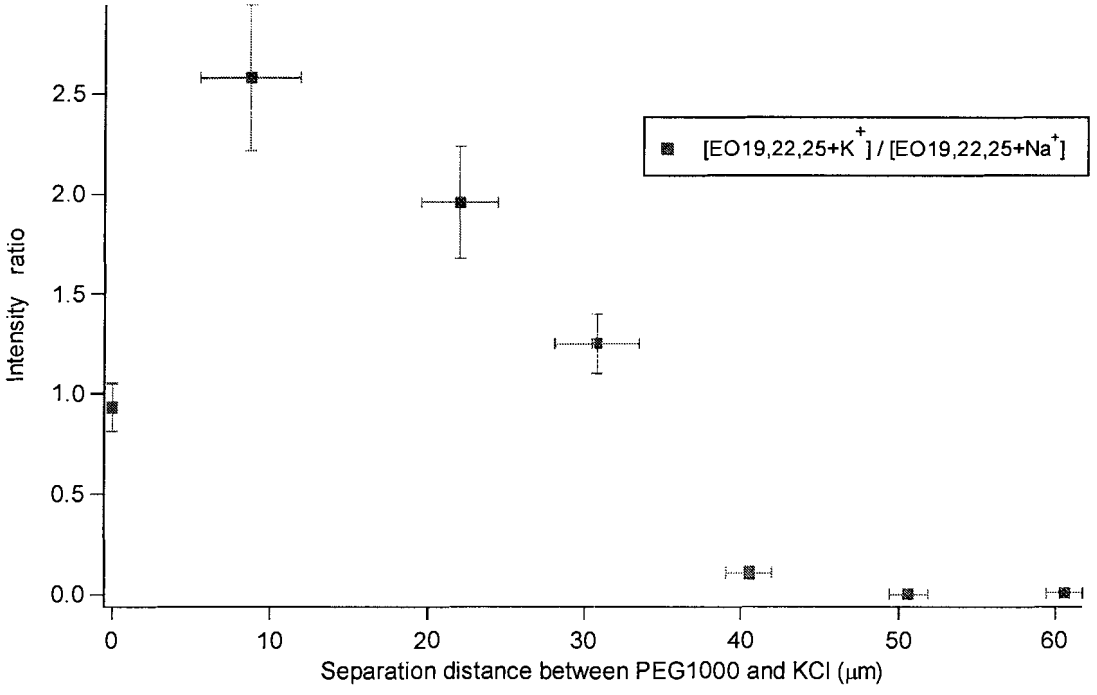

Figure 6.6 Separation distance effect on potassium reaction with PEG1000 in gas phase.

(3) Comparison cation reagents effect on gas-phase cationization

In order to better compare the two different cation reagents, CsCl and KCl, reaction with PEG in gas phase, the data plotted in Figures 6.6 and 6.7 were combined

into one figure (Figure 6.7). We found K^+ reacted with PEG at separation distance up to 40 μm whereas Cs^+ reacted with PEG at separation distance <13 μm. The results suggested that the radial velocity of K^+ was greater than that of Cs^+. This is consistent with the results from other research group, different species of analytes have different radial velocities.[43,45]

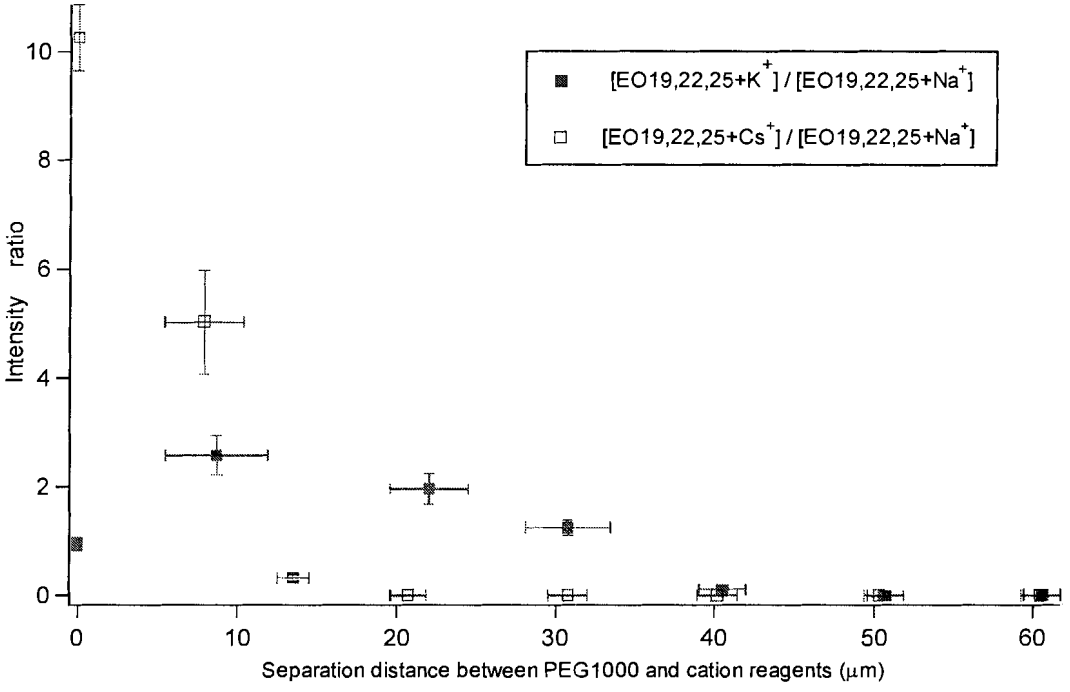

Figure 6.7 Separation distance effect on cationization of PEG in gas phase.

In addition, the intensity ratios of cesium adducts was greater than that of potassium adducts at the same separation distance at the range ≤ 10 μm. A possible reason for this was that the MALDI laser desorption efficiency of Cs^+ was greater than that of K^+, which resulted in an abundance of Cs^+ in the plume to be greater than K^+. To examine the assumption, a mixture of KCl and CsCl at the same concentration (2 M) was measured by MALDI. The mass spectrum (Figure 6.8) confirmed that Cs^+ has better

desorption efficiency in MALDI than K^+. And there was also the possibility that there was a mass and detection bias for Cs^+ versus K^+.

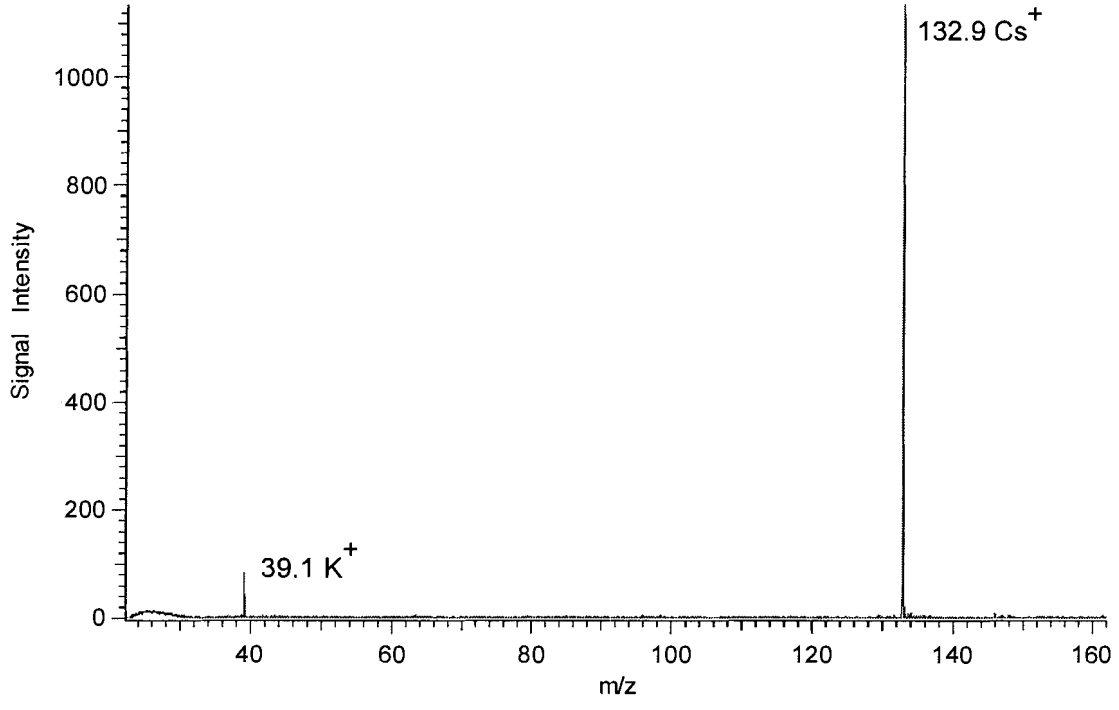

Figure 6.8 MALDI mass spectrum of KCl and CsCl.

6.5.3 Potential for improved quantitative analysis using two-plate methodology

Analyte bradykinin (2-9) concentration range from 0.01 μM to 10 μM was examined while the standard angiotensin I at concentration of 0.1 μM was fixed. When the concentration of bradykinin (2-9) was greater than 5 μM, the MALDI signal of bradykinin (2-9) was saturated, which was not suitable for quantitative measurement. When the concentration of bradyknin (2-9) was below 0.05 μM, the MALDI ion signal of standard, angiotensin I (0.1 μM), was saturated. When the sample ion intensity is saturated, there is significant deviation from a linear relationship between concentration

and signal intensity. The linear response of bradyknin (2-9) at concentration range between 0.05 μM to 5 μM was therefore investigated and plotted in Figure 6.9.

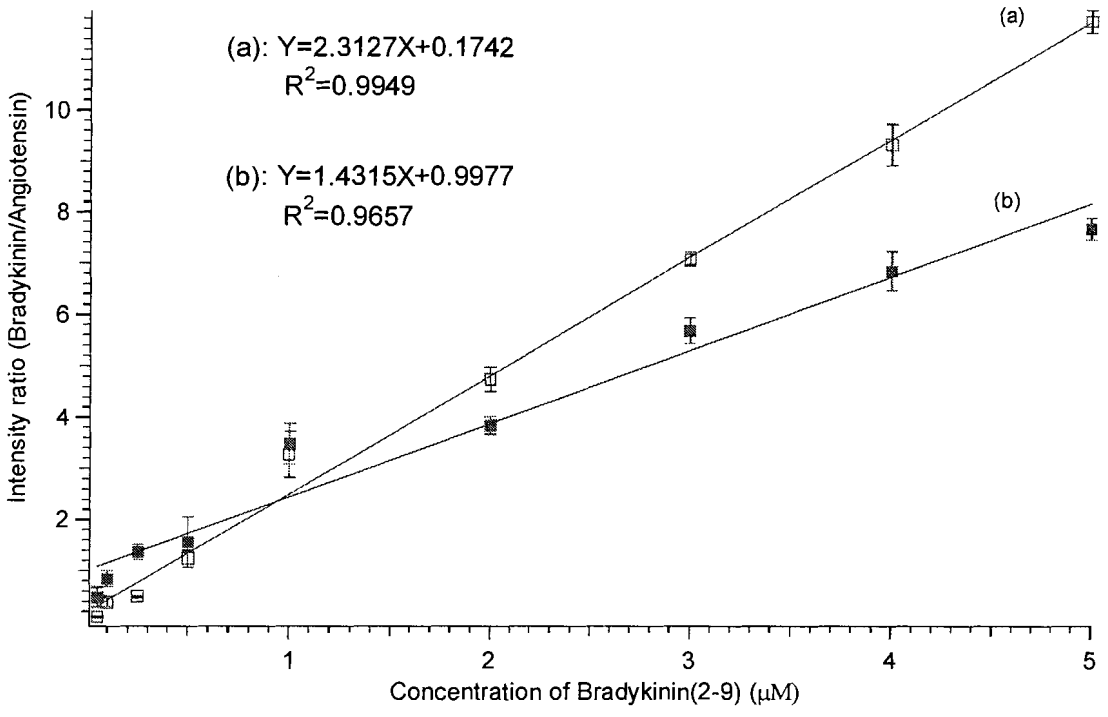

Figure 6.9 **Linear response of bradykinin (2-9) by (a) internal standard method using mixture of analyte bradykinin and standard angiotensin, and (b) a two-plate method with analyte bradykinin on one sample plate and standard angiotensin on another sample plate.**

The linear response of bradykinin (2-9) when using the two-plate method showed that it was comparable to that using an internal standard method (Figure 6.9). At the same dynamic range (0.05 μM – 5 μM), the correlation coefficient value of R^2 for two-plate method was 0.9657, which was slightly less than that of the internal standard method, 0.9949.

The possible reason for the difference of R^2 value was the co-crystallized sample hetegeneity. In MALDI-MS analysis, the "sweet" spots were always searched since the sample was not homogeneity.[116,117] The signal reproducibility "spot-to-spot" was

poor.[116,117] In the internal standard method, the standard co-crystallized with analyte, in which the mixture likely compensated for the sample hetegeneous problem.[116,117]

6.6 Conclusion

A very simple two-plate method was developed and used to study the gas-phase cationization. The results provided experimental data in support of the cation reaction with polymer molecules in gas-phase. The study also found that K^+ reacted with PEG1000 at a greater separation distance that Cs^+. The method of a single laser irradiating two adjacent sample spots simultaneously was also shown its potential for performing quantitative analysis, the results were comparable to the existing methodology.

CHAPTER 7:
CONCLUSION AND FUTURE WORK

MALDI-MS has become a popular tool for proteomics research. It is a relatively new analytical technology that has as its features, relatively simple sample preparation, high mass resolution up to 35,000,[50] as low as femtomole detection[4] and straightforward interpretation of mass spectrum[118]. This thesis described applications of MALDI on proteins or peptides study, such as protein primary structure, sequence coverage of membrane protein, chemical modification sites of protein and ion channel protein-protein interactions.

Hydrophobic proteins including membrane proteins are a challenge for MALDI-MS detection due to their hydrophobic property. Some factors were examined for their performance on hydrophobic protein or peptides in this thesis. (1) We found that the anionic detergent SDS at a low concentration could increase the sequence coverage of a membrane protein bacteriorhodopsin. (2) Three common matrices, CHCA, SA and DHB, were investigated. The results showed that the least polar matrix SA gave the highest sequence coverage of bacteriorhodopsin by the dried-droplet method. (3) Wall-less sample preparation method involving an EDB was demonstrated to be a complementary method with the traditional dried-droplet sample preparation method. A total of 89% sequence coverage of bacteriorhodospin was obtained through a combination of these two sample preparation methodologies.

Another useful application of MALDI is to identify the chemical modification sites of proteins. In chapter 4, two proteins, pheromone binding protein 2 and cytochrome $P450_{cam}$, were modified by chemical reagents. The sites of their covalent modifications were characterized using MALDI-MS. The capability to track such modifications enables investigation of protein topology, structure and function.

Ion channel Kv1.5 is another membrane protein studied in this thesis. Co-immunoprecipitation followed by SDS gel separation, in gel trypsin digestion and MALDI-MS was used to identify a physiologically relevant associated protein. The masses of peptides detected using MALDI were submitted to protein database for peptide mass fingerprinting search. SAP97 was identified. It was also found that SAP97 interacted with Kv1.5 at the C-terminal side of Kv1.5. This mass spectral evidence supported the protein-protein interaction of Kv1.5 and SAP97.

We conducted MALDI gas-phase cationization studies to better understand one type of ionization pathways in this soft ionization technique. We developed a simple two-plate method to examine two adjacent sample spots irradiated by one single laser simultaneously. This two-plate method provides an exclusive pathway to examine the gas-phase reaction. The results provided evidence to support the gas-phase cationization mechanism. We also found that Cs^+ could form adducts of PEG1000 at further separation distance than that of K^+, which helps to characterize the MALDI laser induced plume.

Currently, room temperature ionic liquid matrices are being studied in our group, which in principle are well-suited for the wall-less sample preparation method. Due to the diameter of the orifice in the droplet dispenser is as small as 40 μm, the common solid matrices solution sometimes crystallized at the tip of dispenser during sample

preparation. Use of a liquid matrix could solve this problem. The ionic liquid matrix also minimizes searching for a "sweet spot" by improving homogeneity across the sample, reducing the background noise and improving signal reproducibility.[119-123]

In the future, a non-polar or very weak polar matrix could be examined and evaluated based on its performance of sequence coverage of hydrophobic proteins. The relative polarity of three most common matrices used and their effect on sequence coverage of bacteriorhodopsin were monitored in chapter 3. SA (the least polar matrix) compared to CHCA and DHB gave the highest sequence coverage (SA:59%, CHCA:38% and DHB:31%, using the dried-droplet method). However, these three matrices are all still quite polar molecules. In order to better understand the interaction of matrix and hydrophobic proteins or peptides, as well as the effect on MALDI-MS detection, a non-polar or very weak polar matrix could be examined.

Due to the matrix absorbing the UV laser energy via electronic excitation,[41] most matrices are aromatic compounds, e.g. benzoic derivatives (e.g. DHB) or cinnamic acid derivatives (e.g. SA and CHCA).[27,38] It is very difficult to find a non-polar compound as UV MALDI matrix. The compound dithranol is polar though, it should be studied. Its chemical structure is shown in figure 7.1. Dithranol is mostly used as a matrix to detect synthetic polymers. In a method proposed by Hoteling and Owens, the HPLC retention time of matrix SA was 4.12 min, while it was 7.66 min for dithranol.[80] The difference between retention times indicated that dithranol is much less polar than SA. Based on the finding from chapter 3, the least polar matrix obtained the highest sequence coverage of hydrophobic protein. It is anticipated that dithranol could generate even better sequence coverage of hydrophobic proteins than common more polar matrices.

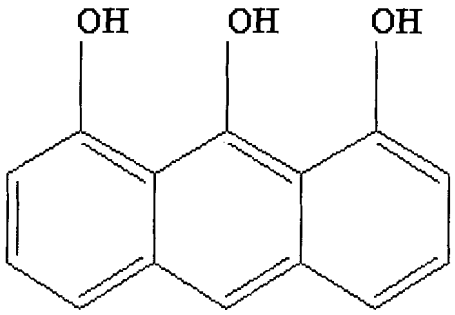

1, 8-dihydroxy-9-anthrone
(Dithranol)

Figure 7.1 The chemical structure of dithranol.

REFERENCE LIST

(1) Karas, M.; Bachmann, D.; Bahr, U.; Hillenkamp, F. Matrix-Assisted Ultraviolet-Laser Desorption of Nonvolatile Compounds. *International Journal of Mass Spectrometry and Ion Processes* **1987**, *78*, 53-68.

(2) Tanaka, K.; Waki, H.; Ido, Y.; Akita, S.; Yoshida, Y. et al. Protein and polymer analyses up to m/z 100 000 by laser ionization time-of-flight mass spectrometry. *Rapid Communications in Mass Spectrometry* **1988**, *2*, 151-153.

(3) Fenn, J. B. Ion Formation from Charged Droplets - Roles of Geometry, Energy, and Time. *Journal of the American Society for Mass Spectrometry* **1993**, *4*, 524-535.

(4) Knochenmuss, R.; Dubois, F.; Dale, M. J.; Zenobi, R. The matrix suppression effect and ionization mechanisms in matrix-assisted laser desorption/ionization. *Rapid Communications in Mass Spectrometry* **1996**, *10*, 871-877.

(5) Gaskell, S. J. Electrospray: Principles and practice. *Journal of Mass Spectrometry* **1997**, *32*, 677-688.

(6) Pitt, A. R. Application of electrospray mass spectrometry in biology. *Natural Product Reports* **1998**, *15*, 59-72.

(7) Loo, J. A. Studying noncovalent protein complexes by electrospray ionization mass spectrometry. *Mass Spectrometry Reviews* **1997**, *16*, 1-23.

(8) Karas, M.; Bahr, U.; Ingendoh, A.; Nordhoff, E.; Stahl, B. et al. Principles and Applications of Matrix-Assisted Uv Laser Desorption Ionization Mass-Spectrometry. *Analytica Chimica Acta* **1990**, *241*, 175-185.

(9) Zhang, N.; Li, L. Effects of common surfactants on protein digestion and matrix-assisted laser desorption/ionization mass spectrometric analysis of the digested peptides using two-layer sample preparation. *Rapid Communications in Mass Spectrometry* **2004**, *18*, 889-896.

(10) Patterson, S. D.; Aebersold, R. Mass-Spectrometric Approaches for the Identification of Gel-Separated Proteins. *Electrophoresis* **1995**, *16*, 1791-1814.

(11) Stuhler, K.; Meyer, H. E. MALDI: More than peptide mass fingerprints. *Current Opinion in Molecular Therapeutics* **2004**, *6*, 239-248.

(12) Karas, M.; Bahr, U. Laser Desorption Ionization Mass-Spectrometry of Large Biomolecules. *Trac-Trends in Analytical Chemistry* **1990**, *9*, 321-325.

(13) Henzel, W. J.; Watanabe, C.; Stults, J. T. Protein identification: The origins of peptide mass fingerprinting. *Journal of the American Society for Mass Spectrometry* **2003**, *14*, 931-942.

(14) Thiede, B.; Hohenwarter, W.; Krah, A.; Mattow, J.; Schmid, M. et al. Peptide mass fingerprinting. *Methods* **2005**, *35*, 237-247.

(15) Wilkins, M. R.; Lindskog, I.; Gasteiger, E.; Bairoch, A.; Sanchez, J. C. et al. Detailed peptide characterization using PEPTIDEMASS - A World-Wide-Web-accessible tool. *Electrophoresis* **1997**, *18*, 403-408.

(16) Rappsilber, J.; Mann, M. What does it mean to identify a protein in proteomics? *Trends in Biochemical Sciences* **2002**, *27*, 74-78.

(17) Lee, K.; Bae, D.; Lim, D. Evaluation of parameters in peptide mass fingerprinting for protein identification by MALDI-TOF mass spectrometry. *Molecules and Cells* **2002**, *13*, 175-184.

(18) Mathews, C. K.; Van Holde, K. E.; Ahern, K. G. *Biochemistry*; 3rd ed.; Benjamin Cummings: San Francisco, Calif., 2000; xxviii, 1186.

(19) Walsh, G. *Proteins : biochemistry and biotechnology*; J. Wiley: Chichester ; New York, 2002; x, 547.

(20) Kellner, R.; Lottspeich, F.; Meyer, H. E. *Microcharacterization of proteins*; 2nd ed.; Wiley-VCH: Weinheim ; New York, 1999; xxi, 325.

(21) Walsh, G. *Proteins biochemistry and biotechnology*, 2002.

(22) Chen, S. L.; Huddleston, M. J.; Shou, W. Y.; Deshaies, R. J.; Annan, R. S. et al. Mass spectrometry-based methods for phosphorylation site mapping of hyperphosphorylated proteins applied to Net1, a regulator of exit from mitosis in yeast. *Molecular & Cellular Proteomics* **2002**, *1*, 186-196.

(23) Mathews, C.; H., V.; Ahern, K. G. *Biochemistry*, 1998.

(24) Alberts, B. The cell as a collection of protein machines: Preparing the next generation of molecular biologists. *Cell* **1998**, *92*, 291-294.

(25) Gavin, A. C.; Bosche, M.; Krause, R.; Grandi, P.; Marzioch, M. et al. Functional organization of the yeast proteome by systematic analysis of protein complexes. *Nature* **2002**, *415*, 141-147.

(26) Moran, L. A.; Rawn, J. D. *Biochemistry*; 2nd ed.; Neil Patterson Publishers: Englewood Cliffs, NJ, 1994; 1 v. (various pagings).

(27) Hillenkamp, F.; Karas, M.; Beavis, R. C.; Chait, B. T. Matrix-Assisted Laser Desorption Ionization Mass-Spectrometry of Biopolymers. *Analytical Chemistry* **1991**, *63*, A1193-A1202.

(28) Bogan, M. J.; Agnes, G. R.; Pio, F.; Cornell, R. B. Interdomain and membrane interactions of CTP : phosphocholine cytidylyltransferase revealed via limited proteolysis and mass spectrometry. *Journal of Biological Chemistry* **2005**, *280*, 19613-19624.

(29) Moran, L. A.; Scrimgeour, K. G.; Horton, H. R.; Ochs, R. S.; Rawn, J. D. *Biochemistry*; second edition ed., 1994.

(30) Cadene, M.; Chait, B. T. A robust, detergent-friendly method for mass spectrometric analysis of integral membrane proteins. *Analytical Chemistry* **2000**, *72*, 5655-5658.

(31) Cohen, S. L.; Chait, B. T. Influence of matrix solution conditions on the MALDI-MS analysis of peptides and proteins. *Analytical Chemistry* **1996**, *68*, 31-37.

(32) Redeby, T.; Emmer, A. Membrane protein and peptide sample handling for MS analysis using a structured MALDI target. *Analytical and Bioanalytical Chemistry* **2005**, *381*, 225-232.

(33) Redeby, T.; Roeraade, J.; Emmer, A. Simple fabrication of a structured matrix-assisted laser desorption/ionization target coating for increased sensitivity in mass spectrometric analysis of membrane proteins. *Rapid Communications in Mass Spectrometry* **2004**, *18*, 1161-1166.

(34) Kellner, R.; Lottspeich, F.; Meyer, H. E. *Microcharacterization of proteins*; 2nd Edittion ed., 1998.

(35) Wang, B. H.; Dreisewerd, K.; Bahr, U.; Karas, M.; Hillenkamp, F. Gas-Phase Cationization and Protonation of Neutrals Generated by Matrix-Assisted Laser Desorption. *Journal of the American Society for Mass Spectrometry* **1993**, *4*, 393-398.

(36) Vastola, F. J.; Mumma, R. O.; Pirone, A. J. Analysis of Organic Salts by Laser Ionization. *Organic Mass Spectrometry* **1970**, *3*, 101-103.

(37) Karas, M.; Hillenkamp, F. Laser Desorption Ionization of Proteins with Molecular Masses Exceeding 10000 Daltons. *Analytical Chemistry* **1988**, *60*, 2299-2301.

(38) Strupat, K.; Kampmeier, J.; Horneffer, V. Investigations of 2,5-DHB and succinic acid as matrices for UV and IR MALDI. Part II: Crystallographic and mass spectrometric analysis. *International Journal of Mass Spectrometry* **1997**, *169*, 43-50.

(39) Strupat, K.; Karas, M.; Hillenkamp, F. 2,5-Dihydroxybenzoic Acid - a New Matrix for Laser Desorption Ionization Mass-Spectrometry. *International Journal of Mass Spectrometry and Ion Processes* **1991**, *111*, 89-102.

(40) Karas, M.; Kruger, R. Ion formation in MALDI: The cluster ionization mechanism. *Chemical Reviews* **2003**, *103*, 427-439.

(41) Dreisewerd, K. The desorption process in MALDI. *Chemical Reviews* **2003**, *103*, 395-425.

(42) Bahr, U.; Karas, M.; Hillenkamp, F. Analysis of Biopolymers by Matrix-Assisted Laser-Desorption Ionization (Maldi) Mass-Spectrometry. *Fresenius Journal of Analytical Chemistry* **1994**, *348*, 783-791.

(43) Puretzky, A. A.; Geohegan, D. B. Gas-phase diagnostics and LIF-imaging of 3-hydroxypicolinic acid maldi-matrix plumes. *Chemical Physics Letters* **1998**, *286*, 425-432.

(44) Zenobi, R.; Knochenmuss, R. Ion formation in MALDI mass spectrometry. *Mass Spectrometry Reviews* **1998**, *17*, 337-366.

(45) Puretzky, A. A.; Geohegan, D. B.; Hurst, G. B.; Buchanan, M. V.; Luk'yanchuk, B. S. Imaging of vapor plumes produced by matrix assisted laser desorption: A plume sharpening effect. *Physical Review Letters* **1999**, *83*, 444-447.

(46) Knochenmuss, R.; Zenobi, R. MALDI ionization: The role of in-plume processes. *Chemical Reviews* **2003**, *103*, 441-452.

(47) Knochenmuss, R.; Stortelder, A.; Breuker, K.; Zenobi, R. Secondary ion-molecule reactions in matrix-assisted laser desorption/ionization. *Journal of Mass Spectrometry* **2000**, *35*, 1237-1245.

(48) Karas, M.; Bahr, U.; Strupat, K.; Hillenkamp, F.; Tsarbopoulos, A. et al. Matrix Dependence of Metastable Fragmentation of Glycoproteins in Maldi Tof Mass-Spectrometry. *Analytical Chemistry* **1995**, *67*, 675-679.

(49) Siuzdak, G. *Mass spectrometry for biotechnology*; Academic Press: San Diego, Calif., 1996; xvi, 161.

(50) Weickhardt, C.; Moritz, F.; Grotemeyer, J. Time-of-flight mass spectrometry: State-of-the-art in chemical analysis and molecular science. *Mass Spectrometry Reviews* **1996**, *15*, 139-162.

(51) Feng, X.; Agnes, G. R. Single isolated droplets with net charge as a source of ions. *Journal of the American Society for Mass Spectrometry* **2000**, *11*, 393-399.

(52) Bogan, M. J.; Agnes, G. R. MALDI-TOF-MS analysis of droplets prepared in an electrodynamic balance: "Wall-less" sample preparation. *Analytical Chemistry* **2002**, *74*, 489-496.

(53) Bogan, M. J.; Agnes, G. R. Time-of-flight mass spectrometric analysis of ions produced from adjacent sample spots irradiated simultaneously by a single 337 nm laser. *Rapid Communications in Mass Spectrometry* **2003**, *17*, 2557-2562.

(54) Bogan, M. J.; Agnes, G. R. Wall-less sample preparation of mu m-sized sample spots for femtomole detection limits of proteins from liquid based UV-MALDI matrices. *Journal of the American Society for Mass Spectrometry* **2004**, *15*, 486-495.

(55) Bogan, M. J.; Agnes, G. R. Preliminary investigation of electrodynamic charged droplet processing to couple capillary liquid chromatography with matrix-assisted laser desorption/ionization mass spectrometry. *Rapid Communications in Mass Spectrometry* **2004**, *18*, 2673-2681.

(56) Bogan, M. J.; Bakhoum, S. F. W.; Agnes, G. R. Promotion of alpha-cyano-4-hydroxycinnamic acid and peptide cocrystallization within levitated droplets with net charge. *Journal of the American Society for Mass Spectrometry* **2005**, *16*, 254-262.

(57) Haddrell, A. E.; Agnes, G. R. A class of heterogeneous/multiphase organic reactions studied on droplets/particles levitated in a laboratory environment: aldehyde plus 1,8-diaminonaphthalene equals imine. *Atmospheric Environment* **2004**, *38*, 545-556.

(58) Haddrell, A. E.; Agnes, G. R. Organic cation distributions in the residues of levitated droplets with net charge: Validity of the partition theory for droplets produced by an electrospray. *Analytical Chemistry* **2004**, *76*, 53-61.

(59) Haddrell, A. E.; Ishii, H.; van Eeden, S. F.; Agnes, G. R. Apparatus for preparing mimics of suspended particles in the troposphere and their controlled deposition onto individual lung cells in culture with measurement of downstream biological response. *Analytical Chemistry* **2005**, *77*, 3623-3628.

(60) Bakhoum, S. F. W.; Agnes, G. R. Study of chemistry in droplets with net charge before and after Coulomb explosion: Ion-induced nucleation in solution and implications for ion production in an electrospray. *Analytical Chemistry* **2005**, *77*, 3189-3197.

(61) Bakhoum, S. F. W.; Bogan, M. J.; Agnes, G. R. Archiving and absolute quantitation of solutes separated by single charged droplet coulomb explosion. *Analytical Chemistry* **2005**, *77*, 3461-3465.

(62) Brèandâen, C.-I.; Tooze, J. *Introduction to protein structure*; 2nd ed.; Garland Pub.: New York, 1999; xiv, 410.

(63) Weinglass, A. B.; Whitelegge, J. P.; Kaback, H. R. Integrating mass spectrometry into membrane protein drug discovery. *Current Opinion in Drug Discovery & Development* **2004**, *7*, 589-599.

(64) Wu, C. C.; Yates, J. R. The application of mass spectrometry to membrane proteomics. *Nature Biotechnology* **2003**, *21*, 262-267.

(65) Abdulaev, N. G.; Ovchinnikov, Y. A. Some Approaches to Determining the Primary Structure of Membrane-Proteins. *Methods in Enzymology* **1982**, *88*, 723-729.

(66) Pomerleau, V.; Harveygirard, E.; Boucher, F. Lipid-Protein Interactions in the Purple Membrane - Structural Specificity within the Hydrophobic Domain. *Biochimica Et Biophysica Acta-Biomembranes* **1995**, *1234*, 221-224.

(67) Ovchinnikov, Y. A. Ion Channels - Structure and Function. *Biochemical Society Symposium* **1982**, 103-137.

(68) Ovchinnikov, Y. A.; Abdulaev, N. G.; Feigina, M. Y.; Kiselev, A. V.; Lobanov, N. A. Structural Basis of the Functioning of Bacteriorhodopsin - Overview. *Febs Letters* **1979**, *100*, 219-224.

(69) Henderson, R.; Unwin, P. N. T. 3-Dimensional Model of Purple Membrane Obtained by Electron-Microscopy. *Nature* **1975**, *257*, 28-32.

(70) Schobert, B.; Cupp-Vickery, J.; Hornak, V.; Smith, S. O.; Lanyi, J. K. Crystallographic structure of the K intermediate of bacteriorhodopsin: Conservation of free energy after photoisomerization of the retinal. *Journal of Molecular Biology* **2002**, *321*, 715-726.

(71) van Montfort, B. A.; Doeven, M. K.; Canas, B.; Veenhoff, L. M.; Poolman, B. et al. Combined in-gel tryptic digestion and CNBr cleavage for the generation of peptide maps of an integral membrane protein with MALDI-TOF mass spectrometry. *Biochimica Et Biophysica Acta-Bioenergetics* **2002**, *1555*, 111-115.

(72) van Montfort, B. A.; Canas, B.; Duurkens, R.; Godovac-Zimmermann, J.; Robillard, G. T. Improved in-gel approaches to generate peptide maps of integral membrane proteins with matrix-assisted laser desorption/ionization time-of-flight mass spectrometry. *Journal of Mass Spectrometry* **2002**, *37*, 322-330.

(73) Yu, Y. Q.; Gilar, M.; Lee, P. J.; Bouvier, E. S. P.; Gebler, J. C. Enzyme-friendly, mass spectrometry-compatible surfactant for in-solution enzymatic digestion of proteins. *Analytical Chemistry* **2003**, *75*, 6023-6028.

(74) Yu, Y. Q.; Gilar, M.; Gebler, J. C. A complete peptide mapping of membrane proteins: a novel surfactant aiding the enzymatic digestion of bacteriorhodopsin. *Rapid Communications in Mass Spectrometry* **2004**, *18*, 711-715.

(75) Blonder, J.; Conrads, T. P.; Yu, L. R.; Terunuma, A.; Janini, G. M. et al. A detergent- and cyanogen bromide-free method for integral membrane proteomics: Application to Halobacterium purple membranes and the human epidermal membrane proteome. *Proteomics* **2004**, *4*, 31-45.

(76) Blonder, J.; Goshe, M. B.; Moore, R. J.; Pasa-Tolic, L.; Masselon, C. D. et al. Enrichment of integral membrane proteins for proteomic analysis using liquid chromatography-tandem mass spectrometry. *Journal of Proteome Research* **2002**, *1*, 351-360.

(77) Zhang, N.; Li, N.; Li, L. Liquid chromatography MALDI MS/MS for membrane proteome analysis. *Journal of Proteome Research* **2004**, *3*, 719-727.

(78) Bird, G. H.; Lajmi, A. R.; Shin, J. A. *Anal. Chem.* **2002**, *74*, 219-225.

(79) Magdassi, S. *Surface activity of proteins : chemical and physicochemical modifications*; Marcel Dekker: New York, 1996; viii, 327.

(80) Hoteling, A. J.; Erb, W. J.; Tyson, R. J.; Owens, K. G. Exploring the importance of the relative solubility of matrix and analyte in MALDI sample preparation using HPLC. *Analytical Chemistry* **2004**, *76*, 5157-5164.

(81) Gerber, G. E.; Khorana, H. G. Primary Structure of Bacteriorhodopsin - Sequencing Methods for Membrane-Proteins. *Methods in Enzymology* **1982**, *88*, 56-74.

(82) Hoteling, A. J.; Mourey, T. H.; Owens, K. G. Importance of solubility in the sample preparation of poly(ethylene terephthalate) for MALDI TOFMS. *Analytical Chemistry* **2005**, *77*, 750-756.

(83) Kyte, J.; Doolittle, R. F. A Simple Method for Displaying the Hydropathic Character of a Protein. *Journal of Molecular Biology* **1982**, *157*, 105-132.

(84) Smirnov, I. P.; Zhu, X.; Taylor, T.; Huang, Y.; Ross, P. et al. Suppression of alpha-cyano-4-hydroxycinnamic acid matrix clusters and reduction of chemical noise in MALDI-TOF mass spectrometry. *Analytical Chemistry* **2004**, *76*, 2958-2965.

(85) Fligge, T. A.; Kast, J.; Bruns, K.; Przybylski, M. Direct monitoring of protein-chemical reactions utilising nanoelectrospray mass spectrometry. *Journal of the American Society for Mass Spectrometry* **1999**, *10*, 112-118.

(86) Glocker, M. O.; Nock, S.; Sprinzl, M.; Przybylski, M. Characterization of surface topology and binding area in complexes of the elongation factor proteins EF-Ts and EF-Tu center dot GDP from Thermus thermophilus: A study by protein chemical modification and mass spectrometry. *Chemistry-a European Journal* **1998**, *4*, 707-715.

(87) Odani, H.; Matsumoto, Y.; Shinzato, T.; Usami, J.; Maeda, K. Mass spectrometric study on the protein chemical modification of uremic patients in advanced Maillard reaction. *Journal of Chromatography B-Analytical Technologies in the Biomedical and Life Sciences* **1999**, *731*, 131-140.

(88) Plettner, E.; Lazar, J.; Prestwich, E. G.; Prestwich, G. D. Discrimination of pheromone enantiomers by two pheromone binding proteins from the gypsy moth Lymantria dispar. *Biochemistry* **2000**, *39*, 8953-8962.

(89) Kowcun, A.; Honson, N.; Plettner, E. Olfaction in the gypsy moth, Lymantria dispar - Effect of pH, ionic strength, and reductants on pheromone transport by pheromone-binding proteins. *Journal of Biological Chemistry* **2001**, *276*, 44770-44776.

(90) Honson, N.; Johnson, M. A.; Oliver, J. E.; Prestwich, G. D.; Plettner, E. Structure-activity studies with pheromone-binding proteins of the gypsy moth, Lymantria dispar. *Chemical Senses* **2003**, *28*, 479-489.

(91) Sandler, B. H.; Nikonova, L.; Leal, W. S.; Clardy, J. Sexual attraction in the silkworm moth: structure of the pheromone-binding-protein-bombykol complex. *Chemistry & Biology* **2000**, *7*, 143-151.

(92) Merritt, T. J. S.; LaForest, S.; Prestwich, G. D.; Quattro, J. M.; Vogt, R. G. Patterns of gene duplication in lepidopteran pheromone binding proteins. *Journal of Molecular Evolution* **1998**, *46*, 272-276.

(93) Klingenberg, M. Pigments of Rat Liver Microsomes. *Archives of Biochemistry and Biophysics* **1958**, *75*, 376-386.

(94) Garfinkel, D. Studies on Pig Liver Microsomes .1. Enzymic and Pigment Composition of Different Microsomal Fractions. *Archives of Biochemistry and Biophysics* **1958**, *77*, 493-509.

(95) Omura, T.; Sato, R. A New Cytochrome in Liver Microsomes. *Journal of Biological Chemistry* **1962**, *237*, 1375-1376.

(96) Ortiz de Montellano, P. R. *Cytochrome P-450 : structure, mechanism, and biochemistry*; Plenum Press: New York, 1986; x, 556.

(97) Schlichting, I.; Jung, C.; Schulze, H. Crystal structure of cytochrome P-450cam complexed with the (1S)-camphor enantiomer. *Febs Letters* **1997**, *415*, 253-257.

(98) Haniu, M.; Tanaka, M.; Yasunobu, K. T.; Gunsalus, I. C. Amino-Acid-Sequence of the Pseudomonas-Putida Cytochrome-P-450 .1. Sequences of Tryptic and Clostripain Peptides. *Journal of Biological Chemistry* **1982**, *257*, 2657-2663.

(99) Haniu, M.; Yasunobu, K. T.; Gunsalus, I. C. Modification of the Cysteine Residues of Cytochrome P-450cam with 2-Bromoacetamido-4-Nitrophenol. *Biochemical and Biophysical Research Communications* **1982**, *107*, 1075-1081.

(100) Unger, B. P.; Gunsalus, I. C.; Sligar, S. G. Nucleotide-Sequence of the Pseudomonas-Putida Cytochrome P-450cam Gene and Its Expression in Escherichia-Coli. *Journal of Biological Chemistry* **1986**, *261*, 1158-1163.

(101) Bech, L. M.; Breddam, K. Chemical Modifications of a Cysteinyl Residue Introduced in the Binding-Site of Carboxypeptidase-Y by Site-Directed Mutagenesis. *Carlsberg Research Communications* **1988**, *53*, 381-393.

(102) Eldstrom, J.; Doerksen, K. W.; Steele, D. F.; Fedida, D. N-terminal PDZ-binding domain in Kv1 potassium channels. *Febs Letters* **2002**, *531*, 529-537.

(103) Eldstrom, J.; Choi, W. S.; Steele, D. F.; Fedida, D. SAP97 increases Kv1.5 currents through an indirect N-terminal mechanism. *Febs Letters* **2003**, *547*, 205-211.

(104) Sheng, M.; Sala, C. PDZ domains and the organization of supramolecular complexes. *Annual Review of Neuroscience* **2001**, *24*, 1-29.

(105) Godreau, D.; Vranckx, R.; Maguy, A.; Goyenvalle, C.; Hatem, S. N. Different isoforms of synapse-associated protein, SAP97, are expressed in the heart and have distinct effects on the voltage-gated K+ channel Kv1.5. *Journal of Biological Chemistry* **2003**, *278*, 47046-47052.

(106) Cabral, J. H. M.; Petosa, C.; Sutcliffe, M. J.; Raza, S.; Byron, O. et al. Crystal structure of a PDZ domain. *Nature* **1996**, *382*, 649-652.

(107) Hata, Y.; Nakanishi, H.; Takai, Y. Synaptic PDZ domain-containing proteins. *Neuroscience Research* **1998**, *32*, 1-7.

(108) Murata, M.; Buckett, P. D.; Zhou, J.; Brunner, M.; Folco, E. et al. SAP97 interacts with Kv1.5 in heterologous expression systems. *American Journal of Physiology-Heart and Circulatory Physiology* **2001**, *281*, H2575-H2584.

(109) Marfatia, S. M.; Byron, O.; Campbell, G.; Liu, S. C.; Chishti, A. H. Human homologue of the Drosophila discs large tumor suppressor protein forms an oligomer in solution - Identification of the self-association site. *Journal of Biological Chemistry* **2000**, *275*, 13759-13770.

(110) Marvin, L.; Millar, A.; Saulot, V.; Machour, N.; Charlionet, R. et al. Identification of proteins from one-dimensional sodium dodecyl sulfate-polyacrylamide gel electrophoresis using electrospray quadrupole-time-of-flight tandem mass spectrometry. *Rapid Communications in Mass Spectrometry* **2000**, *14*, 1287-1292.

(111) Mann, M.; Hendrickson, R. C.; Pandey, A. Analysis of proteins and proteomes by mass spectrometry. *Annual Review of Biochemistry* **2001**, *70*, 437-473.

(112) Perkins, D. N.; Pappin, D. J. C.; Creasy, D. M.; Cottrell, J. S. Probability-based protein identification by searching sequence databases using mass spectrometry data. *Electrophoresis* **1999**, *20*, 3551-3567.

(113) Rashidezadeh, H.; Guo, B. C. Investigation of metal attachment to polystyrenes in matrix-assisted laser desorption ionization. *Journal of the American Society for Mass Spectrometry* **1998**, *9*, 724-730.

(114) Kinsel, G. R.; Edmondson, R. D.; Russell, D. H. Profile and flight time analysis of bovine insulin clusters as a probe of matrix-assisted laser desorption/ionization ion formation dynamics. *Journal of Mass Spectrometry* **1997**, *32*, 714-722.

(115) Zhang, W. Z.; Chait, B. T. Radial velocity distributions of molecular ions produced by matrix-assisted laser desorption/ionization. *International Journal of Mass Spectrometry and Ion Processes* **1997**, *160*, 259-267.

(116) Gusev, A. I.; Wilkinson, W. R.; Proctor, A.; Hercules, D. M. Improvement of Signal Reproducibility and Matrix/Comatrix Effects in Maldi Analysis. *Analytical Chemistry* **1995**, *67*, 1034-1041.

(117) Gusev, A. I.; Wilkinson, W. R.; Proctor, A.; Hercules, D. M. Direct quantitative analysis of peptides using matrix assisted laser desorption ionization. *Fresenius Journal of Analytical Chemistry* **1996**, *354*, 455-463.

(118) Aebersold, R.; Mann, M. Mass spectrometry-based proteomics. *Nature* **2003**, *422*, 198-207.

(119) Li, Y. L.; Gross, M. L. Ionic-liquid matrices for quantitative analysis by MALDI-TOF mass spectrometry. *Journal of the American Society for Mass Spectrometry* **2004**, *15*, 1833-1837.

(120) Li, Y. L.; Gross, M. L.; Hsu, F. F. Ionic-liquid matrices for improved analysis of phospholipids by MALDI-TOF mass spectrometry. *Journal of the American Society for Mass Spectrometry* **2005**, *16*, 679-682.

(121) Armstrong, D. W.; He, L. F.; Liu, Y. S. Examination of ionic liquids and their interaction with molecules, when used as stationary phases in gas chromatography. *Analytical Chemistry* **1999**, *71*, 3873-3876.

(122) Armstrong, D. W.; Zhang, L. K.; He, L. F.; Gross, M. L. Ionic liquids as matrixes for matrix-assisted laser desorption/ionization mass spectrometry. *Analytical Chemistry* **2001**, *73*, 3679-3686.

(123) Mank, M.; Stahl, B.; Boehm, G. 2,5-Dihydroxybenzoic acid butylamine and other ionic liquid matrixes for enhanced MALDI-MS analysis of biomolecules. *Analytical Chemistry* **2004**, *76*, 2938-2950.